Removal of trace organic contaminants from water by pervaporation

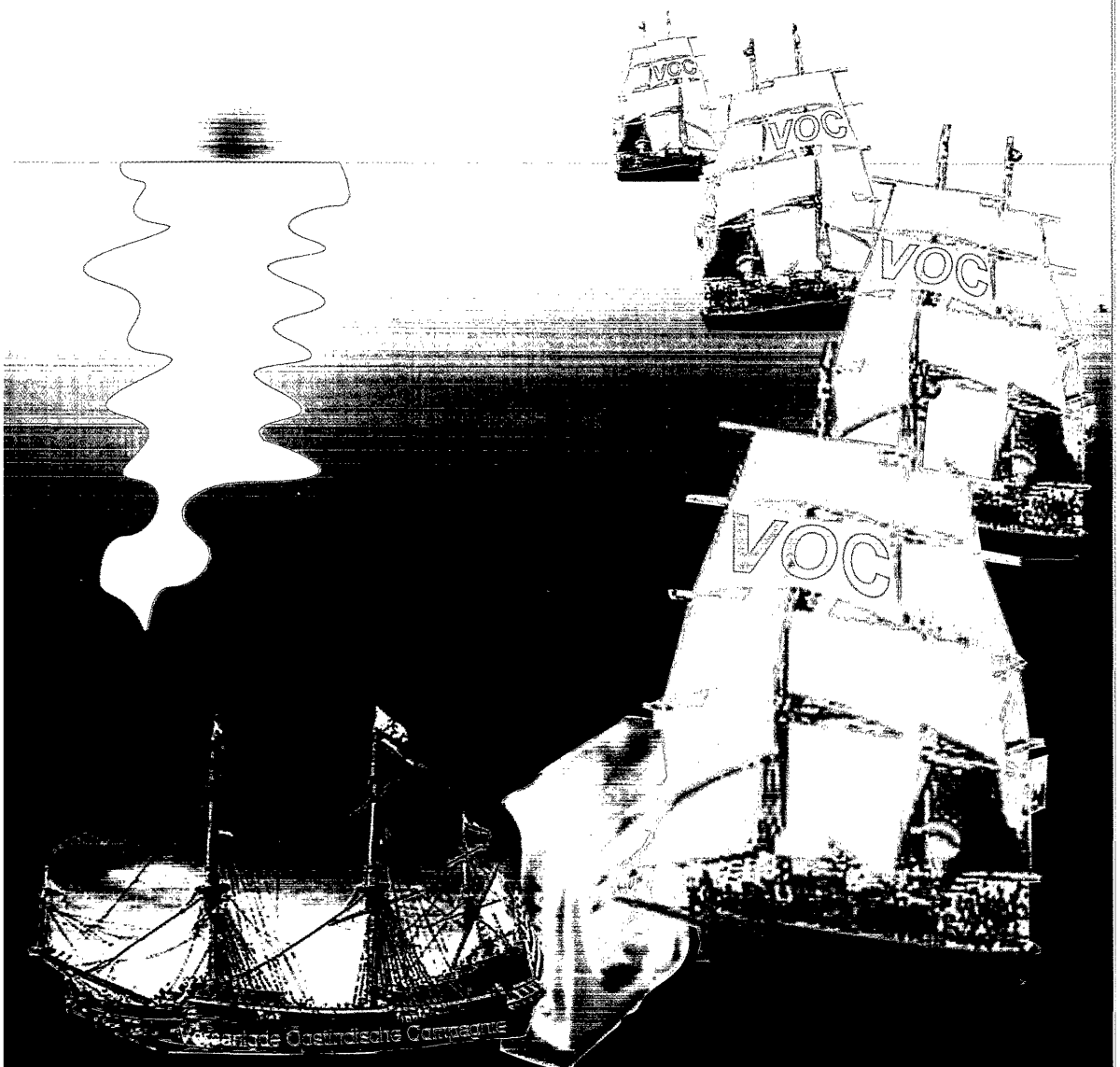

40

Erik Meuleman

REMOVAL OF TRACE ORGANIC CONTAMINANTS

FROM WATER BY PERVAPORATION

PROEFSCHRIFT

ter verkrijging van
de graad van doctor aan de Universiteit Twente,
op gezag van de rector magnificus,
prof. dr. F.A. van Vught,
volgens besluit van het College voor Promoties
in het openbaar te verdedigen
op vrijdag 21 maart te 15.00 uur.

door

Erik Everhardus Bernardus Meuleman

geboren op 20 oktober 1967
te Goor

Dit proefschrift is goedgekeurd door de promotor prof. dr. ing. H. Strathmann en de assistent-promotor dr. ing. M.H.V. Mulder.

Acknowledgement

The European Commission is highly acknowledged for supporting the work described in this thesis in the framework of the 'International Scientific Cooperation Programme' (Contract nr: CI1 - CT 920081 BR).

ISBN 90 365 09 343

Printed by Print Partners Ipskamp, Enschede (NL).

This thesis is printed on 100% recycled paper.

Cover: *Removal of a 'VOC' from water by a transverse flow membrane module.*
Omslag: *De verwijdering van een 'VOC' uit water met behulp van een dwars-aangestroomde membraan-module.*

VOORWOORD

Dit boek is het proefschrift, waaraan ik de laatste vier jaar heb mogen werken. Dit werk vormt voor mij min of meer de afsluiting van een gedeelte van m'n leven waarin opleiding centraal stond, hoewel promotiewerk soms meer managen is dan opleiding. Het VWO ging met twee vingers in de neus, waarvoor ik weinig trots voelde. De ir-titel deed me daarentegen al wat meer. Het gevoel echter dat bij het gereed komen van dit boekje naar bovenkomt benadert het ultieme.

Doordat er de eerste twee jaren geen goede komposiet-membranen konden worden geproduceerd, heeft het bijna drie jaar geduurd voordat er goede pervaporatie-experimenten konden worden uitgevoerd. Dit heeft ervoor gezorgd dat een onnavolgbare eindsprint moest worden ingezet, waarin metingen uitvoeren, resultaten verwerken, schrijven en eten en slapen centraal stonden. Ik hoop dan ook dat dit werk door vele mensen wordt gelezen en gebruikt.

Daar staat tegenover dat ik het eerste anderhalve jaar een super-leven heb gehad, waarin ik het project naar eigen inzicht kon uitvoeren (dat bleef zo). Verder heerste er een welhaast perfecte sfeer in de groep die expliciet tot uitdrukking werd gebracht met trouwe stap-maatjes als JMD, JPB, AK en andere membraners, met wie we feestend waren afgebeeld in de Volkskrant onder de kop: "Enschede, studenten-stad nummer 1".

Dat het heeft mogen lukken binnen vier en een half jaar heb ik aan vele mensen en studenten te danken. Zonder anderen tekort willen doen zal ik toch enkele noemen. Ten eerste ben ik de meeste dank verschuldigd aan Marcel Mulder die het project-voorstel heeft gedaan, de grote lijnen van het onderzoek op de voet volgde, veel tijd stak in het fatsoeneren van de engelse teksten in dit proefschrift en de resultaten voorzag van kritische noten (tot het bittere einde). Verder heeft Heiner Strathmann zijn steen bijgedragen door tussentijdse diskussies en door op het laatst nog blunders uit belangrijke vergelijkingen te halen die erin waren geslopen. Grote bijdragen zijn geleverd door Lydia Versteeg (Hfs 7), Jeroen Willemsen (Hfs 3), Frank Huijs (Hfs 6, App A), Bert Bosch (Hfs 4), Krista Bouma (Hfs 6 en 7), Kees Plug (Hfs 5, 6 en 7) en Jianjun Qin (Hfs 5) die als afstudeerder, KIPper of als buitenlandse gast-medewerker met veel plezier, veel werk hebben verzet en gemotiveerd bleven terwijl de resultaten toch soms (heel) erg tegenvielen. Dat waardeer ik nog steeds enorm. Betty Folkers wil bedanken voor de bruikbare last-minute metingen in Hfs 3. Tevele om op te noemen, maar aan de basis van menig idee, zijn de 2.3- en 3.1-praktikanten. Voor dagelijkse (praktische) problemen kon ik gelukkig altijd terecht bij Koops-San, Clemens, Herman, John H., Greet en Zandrie. Verder wil ik het vakgroepbestuur bedanken voor de goeie computer-voorzieningen (Mac's voor allerlei presentatie-werk en enkele MS-Dom-bakken voor het rekenwerk) en het instemmen met vele (buitenlandse) cursus-, congresbezoeken en een achtweeks verblijf in Rio.

Naast de praktische bijdrage hebben voornoemden ook bijgedragen tot de prettige werksfeer. Kamergenoten Toshio, Alie en op het laatst Annemieke waren altijd goedgeluimde aanspreekpunten en klaagden nooit over mijn op het eerste

gezicht onopgeruimde buro dat in schril kontrast afstak tegen hun buro's. Ze begrepen dat ik werkte volgens de *pyramides - law* (the important things lie on top). Dat brengt me in Rio. Claudio Habert and Ronaldo Nobrega introduced me to this very handy law. Further, Cristiano Borges and Harry Futselaar guided me well, which enabled me to do much in a short time (where commonly it is the reverse). Also, the atmosphere of this group was perfect which resulted in quite some parties at great locations with spectacular views. I want to thank Justino for filling the weekends extraordinarily and the introduction to Rio at night- and beach time, well done you stupid Carioca!!! Rick Vandervaart heb ik pas goed leren kennen op een cursus in Bath en werd een goeie vriend die door mij (?) in Rio kwam. Achteraf niet zo gek dat ik hem daar zo weinig zag ... ;-D

Een groot gedeelte van m'n vrije tijd ging op aan voetbal. Bewust koos ik om te spelen tussen de 'gewone' mensen bij de Richtersbleek; ff weg uit het academische milieu. Gelijk de eerste week was ik onder de indruk van de (aggressieve) tattoos, de stoere verhalen over carnaval waarin met veel trots van stekkerieje (=steekpartij(?)) verslag werd gedaan en waar een meter bier geen 11 glazen, maar eerder 11 kratten zijn (± 1 m^3). Na een tijdje ga je ze beter leren kennen en blijken het goeie jongens te zijn, waarmee je wekelijks goed kunt voetballen (liefst met 'geluud'). Het laatste halve jaar zijn ook zij goed met mijn geestelijke afwezigheid omgegaan.

Mijn eigen en Susan's familie wil ik hier bedanken, mede vanwege de door hun getoonde belangstelling en motivatie ben ik gekomen waar ik nu ben. Als laatste en als belangrijkste kan ik Susan op deze manier onmogelijk genoeg bedanken.

Erik

SUMMARY

Pervaporation is a membrane process in which a liquid mixture is enriched in one component due to selective transport across a dense film of one or more of the feed components. The driving force is the partial pressure difference of the permeating compounds. A lower partial pressure in the permeate is established by the use of a vacuum or a carrier gas.

Volatile organic *contaminants* (VOCs) are considered to be one of the most toxic pollutants. These compounds occur in groundwater and waste water streams. *Chapter 1* gives an overview of typical VOC-pollution sources and concentrations of the VOC in water. The most severe pollutants are toluene, benzene and trichloro-ethylene. It may be concluded that groundwater has typical concentrations below 10 ppm, while industrial streams can have VOC-concentrations of 100 to 10,000 ppm. Therefore, the VOCs have to be removed from water. Pervaporation is a novel technique which can accomplish this.

Chapter 2 describes the state-of-the-art of the removal of VOCs from water by pervaporation and compares this process to other more conventional processes such as carbon adsorption, air stripping or bio-filtration. Within a feed concentration range of the VOC between 100 and 10,000 ppm pervaporation is not only technically feasible but also environmentally attractive and economically viable. The VOCs can be removed in a pure state with pervaporation in contrast to many conventional separation methods and can easily be re-used, post-treated or properly disposed. PDMS (polydimethylsiloxane) is commonly used as the permselective membrane. However, other materials such as EPDM (ethylene-propylene terpolymer), PEBA (polyether-block-polyamides) and POT (polyoctenamer) show higher selectivities for many feed mixtures, while the VOC-fluxes are about the same.

Due to boundary layer limitations in the feed the mass transfer coefficient (k_L) is one of the main process efficiency determining parameters. Transverse flow membrane modules show the best properties (i.e. high k_L and high membrane surface per volume) but are still only produced on pilot-plant scale. Currently, plate-and-frame and spiral wound modules with composite membranes containing PEBA or PDMS are commercially available. The adverse effects of the boundary layer may be reduced by the use of thicker membranes or higher permeate pressures.

In *Chapter 3* several ethylene-propylene-diene terpolymers (EPDM) and crosslinking procedures have been investigated using pervaporation, vapor sorption, liquid sorption and gas permeation experiments. The EPDM parameters that have been changed are ethylene content, molecular weight, choice of third monomer and type of branching. Various crosslinking procedures were carried out.

The permeability coefficients were determined from pervaporation experiments and were about 40,000 Barrer for toluene and 700 Barrer for water. From vapor sorption measurements a value of 22,000 Barrer for toluene was obtained which is similar to the value obtained from pervaporation experiments. This indicates that, indeed, the presence of water does not influence the toluene flow during pervaporation.

No clear differences were found for both EPDM-variation and different crosslinking procedures.

In *Chapter 4*, the resistances-in-series model, the modified solution-diffusion model, the Flory-Rehner theory and the film theory have been used to calculate the diffusion coefficients of two components of a liquid feed mixture from actual pervaporation experiments. The toluene and water fluxes through EPDM membranes of various thicknesses have been modeled for different mass transfer coefficients in the feed boundary layer (k_L). Concentration independent diffusion coefficients have been determined by numerical methods. Diffusion coefficients of $3.2 \cdot 10^{-12}$ m^2/s and $1.4 \cdot 10^{-11}$ m^2/s were found for toluene and water, respectively. The use of concentration dependent diffusion coefficients did not improve the results.

It is shown that the toluene flux depends strongly on the k_L. Furthermore, the membrane resistance has a significant effect on the toluene flux only for very high values of k_L ($>10^{-4}$ m/s). The water flux increases linearly with the reciprocal value of the membrane thickness and is not affected by the boundary layer resistance. The small increase of the water flux due to the toluene concentration increase in the feed, can adequately be described by the presented model.

It is also shown that selective layers of about 5 to 50 μm may be most efficient.

Since thin layers of the selective layer are not strong enough they have to be supported by another layer. This layer should provide the mechanical strenght and it should not show any resistance to mass transfer. The spinning of such porous support capillaries is described in *Chapter 5*. Poly(ether imide) and poly(ether sulfone) capillaries were spun by a dry-wet spinning technique with 1-methyl-5-pyrrolidone as the solvent and water as the nonsolvent. Several high and low molecular additives were added to the polymer solution; poly(vinyl pyrrolidone), lithium nitrate, water and diethylene glycol. Characterization has been performed by gas permeation, liquid-liquid displacement and scanning electron microscopy. Several porous ultrafiltration membranes were selected as support for composite membranes. A whole range of pore sizes and pressure-normalized gas fluxes were covered. The support with the lowest overall porosity had a P/l-value of 0.03 cm^3(STP)/ (cm^2.s.cmHg) and a narrow pore radius distribution of 6 to 10 nm with a maximum pore radius of 20 nm. The support with the highest porosity had a P/l-value of 0.8 cm^3(STP)/ (cm^2.s.cmHg) and a maximum surface pore radius of 0.6 μm.

Chapter 6 describes the preparation of composite membranes by a dip-

coating technique with a polymer solution which contains ethylene-propylene terpolymer (EPDM) in an appropriate solvent. One of the main problems is the penetration of the coating-solution into the pores of the support material. Investigations were performed to prevent penetration. Prior to coating, some capillaries were pre-filled with different liquids, such as hexane, water and a thermo-reversible gel to prevent penetration. It was concluded that water and hexane gave the best results, however, penetration could not be prevented completely. With a coating-solution of 5 wt-% EPDM in hexane, 4 coating steps were needed to obtain defect-free membranes. This was concluded from gas permeation measurements, in which the composite membrane showed the same or higher selectivity than the intrinsic selectivity of the pure EPDM. Only one step was needed when a 10 wt-% EPDM solution was used. However, for these membranes the theoretical toplayer thickness is still higher than the toplayer thickness observed by scanning electron microscopy. Further, the gas selectivities are in between the intrinsic selectivity of the toplayer and the porous support material. This implicates that the toplayer material intrudes into the pores of the support.

The best properties are obtained with the relatively high porous PES-supports. In this case, the selectivity of the composite membrane is nearly equal to the intrinsic selectivity of the toplayer material and the effective thickness as determined from CO_2 permeation is close to the observed thickness as determined from scanning electron microscopy.

At last in Chapter 7 composite membranes with poly(ether sulfone) (PES) or poly(ether imide) (PEI) as porous support layer and with ethylene-propylene terpolymer (EPDM) as toplayer were used in the removal of volatile organic contaminants (VOCs) by pervaporation. The toluene flux through the membrane was between 5 and 50 $g/m^2.h$ at a toluene concentration in the feed of 250 ppm. The toluene flux was mainly affected by the toplayer thickness and the feed flow velocity. The water flux decreased with increasing toplayer thickness and ranged from 1.5 to 12 $g/m^2.h$. The separation factor ranged between 5,000 and 90,000 and increased with toplayer thickness and feed flow velocity. Composite membranes with a highly porous PES support showed a better performance than membranes with a less porous PEI support.

The composite membranes were built in transverse flow modules (TFM) and longitudinal outside flow modules (LOM) and pervaporation experiments were carried out with these modules. From the velocity-variation method and the resistances-in-series model a value for the mass transfer coefficient in the liquid boundary layer (k_L) was determined. At a Reynolds number of 2,400 the TFM had a k_L of $6.7.10^{-5}$ m/s. For the LOM a k_L value of $5.7.10^{-5}$ m/s was found at extreme high Reynolds numbers of 11,000.

SAMENVATTING VOOR DE 'LEEK'

Dit boekje (proefschrift) beschrijft hoe een zuiveringstechniek (**pervaporatie**) sterk verbeterd kan worden. Het doel van dit promotie-onderzoek was te kijken naar hoe je met behulp van pervaporatie bepaalde stoffen uit water kunt verwijderen. Meestal komen deze stoffen in zeer lage concentraties voor (minder dan 1 %). Hierbij kan het gaan om waardevolle stoffen, zoals bijvoorbeeld allerlei natuurlijke geur- en smaakstoffen die in fruit-vocht zitten, maar ook om gevaarlijke stoffen, zoals bijvoorbeeld benzeen en tri die zelfs bij extreem lage concentraties kankerverwekkend kunnen zijn! Deze laatste stoffen werden vroeger onder andere veel als ontvetter gebruikt en worden nu (hoewel in véél mindere mate) nog steeds gebruikt.

Er zijn talloze oorzaken van watervervuiling. Denk maar eens aan de paar druppeltjes benzine die je steeds morst bij het tanken. En jij bent niet de enige! Benzine bestaat voornamelijk uit benzeen, **tolueen**, ethyl-benzeen en xylenen (**BTEX**). Tijdens regen worden deze gevaarlijke stoffen meegespoeld, de grond in. Hier hoopt het zich in de jaren op en de grond moet dus uiteindelijk worden gereinigd. Naast deze bron van vervuiling zijn er nog talloze meer. Cijfers die de vervuiling door de verschillende bedrijfstakken weergeven staan in *Hoofdstuk 1*.

In *Hoofdstuk 2* wordt de zuiveringstechniek 'pervaporatie' uitgelegd. Tevens geeft het een overzicht van wat er in het afgelopen decenium al is geschreven over pervaporatie. Een voorbeeld van pervaporatie is het volgende: een mengsel van tolueen in water wordt in kontakt gebracht met een heel **dun laagje rubber** (**EPDM**). Dit rubber zuigt het tolueen als een gek op, terwijl het water nauwelijks het rubber in wil. Dit kun je je voorstellen als je eens denkt aan je rubberen-schoenzolen, waarmee niets gebeurd als ze in water staan, terwijl ze kapot-zwellen als ze in een plas benzine staan. Bij pervaporatie wordt tolueen aan de andere kant van het rubber heel hard uit het rubber gezogen, zodat het rubber niet kapot-zwelt. Stel dat het mengsel aan de ene kant van het rubber 0,025 % (=250 ppm) tolueen en 99, 975 % water bevat, dan komt er aan de andere kant meer dan 90 % tolueen! Omdat oliën en dus ook tolueen lichter zijn dan water, drijft het tolueen bij die hoge concentratie op water en kun je het er zo afhalen en hergebruiken of vernietigen.

In *Hoofdstuk 3* blijkt dat EPDM een hele gewone rubber is die veel als dakbedekking of in bumpers van auto's wordt gebruikt en het is daardoor goedkoop.

In *Hoofdstuk 4* wordt een computer-model toegepast om te berekenen hoe dik het rubber-laagje (**membraan**) moet zijn om water efficient te kunnen zuiveren. Meestal geldt hoe dunner het laagje, hoe sneller de stoffen er door gaan. In het begin van mijn onderzoek is gebleken dat het tolueen zo snel door het dunne membraan gaat, dat vlak aan het membraan-oppervlak veel minder tolueen zit dan in het mengsel zelf. De aanvoer van tolueen vanuit het mengsel

naar het membraan-oppervlak moet dus worden verhoogd. Dit kan door het mengsel harder langs het membraan-oppervlak te laten stromen. Dit is vergelijkbaar met het sneller drogen van natte voetbalvelden als het harder waait. Hetzelfde gaat op voor natte was; hoe harder het waait, hoe sneller het droogt. Wij hebben hiermee rekening gehouden en hebben een **membraan-houder** gemaakt die op de voorkant van dit boekje staat afgebeeld. Hierdoor is de aanvoer van tolueen sterk verbeterd. Gevolg is dat het membraan toch heel dun mag zijn (circa 5 tot 50 µm[1]). Omdat dit te dun is om sterk genoeg te zijn moet het worden ondersteund. De produktie van deze **steunlaag** is beschreven in *Hoofdstuk 5*. Normaal is deze steunlaag een ander soort membraan die werkt als een zeef met hele kleine gaatjes. Dat is goed te zien op de plaatjes in dit hoofdstuk.

In *Hoofdstuk 6* wordt beschreven hoe een dun laagje EPDM-rubber op de steunlaag wordt aangebracht. De dikte (dunte) van dit laagje kan worden geregeld met de manier waarop het laagje wordt aangebracht. Ook in dit hoofdstuk zijn plaatjes opgenomen van typische **composiet-membranen**[2] die duidelijk het dunne en dichte laagje EPDM op de poreuze steunlaag laten zien. Door te meten hoeveel sneller koolstof-dioxide (CO_2 of koolzuurgas) door het composiet-membraan gaat dan stikstof (N_2), kun je zien of het membraan goed is.

Tenslotte worden in *Hoofdstuk 7* verschillende membranen vergeleken op hun vermogen om tolueen uit water halen. Hoewel in het mengsel minder dan 0,025 % tolueen zit en 99,975 % water laten de meeste membranen inderdaad veel meer tolueen door dan water! Het blijkt daar ook dat membranen die worden aangestroomd met onze nieuwe membraan-houder meer tolueen doorlaten dan dezelfde membranen die zijn ingebouwd in een oudere type membraan-houder.

De composiet-membranen die in dit onderzoek zijn gemaakt geven de beste prestaties voor de verwijdering van BTEX en snel verdampende chloorhoudende koolwaterstoffen uit water, die er in de wereld zijn getest op laboratorium-schaal en beschreven in de literatuur. Het grote voordeel ten opzichte van andere membraan-materialen dan EPDM wordt voornamelijk veroorzaakt door een combinatie van de lage hoeveelheid water die door het EPDM gaat (waardoor de koelingskosten veel lager zijn) en de hoge hoeveelheid tolueen door het toegepaste aanstromingsconcept.

Alles overziend kunnen we vaststellen dat de zuiveringstechniek 'pervaporatie' weinig gebruikt zal worden om grondwater te reinigen. De concentraties van de organische stoffen in het grondwater zijn daarvoor te laag (< 10 ppm). Echter aan het eind van bijvoorbeeld een productie-proces in een fabriek zijn de concentraties wel hoog genoeg. Vooral op olieplatforms waar de concentraties gevaarlijke stoffen in water hoog zijn en waar maar weinig ruimte voorhanden is, zou pervaporatie goed kunnen worden ingezet.

---

1 1 µm is gelijk aan 0.001 mm, oftewel 1000 µm is 1 mm.

2 composiet-membranen zijn membranen die uit meer dan 1 materiaal zijn opgebouwd.

CONTENTS

LEVENSLOOP

1

REMOVAL OF VOCs FROM WATER BY PERVAPORATION

A SHORT INTRODUCTION

1.1 POLLUTION SOURCES OF VOLATILE ORGANIC COMPONENTS

Volatile organic contaminants, abbreviated as VOCs, are considered to be one of the most toxic pollutants. Aromatic hydrocarbons (e.g. benzene, toluene, xylene, etc.) and halogenated hydrocarbons (e.g. chloro-ethylene, chloro-methane, chloro-ethane, etc.) are present in industrial effluent streams. Also the area around gasoline stations and municipal effluents may contain various VOCs.

Since the mid 80's a strong decrease in emission rate of VOCs is observed [1] due to a stricter governmental legislation [2]. In The Netherlands , however, in 1993, still 35 kton/yr was emitted into the air and a considerable amount of 5.5 kton/yr entered the environment via the water [3]. These values refer to halogenated hydrocarbon and aromatic compounds. If all volatile organic compounds are included, an emission of 150 kton/yr to the atmosphere was estimated for The Netherlands by industrial activities [3]. Apart from pollution, the emission of these solvents also results in a loss of potential resources and energy [4]. If these solvents were recovered, the pollution of the environment would be reduced and materials and energy would be recovered. This thesis will be focused on the removal of VOCs from water.

1.1.1 Halogenated hydrocarbons

Many highly toxic components belong to the group of halogenated hydrocarbons. In the following overview, some were selected because of their toxic or carcinogenic character [5]. These compounds are trichloro-ethylene, tetrachloro-ethylene, tetrachloro-methylene and trichloromethane, which are commonly known as tri, per, tetra and chloroform, respectively. The total emission over 1993 for these components is listed in table 1.

Table 1 *Industrial emissions of chlorinated hydrocarbons into air and water in 1993 [3].*

Component	air [ton/yr]	water [ton/yr]
Tetrachloro-ethylene (per)	1,260	0.83
Trichloro-ethylene (tri)	1,000	1.91
Tetrachloromethane (tetra)	169	0.28
Trichloromethane (chloroform)	36	0.61
Aliphatic halogenated, total	12,400	5.37

Tri is the most severe pollutant with 1.9 ton/yr. The use of trichloro-ethylene was strongly reduced over the last years due to stricter legislation. Table 2 shows the emission of a certain component per type of industry as percentages of the total emission.

Table 2 *Emission of chlorinated hydrocarbons to water by various industries in 1993 [3]. Numbers are in % of total as tabulated in table 1.*

Industry type	Per	Tri	Tetra	Chloroform
Bulk chemicals	29	8	59	80
Textile and clothing	5	36	-	-
Metallurgy	6	-	-	-
Fibers	-	-	39	7
Pharmaceutical	-	19	-	8
Storage and warehouse	56	34	-	-
other	4	3	2	5

1.1.2 Aromatic hydrocarbons

Also many aromatic hydrocarbons are toxic or carcinogenic [5]. A well known mixture is BTEX consisting of benzene, toluene, ethylbenzene and xylenes. The total emission during 1993 in The Netherlands for these components is listed in table 3. The most widely spread pollutant to water is toluene with 30 ton/yr and its emission was decreased by 70% in 1993 compared to 1992 [3]. On the other hand, benzene is the second largest pollutant and much more carcinogenic. Table 4 shows percentages of the total emission of different components for various industries.

Table 3 *Industrial emissions of aromatic hydrocarbons into air and water in 1993 [3].*

Component	air [ton/yr]	water [ton/yr]
Benzene	841	22
Toluene	10,700	30
Ethylbenzene	1,400	nr*
Xylene	3,470	7
Aromatic, total	21,500	169

* nr is not reported

Table 4 *Emission of aromatic contaminants to water per type of industry in 1993 [3]. Numbers are in % of total as tabulated in table 3.*

Industry type	Benzene	Toluene	Xylenes
Bulk chemicals	67	60	99
Petroleum	20	1	-
Public services	6	12	-
other	7	27	1

1.2 WASTEWATER STREAMS

Clean technology is the only alternative to reduce pollution problems. However, for the near future, this alternative is not assessable for many industrial processes. Therefore remediation of polluted effluents ('cleaning technology') is still the current solution. The best place to remove polluting components from an effluent stream is close to the process where they are discharged. It may then be possible to recycle these components. Once various effluent streams have been mixed recycling becomes increasingly difficult. Table 5 lists typical concentrations of a VOC containing effluent stream of the AKZO-NOBEL site in Delfzijl (NL) and at DSM Geleen (NL) [6]. This table shows that contamination occurs below the 10,000 ppb range. The wastewaters on oil platforms are a different case. These streams are almost completely saturated with hydrocarbons [7], which implies concentrations of 100 to 10,000 ppm. In near future these streams will be treated according to a European legislation. Another highly contaminated wastewater stream occurs at a natural gas dehydration unit of Elf Petroland at Harlingen (NL). At this site concentrations of 3,000 ppm with fluctuations up to 10,000 ppm have to be treated [8], which is above the saturation concentration.

Table 5 *Typical wastewater composition of the AKZO-NOBEL site in Delfzijl and the DSM site in Geleen (1994) [6].*

component	AKZO-NOBEL [µg/l]*	DSM [µg/l]*
tri	100	-
per	500	-
chloroform	1,750	-
tetra	850	-
dichloormethane	5,000	-
benzene	-	6,000
toluene	-	2,000
xylene	-	380

* µg/l is commonly used in wastewater literature. 1 µg/l = 1 ppb or 10^{-3} ppm

1.3 GROUNDWATER

In the early 90's the Dutch government made an overview of contaminated sites. In addition, TauwMilieu BV published a list of another 48 contaminated sites. Typical concentrations for BTEX were in the range of 10 to 370 ppb and 10 - 760 ppb for the chlorinated hydrocarbons [9]. Higher BTEX concentrations of typically tens of ppm's can be found in places with storage tanks of gasoline in the ground [10]. Table 6 shows a typical sample well composition.

Table 6 *Groundwater composition at a certain industrial site (1996) [10] and the allowable limits and the intervention value [9].*

component	benzene	ethylbenzene	toluene	xylene
industrial site [µg/l]	14,000	150	3,200	1,300
allowable limits [µg/l]	0.01	0.05	0.05	0.05
intervention-value [µg/l]	30	150	1,000	70

Table 6 also lists the allowable limits (concentration of a component in water above which it should be treated) and the intervention-value (concentration of a component in water above which it has to be treated). The allowable limits for these VOCs typically approach the detection limit. An extremely contaminated groundwater stream with chlorinated hydrocarbons (250 ppm) and aromatics (400 ppm) is treated on site (Diosynth, Oss, NL) [11].

1.4 OUTLINE OF THIS THESIS

Pervaporation is a relatively new technique which can be applied to remove organics from water. The main objective of this study is the preparation of high

performance composite capillaries which can be used in transverse flow modules to remove volatile organic contaminants (VOCs) from water.

In Chapter 2 a literature review is given about the removal of volatile organic contaminants from water. Various membrane materials are listed and the performance of composite membranes are tabulated. Another part of Chapter 2 compares the costs of pervaporation with several conventional processes. From literature it was concluded that poly(dimethyl siloxane) (PDMS) is most commonly used due to its high VOC fluxes. However, ethylene-propylene terpolymer (EPDM) shows the most promising performance of all materials due to a very low water flux and a moderate VOC flux. The employment of composite membranes makes it possible to adjust the toplayer thickness to obtain the same toluene flux as found in PDMS. However, the water flux is much lower in case of EPDM.

In Chapter 3 several EPDM types were investigated. The structure-property relationship, such as molecular weight and ethylene content to differences in permeability coefficients of water, toluene and gases such as CO_2, O_2 and N_2 was studied. Pervaporation experiments were carried out with homogeneous EPDM films as the selective barrier.

Chapter 4 models the performance of the pervaporation process with the feed flow velocity and the EPDM film thickness as the main variables. Flux values of water and toluene as found in literature were used.

Composite membranes combine a high flux with the intrinsic selectivity of the used barrier materials. The preparation and characterization of the capillary supports is discussed in Chapter 5. Important properties of this support are porosity and pore size. These parameters can be varied by changing the spinning dope solution and the residence time of the nascent fiber in the air gap during the spinning process. The support structures have been characterized by scanning electron microscopy (SEM), permeation experiments and liquid-liquid displacement measurements.

Chapter 6 describes the coating of the porous sublayers with a selective dense EPDM film by a dip-coating technique. The composite membranes are characterized with SEM and gas permeation measurements.

Chapter 7 describes the pervaporation results with two different module types: a transverse flow module and a longitudinal outside flow module. Via the 'velocity-variation' method and the resistances-in-series model the boundary layer and the membrane resistance were determined.

REFERENCES

[1] Plas, A.van der, P.Verhoeve, *Trends in de industriële emissies van prioritaire stoffen*, Publicatiereeks emissieregistratie, nr 18, Ministerie van VROM, 1994.

[2] Projektgroep koolwaterstoffen 2000, *Bestrijdingsstrategie voor de emissies van vluchtige organische stoffen*, Ministerie van VROM, 1989.

[3] Berdowski, J.J.M., W.J.Jonker, P.Verhoeve, *Emissies in Nederland, bedrijfsgroepen en regio's 1993 en ramingen 1994*, Publicatiereeks emissieregistratie, nr 27, Ministerie van VROM, 1995.

[4] Blume, I., M.H.V.Mulder, H.M.G.Temmink, P.H.M.Feron, K.Weijers, J.Dilweg, *Verwijdering*

van vluchtige organische componenten uit lucht m.b.v. membranen, Programma commissie membraantechnologie, C.P.M. van Ginneken (secr.), Tebodin BV, Hengelo (NL), 1991.

[5] Trouwborst, T., *Bronnen van verontreininging van grondwater en hun betekenis,* H2O, 14 (1981) 4-10.

[6] Klaassen, R., A.E.Jansen, G.I.H.M.Oesterholt, B.A.Bult, *Pertraction of hydrocarbons from wastewater streams,* Final report, TNO-ME en TauwMilieu BV, 1994.

[7] Nijhuis, H.H., *Removal of trace organics from water by pervaporation (a technical and economic analysis),* PhD-Thesis, University of Twente, Enschede (NL), 1990.

[8] AKZO Nobel, *MPPE unit Harlingen, NL,* Brochure AKZO Nobel, 1996.

[9] *Inventarisatie praktijkgegevens van grondwaterreinigingstechnieken,* Eindrapport, TauwMilieu BV, 1994.

[10] Olde Scholtenhuis, F.H.A., Private communication, Envinex milieutechniek BV, 1996.

[11] AKZO Nobel, *MPPE unit Oss, NL,* Brochure AKZO Nobel, 1996.

2

REMOVAL OF VOLATILE ORGANIC CONTAMINANTS FROM WATER BY PERVAPORATION

STATE-OF-THE-ART

SUMMARY

The state-of-the-art of the removal of volatile organic *contaminants* (VOCs) from water by pervaporation is described in this chapter. This process is technically feasible, environmentally attractive and economically viable. The VOCs can be removed in a pure state with pervaporation in contrast to many conventional separation methods and can easily be re-used, post-treated or properly disposed. PDMS (polydimethylsiloxane) is commonly used as the permselective membrane. However, other materials such as EPDM (ethylene-propylene terpolymer), PEBA (polyether-block-polyamides) and POT (polyoctenamer) show higher selectivities for many feed mixtures, while the VOC-fluxes are about the same. Due to boundary layer limitations at the feed side of the membrane the mass transfer coefficient (k_L) is one of the main process efficiency determining parameters. Transverse flow membrane modules show the best properties (i.e. high k_L and high membrane surface per volume) but are still only produced on pilot-plant scale. Currently, plate-and-frame and spiral wound modules with composite membranes containing PEBA or PDMS are commercially available. The adverse effects of the boundary layer may be reduced by the use of thicker membranes or higher permeate pressures.

2.1 HISTORY OF PERVAPORATION

Kober, at the research laboratories of the New York State Department of Health, first termed pervaporation as a coupling of permeation and evaporation in a publication in 1917 [1]. The first major research effort was performed by Binning et al. in the late 1950's [2]. By 1965 it was possible to separate aqueous-organic mixtures by pervaporation. However, the process could not compete with conventional techniques, since the available homogeneous membranes were lacking high selectivities and high fluxes. The goals of these preliminary studies were aimed to find alternative techniques for separations which were difficult to accomplish with distillation, such as the separation of isomeric and azeotropic mixtures. Energy costs were at that time of only little importance.

The energy crises in the early 1970's draw full attention to less energy consuming techniques to replace at least partly the energy-intensive distillation operations. Nowadays, large-scale plants are successfully in operation and there is a great potential for future growth in research and commercial applications [3]. Néel [4] indicated that about 200 pervaporation plants are in operation mainly for dehydration of solvents, but also for the separation of organic-organic mixtures and the removal of organics from water.

2.2 REMOVAL OF ORGANIC CONTAMINANTS FROM WATER BY PERVAPORATION

Volatile organic contaminants, abbreviated to VOCs, are now considered to be one of the most threatening pollutants. Examples are aromatic hydrocarbons (e.g. benzene, toluene, xylene, etc.) and halogenated hydrocarbons (e.g. trichloro ethylene, chloroform, chloroethane, etc.) which can be found in industrial effluent streams and groundwater.

Conventional techniques which are used for the removal of VOCs from water are activated carbon adsorption (ACA) and air stripping (AS). In the ACA-technique water with organics is pumped across activated carbon, where adsorption takes place. When the complete surface of the carbon is occupied, the adsorption material has either to be disposed or regenerated. In particular, this part of the process can be very expensive, depending on the kind of pollutant, the adsorption system and, if used, the regeneration technique. With AS the volatile organic components can be removed from water by air or steam. The off-gases of this process must be post-treated, which can be accomplished by biofiltration or ACA [5,6]. Pervaporation is a new technique to remove VOCs from water.

The VOCs usually occur at low concentrations (< 10 ppm) and sometimes at relative high concentrations (100 - 10,000 ppm) [7]. In the latter case, pervaporation is very useful (10 - 100,000 ppm [8]). Fig.1 shows the optimal concentration range of different treatment techniques. Although economically not interesting it is possible to achieve VOC-concentrations in water below the ppm-range by pervaporation [9]. Initially, pervaporation was applied to remove

and recover VOCs from groundwater or wastewater as an economical more attractive process under certain conditions compared to the conventional techniques [10-13]. Later, other applications were found based on the same process. These applications involve the extraction of organic substances from fermentation broths [14,15] and the recovery of valuable aroma compounds [16]. Lately, the same process is used to enrich a VOC-content in an aqueous solution to increase the detection range of an analysis method [17].

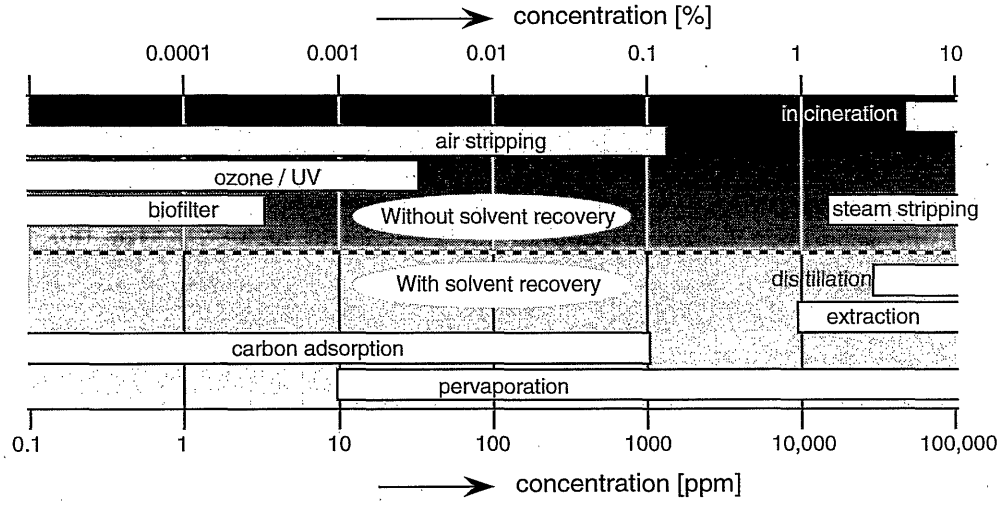

Figure 1 *Separation processes to remove volatile organic solvents from water [8].*

2.3 PRINCIPLES OF PERVAPORATION

Pervaporation is a membrane process, in which a liquid mixture (feed) is brought in contact with the upstream side of a membrane while the permeate is removed as a vapor at the downstream side. A partial pressure difference of the components is the driving force for mass transport through the membrane. At the permeate side a lower partial pressure of the permeating components is applied by a condenser operated at low temperature, or by a vacuum or an inert carrier gas stream. The permeation of molecules through the dense membrane occurs basically in three steps:

- selective sorption of molecules into the membrane at the feed side from a liquid mixture
- selective diffusion through the membrane
- desorption into a vapor phase at the permeate side.

The concentration of the VOC in the permeate is typically much higher than the saturated concentration and, after condensation, the permeate spontaneously phase separates into a VOC phase saturated with water and a water phase saturated with VOC. The first phase could be used as a product and the second phase can be recycled to the feed of the pervaporation process (fig.2).

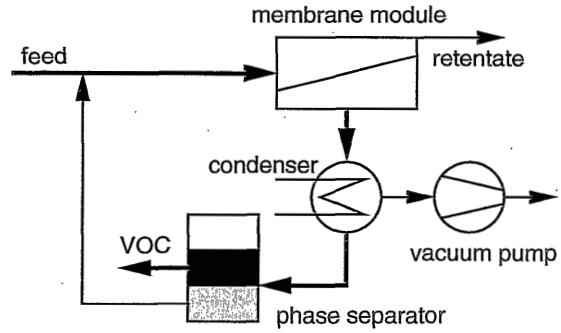

Figure 2 *Schematical representation of the pervaporation process.*

The performance of the pervaporation process is commonly described by the flux (J), the separation factor (α) and/or the enrichment factor (β). The flux of component i across the membrane can be given by

$$J_i = \frac{P_i}{l} \cdot \Delta p_i = k_m \cdot \Delta p_i \ , \qquad (1)$$

in which P_i is the permeability coefficient of component i, J_i is its flux, l is the membrane thickness and Δp_i is the partial pressure difference of component i across the membrane and k_m is the mass transfer coefficient of the membrane.
The separation factor is defined as

$$\alpha_{i,j} = \frac{y_i / y_j}{x_i / x_j} \ , \qquad (2)$$

where y is the concentration in the permeate of component i and j, respectively and x is the concentration of the component in the feed. For α x and y can have any dimension such as mole and weight per volume or mole and weight fractions because the dimensions of each component are divided by each other.

Another parameter, which is used to describe the separation properties of the membrane, is the enrichment factor. This is the ratio of the concentration of component i in the permeate and the feed

$$\beta = y_i / x_i \ . \qquad (3)$$

Now x and y have to be in mole concentration or fraction, otherwise one may end up with the ratio of the molecular weights for non-selective membranes. The separation is described better by α than by β, since α relates the enrichment to both components and increases to infinite for perfect semipermeable membranes, while β describes only one component. However, β is commonly used because it is easier incorporated into mass balances [18]. On the other hand, direct relations between α and β can be obtained by combining eqns (2) and (3)

$$\alpha = \frac{1 - x_i}{1 - \beta x_i} \cdot \beta \quad \text{or} \quad \beta = \frac{\alpha}{1 + (\alpha - 1)\, x_i} \quad . \tag{4}$$

The importance of flux and separation factor for the economical feasibility of the process can easily be demonstrated. In the pervaporation process the heat of vaporization of the permeated liquid has to be supplied. Thus, the more selective the membrane, the less water permeates and the less condensation energy is needed to achieve a certain separation. An increase in the permeation rate of the VOC at constant selectivity leads to a decrease in membrane area. In addition, a smaller membrane area implies lower investment and replacement costs.

In the removal of VOCs from water boundary layer resistances occur at the feed side of the membrane, because the VOC-flux across the liquid boundary layer can not keep up with the VOC-flux across the membrane. This is due to the high selectivity of the membrane towards the VOC, the high permeation rate of the VOC across the membrane combined with a low VOC concentration in the feed. Fig.3 shows this phenomenon schematically.

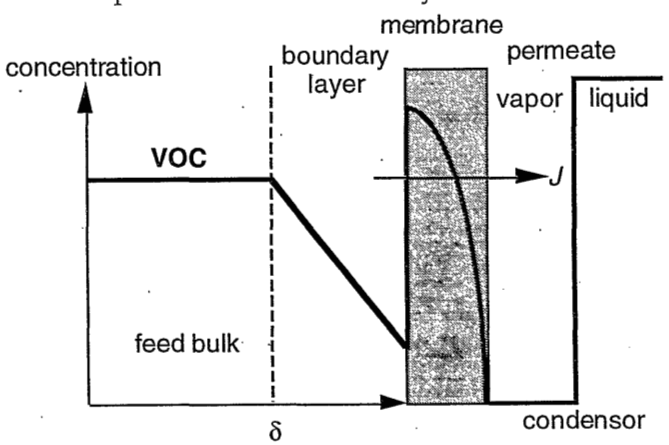

Figure 3 *Concentration profile of VOC from the bulk of the feed side to the permeate side of the membrane.*

The flux equation of component i (J_i) is preferably described by eqn (5) with the partial pressure difference (Δp_i) as the driving force and k_{ov} as the overall mass transfer coefficient,

$$J_i = k_{ov} \cdot \Delta p_i \quad . \tag{5}$$

According to the resistance-in-series model the mass transfer coefficient equals the sum of the resistances of the liquid boundary ($1/k_L$) and the membrane ($1/k_M$)

$$\frac{1}{k_{ov}} = \frac{1}{k_M} + \frac{1}{k_L} \quad . \tag{6}$$

2.4 VOC REMOVAL FROM WATER BY PERVAPORATION; state-of-the-art

For the pervaporative removal of VOCs from water high VOC fluxes and selectivities are prefered. In this paragraph, the intrinsic properties of selective homogeneous films will be reviewed. The performance of composite membranes is summarized and some specialty membranes are discussed. At last different membrane module types are considered in respect to the mass transfer coefficient in the feed.

2.4.1 Homogeneous membranes

In the late 80's most of the research was concentrated on screening polymers to find suitable membrane materials for the removal of VOCs from water. It was found that the class of elastomers and the glassy PTMSP (poly(trimethyl silyl propyne)) are very favorable to be applied. Now, PDMS (polydimethylsiloxane) is the most commonly used polymer because of its high selectivity, high permeability and its chemical stability. However, other polymers show better pervaporation properties for many separations. PEBA (polyether-block-polyamides) was found to have higher selectivities for (low) volatile aromatics [19,20]. NBR (nitrile butadiene rubber), POT (polyoctenamer) and EPDM (ethylene-propylene terpolymer) showed even higher selectivities for toluene and trichloroethylene [21] (fig.4). Table 1 shows a literature overview concerning the removal of VOCs from water by pervaporation of different materials with various membrane module types. Intrinsic membrane selectivities refer to the case in which no boundary layer effects would occur. Furthermore, the selectivities are not only resulting from the membrane but also from the evaporation step as found in distillation (i.e. for toluene in water the selectivity by evaporation is 10,000). From table 1 it is clear that for a certain component the permeabilities may be different for different researchers, which can not only be blamed to the temperature difference. These deviations are mainly explained by the error in the determination of the toluene flux and the error in the determination of the mass transfer coefficient.

Modified PDMS and zeolite filled PDMS were also investigated, however, this did not result in real improvements. For the separation of chloroform from water, the best result was obtained from a functionalized PDMS membrane with 10% functional loading[1] of octane on the Si-atoms in the PDMS-chain. The maximum water permeability decreased by a factor of 2.5, while the organic flux decreased by a factor of 1.8 [22]. The maximum separation factor found was 12,200 which is slightly higher than for pure PDMS.

[1] A CH_3-group of 10% of the Si-atoms has been exchanged for an octyl group

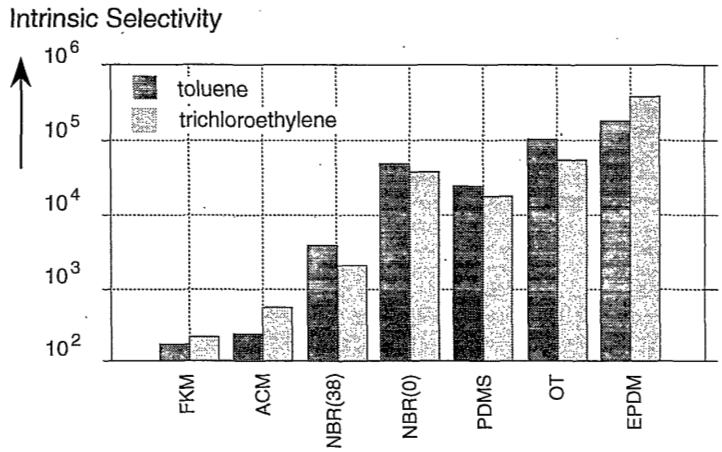

Figure 4 *Intrinsic membrane selectivity of toluene and trichloro-ethylene for elastomeric membranes [21].*

2.4.2 Composite membranes

A composite membrane consists of a thin selective toplayer on a porous support which has little resistance to the mass transport and provides the mechanical strength for the toplayer. Composite membranes combine the selective properties of a dense homogeneous film with high permeation rates.

Table 2 summarizes the most important data found in literature. Blume and Pinnau [19] patented highly selective PEBA composites in spiral wound modules. In literature MTR (Membrane Technology and Research, Inc) refers to their membranes as either "high flux and low selectivity membrane" or "low flux and high selective membrane". Borges [27] developed composite capillary membranes with the high selective POT and EPDM as the toplayers. Most of the other composite membranes described in literature are made with PDMS as the barrier material. Commonly used support materials are ultrafiltration membranes of PES (poly(ether sulfone)), PSf (polysulfone), PEI (poly(ether imide)) or PAN (polyacrylonitril).

In table 2 the composite membranes as characterized in Chapter 7 of this thesis show clearly higher VOC fluxes than the other composite membranes, which is due to the high mass transfer coefficient in the boundary layer. Also the selectivity is higher, due to the low permeability of water in EPDM and the high VOC-fluxes. No data were found for membranes made by GKSS or GFT-Carbone Lorraine. Their organophilic composite membranes were only used for the separation of aroma-compounds, alcohols or high boiling organics from water [16].

Table 1 *State-of-the-art of permeabilities and boundary layer mass transfer coefficients of homogeneous materials.*

Membrane material	Module configuration	T [°C]	Organic compound	P [m^2/s]	α [-]	k_L [m/s]	Ref.
EPDM	flat channel cell, flowrate 2 l/min	25	toluene	$1.1 \cdot 10^{-9}$	100,000*	$1.4 \cdot 10^{-5}$	[22]
	flat channel cell, flowrate 2 l/min	25	trichloroethylene	$2.8 \cdot 10^{-9}$	300,000*	$1.7 \cdot 10^{-5}$	[22]
	flat channel cell, flowrate 3 l/min	26	toluene	$8 \cdot 10^{-9}$	200,000	$2.6 \cdot 10^{-5}$	[23]
PDMS	flat channel cell, flowrate 2 l/min	25	toluene	$8.2 \cdot 10^{-9}$	30,000*	$2.5 \cdot 10^{-5}$	[22]
	flat channel cell, flowrate 2 l/min	25	trichloroethylene	$5.4 \cdot 10^{-9}$	20,000*	$2.3 \cdot 10^{-5}$	[22]
	transversal flow, Re=400	25	trichloroethylene	$2.7 \cdot 10^{-8}$	45,000	$7.0 \cdot 10^{-5}$	[24]
	inside longitudinal flow, Re = 670	25	trichloroethylene	$2.7 \cdot 10^{-8}$	13,000	$6.0 \cdot 10^{-5}$	[24]
	stirred cell	nr	toluene	$3.5 \cdot 10^{-8}$	7,000	nr	[25]
	stirred cell	nr	benzene	$7.7 \cdot 10^{-9}$	nr	nr	[25]
	stirred cell	nr	chlorobenzene	$2.2 \cdot 10^{-8}$	nr	nr	[25]
	disc cell, flowrate 1 l/min, (140μm)	30	toluene	$4.3 \cdot 10^{-8}$	2,500	$3.3 \cdot 10^{-5}$	[26]
	disc cell, flowrate 1 l/min, (140μm)	30	methylene chloride	$6.6 \cdot 10^{-9}$	1,200	$2.4 \cdot 10^{-5}$	[26]
	disc cell, flowrate 1 l/min, (140μm)	30	trichloroethane	$3.3 \cdot 10^{-8}$	2,000	$3.2 \cdot 10^{-5}$	[26]
PEBA	stirred cell, 400 rpm	25	toluene	$2.0 \cdot 10^{-9}$	nr	$1.5 \cdot 10^{-5}$	[25]
	disc cell, flowrate 1 l/min, (27μm)	30	toluene	$9.7 \cdot 10^{-10}$	500	$3.3 \cdot 10^{-5}$	[26]
	disc cell, flowrate 1 l/min, (27μm)	30	methylene chloride	$3.2 \cdot 10^{-10}$	450	$2.4 \cdot 10^{-5}$	[26]
	disc cell, flowrate 1 l/min, (27μm)	30	trichloroethane	$5.2 \cdot 10^{-10}$	300	$3.2 \cdot 10^{-5}$	[26]

nr = not reported, * = intrinsic selectivity

Table 2 *Performance of state-of-the-art composite membranes in VOC-removal from water.*

Membrane material	Module configuration	T [°C]	Organic compound	J [g/m2.h]	α_{ov} [-]	k_L [m/s]	Ref.
EPDM/PSf	Stirred cell	25	Toluene (250ppm)	25	7,000	$1 - 3 \cdot 10^{-5}$	[28]
EPDM/PEI	Longitudinal outside, Re = 5,000	25	TCE (250ppm)	60	12,000	$1.8 \cdot 10^{-5}$	[27]
	Longitudinal outside, Re = 5,000	25	DCM (1,000 ppm)	48	2,800	$1.5 \cdot 10^{-5}$	[27]
EPDM/PES	Longitudinal outside, Re = 10,000	26	Toluene (250ppm)	48	52,000	$5.7 \cdot 10^{-5}$	[29]
	Transverse flow, Re = 2400	26	Toluene (250ppm)	45	35,000	$6.7 \cdot 10^{-5}$	[29]
MTR100	Spiral wound, MTR	40	BTEX (4ppm)	1	> 200	nr	[30]
MTR200	Spiral Wound, MTR	25	1,1,2-TCEa	nr	235	nr	[31]
HDPE/BA	Flat	nr	1,1,2-TCEa (0.135 wt-%)	139	1,100	nr	[34]

EPDM = ethylene-propylene terpolymer, PSf = polysulfon, PEI = polyetherimide, PES = polyethersulfon, PDMS = polydimethylsiloxane, PEBA = polyether-block-polyamide , HDPE = high density polyethylene, BA = *n*-butylacrylate
TCE = trichloroethylene, DCM = dichloromethylene, BTEX = mixture of benzene, toluene, ethylbenzene and xylenes, TCEa = trichloroethane
nr = not reported

2.4.3 Specialty membranes

Masuoka and Ogasawa [32] separated malodorous VOCs from water with TFE-plasma treated PDMS. The selectivity for the removal of trichloroethylene (800 ppm) was 1,000 for the untreated and 3,200 for the modified membrane. However, the flux was below 1 $g/m^2.h$.

Many different chlorinated hydrocarbons were separated from water via zeolite filled PDMS [33]. They found a strong increased flux for these membranes when compared to the pure PDMS membranes.

A more sophisticated technique is plasma-graft filling polymerization. With this technique a porous membrane is filled with a high selective substance. Masuoka and Ogasawa achieved this by filling porous polypropylene with TFE-plasma, but these results were worse than their PDMS-treated films. Yamaguchi et al. [34] show good results for their porous HDPE (high density polyethylene) films filled with grafted polymer of n-butylacrylate. They found a trichloroethane flux of 139 $g/m^2.h$ and a separation factor of 1,100.

2.4.4 Membrane modules

One of the most important properties, when removing sparingly soluble VOCs from water, is the overall mass transfer capacity. This parameter equals the mass transfer coefficient of the feed side (k_L) multiplied by the packing density of the module. An improved membrane module has a higher specific mass transfer coefficient, i.e., a higher k_L and/or a higher membrane area per unit volume (packing ratio). k_L is a function of flow velocity and module geometry. k_L can be increased by either the use of a better spacers as in the case of plate-and-frame and spiral wound modules or a complete different type of module configuration such as a transverse flow system. For the pervaporative removal of VOCs from water plate-and-frame modules and spiral wound modules are commonly used on a commercial scale. Capillary membranes could also be used in three modes: inside flow, outside longitudinal flow and transverse flow. Fig.5 schematically depicts these module types.

The advantages and disadvantages of common membrane modules have been summarized [35], however, the use of transverse flow modules is not discussed.

More recently, Futselaar [36] clearly summarized the advantages of a TFM over more traditional modules for pervaporation. The mass transfer is a factor 10 higher when compared to a longitudinal flow module at a given energy input. Also in spiral wound (SWM) and plate-and-frame (PFM) modules high mass transfer coefficients can be reached with 'special' spacers acting as turbulence promoters [37]. However, the advantage of transverse flow is that the membranes act as turbulence promoters, that is, the turbulence arises at the place where it is needed, at the membrane surface. Consequently, no additional materials have to be used and the specific membrane area is higher for a TFM system than for PFM or SWM systems. Another advantage is that the permeate channel length is

much smaller than in the other type of modules resulting in a lower pressure drop at the permeate side. Futselaar et al. [38] did an extensive cost analysis for the treatment of a VOC containing waste water. They found that the treatment costs with a TFM are the lowest. The second lowest process costs was obtained by the SWM. The transverse flow module is still at an embryonic state. Patents and papers on pilot-plant scale applications for TFMs were published by Futselaar [39], Côté et al. [40], ter Meulen [41], Prasad et al. [42] and Bessarabov et al. [43].

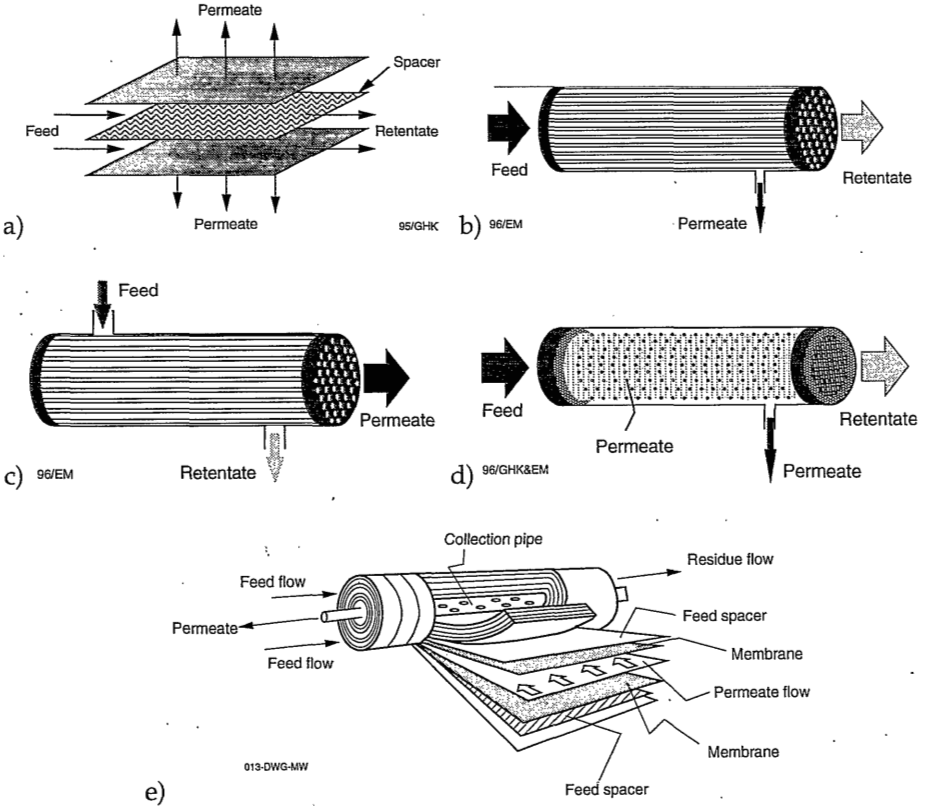

Figure 5 *Schematic drawing showing different membrane modules: a) plate-and-frame, b) inside and c) outside longitudinal flow, d) transverse flow and e) spiral wound module.*

On the other hand, spiral wound modules of MTR are state-of-the-art and successfully used for pervaporation under the tradename Pervap®. Their development proceed steady and in the last 10 years, many patents, publications and papers on the pervaporative removal of VOCs from water with SWMs have been published.

2.5 TREATMENT COSTS

The costs of removal of VOCs from groundwater or wastewater by pervaporation

have been estimated by a number of researchers [12,10,24,37,44]. Nijhuis [10], Lipski and Côté [12] and Hickey et al. [37] compared their pervaporation results with conventional VOC removing processes like active carbon adsorption (ACA), air stripping (AS) and biofiltration (BF). They concluded that, at the concentrations considered, only air stripping is cheaper if no additional air cleaning treatment is added which, however, is not allowed for environmental reasons. For low concentrations (below 10 ppm) ACA is the cheapest technique as for these low concentrations a membrane process can not compete anymore economically with the extreme high active surface area of carbon. At low concentrations the carbon does not have to be regenerated or disposed as often as for high concentrations. Nijhuis concluded that for the removal of VOCs a hybrid operation forms a cost effective alternative for conventional methods. First pervaporation should be used to remove the major part of the VOC and then via ACA a total removal of 99.9% is feasible. For environmentally acceptable processes the treatment costs for the removal of VOCs from water with conventional techniques is higher than \$1 /m^3 and pervaporation has to compete with this.

In the following, costs analysis results for the removal of VOCs from water with pervaporation for specific cases as found in literature are discussed (summarized in table 3). The resulting values of the treatment costs per cubic meter feed are based on membrane performance in pilot-plants. Furthermore, the values depend strongly on several boundary conditions:

1) price of energy,
2) price and life time of membrane and membrane module,
3) influent concentration and recovery of VOC,
4) amount of treated water,
5) mass transfer coefficient of VOC and water.

Therefore, only the values within a certain paper for a specific case may be compared as then most factors are similar.

Kaschemekat et al. [12] studied the performance of their pilot-plant containing a spiral wound module. The feed stream was 2,250 m^3/h containing VOCs (such as chloroform, 1,1,2-trichloroethane, benzene, toluene and naphthas). Enrichment factors of over 200 were obtained. They estimated a total costs to remove benzene from an aqueous feed stream. When the same separation was carried out with composite membranes with higher fluxes but lower selectivities, then the treatment costs increase 10%.

Nijhuis et al. [10] estimated the treatment costs by pervaporation with a SWM for two specific cases (table 3). The relatively small pervaporation unit may be very interesting compared to the other conventional techniques. However, they used in their calculations high selective EPDM composite membranes, which are not yet commercially available. The reason for this choice were the enormous decrease in operation costs (25 %) due to lower condensation costs since the water flux is much lower in the case of composites with an EPDM compared to PDMS as the toplayer material.

Table 3 *Comparison of treatment costs for a VOC containing waste stream*

Contaminant	concentration [ppm]	influent flow [m^3/h]	recovery [%]	selectivity [-]	costs [$/m^3$ feed]	ref.
benzene	1,300	2,250	90	~210	2.40	[12]
benzene	1,300	2,250	90	~830	2.20	[12]
ClHC	10	10	99	45,000	0.65	[10]
hydrocarbons	500	500	99	65,000	0.50	[10]
toluene	500	16	90	500	0.85	[44]
TCEa	500	16	90	450	0.70	[44]
methylene chloride	100	10	90		0.75	[37]
TCE	10	10	99	1,100	0.56*	[24]

ClHC = chlorinated hydrocarbons, TCEa = 1,1,1-trichloro-ethane, TCE = trichloro-ethylene
* transverse flow module

Both Nijhuis and Côté and Lipski did not incorporate the effect of higher permeate pressure into their calculations. Nijhuis stated that this would have a drastic negative effect due to a higher membrane area necessary to remove the same amount of VOC and, hence, higher investment costs. Later, researchers showed the positive effect of increasing the permeate pressure in case of boundary layer limited VOC fluxes [45]. A higher permeate pressure leads to a lower driving force for both the water and the VOC. The water flux will follow eqn (1) and decreases linearly with the pressure difference decrease. However, the VOC flux will decrease relatively less with a decreased pressure difference. This is due to the resistance in the boundary layer; as a result of the lower driving force the flux is lower and the flux through the boundary layer can keep up easier with the lower transmembrane flux. As a consequence the concentration of the organic component at the membrane wall is a little higher. This change in the partial pressure difference may be considered as an effective operation variable. Wijmans and Kamaruddin patented this phenomenon [45].

Ji et al. [44] studied the removal of toluene and 1,1,1-trichloroethane (TCEa) from an aqueous feed flowing through PDMS fibers (IFM). They did extensive work on optimizing the costs and their results are summarized in table 3. If the removal condition is increased from 90 to 99 wt-% then the treatment costs increase by a factor of 1.5, which is similar to that reported by Nijhuis [10]. The condensation costs drops from $42k /yr to $5.6k /yr when the membrane thickness increases from 5 to 55 μm, respectively. These lower costs were mainly due to the 10 times smaller water flux and only to a minor extend to the decrease in VOC flux due to the liquid boundary layer. To overcome the lower VOC flux more membrane area is needed and as a result higher investment costs. An optimal thickness of 25 μm was calculated. Furthermore, they showed that the

treatment costs increase drastically for Reynolds numbers higher than 1000.

Lipski and Côté [24] did their calculations with the boundaries as summarized in table 3. They used PDMS membranes with a thickness of 2 - 150 µm, Reynolds numbers between 100 - 5000 and the membrane module concept as the variables in their calculations. Three different types of modules were compared; an inside flow module (IFM) with both narrow bore fibers and wide bore fibers, a transverse flow module (TFM) and a spiral wound module (SWM). Table 4 shows the cheapest treatment costs for each of the module concepts.

Table 4 *Treatment costs for a TCE containing waste stream [24].*

Module	IFM (narrow)	IFM (wide)	TFM	SWM
PDMS thickness [µm]	75	10	30	30
Reynolds number	500	4000	250	700
Treatment costs [$/m^3]	3.80	1.41	0.56	1.10

IFM = internal flow, TFM = transverse flow, SWM = spiral wound

In their experiments they proved the superior properties of the transverse flow module compared to both the inside and the outside longitudinal flow module, even for thick membranes (160 µm).

It may be concluded that according to many costs evaluations from different researchers the pervaporative removal of VOCs is economically feasible for feed concentrations above 10 ppm up to 10.000 ppm. Moreover, other major advantages of pervaporation are the simple recovery of the VOCs and the small space requirement when compared to conventional techniques [10].

REFERENCES

[1] Kober, P.A., *Pervaporation, perstillation and percristallization*, J.Am.Chem.Soc., 39 (1917) 944-948.

[2] Binning, R.C., R.J.Lee, J.F.Jennings, E.C.Martin, *Separation of liquid mixtures by permeation*, Ind.&Eng.Chem., 53 (1961) 45.

[3] Slater, C.S., P.J. Hickey, *Pervaporation R&D: A chronological and geographic perspective*, Proc. 4th Int. Conf. on Perv. Procs. in the Chem. Ind.; Ft. Lauderdale (USA), Bakish Materials Corp., Englewood, USA, 1989, 476-492.

[4] Néel, J., *Current trends in pervaporation*, in: Drioli, E., A.C.Habert (eds), *Workshop CEE-Brazil on membrane separation process*, Rio de Janeiro, 1992, 182-198.

[5] Dirkse, R.J.A., *Strippen verontreinigd grondwater*, PT-Procestechniek 42 (1987) 4-10.

[6] Byers, W.D., *Control of emissions from an air stripper treating contaminated groundwater*, Environ.Progr. 7 (1988) 17-21.

[7] Meuleman, E.E.B., Chapter 1 of this thesis, 1997

[8] Mulder, M.H.V., *The use of membrane processes in environmental problems. An introduction*, in: Crespo, J.G., K.W.Böddeker (eds), *Membrane processes in separation and purification*, NATO ASI Series, Series E: Applied Sciences Vol 272, Kluwer academic publishers, Dordrecht (NL), 1994.

[9] Psaume, R., Ph.Aptel, Y.Aurelle, J.C.Mora, J.L.Bersillon, *Pervaporation: importance of concentration polarization in the extraction of trace organics from water*, J.Membr.Sci., 36 (1988) 373-

384.

[10] Nijhuis, H.H., *Removal of trace organics from water by pervaporation (a technical and economic analysis)*, PhD-Thesis, University of Twente, Enschede (NL), 1990.

[11] Côté, P., C. Lipski, *Mass transfer limitations in pervaporation for water and waste water treatment*, Proc. 3rd Int. Conf. on Perv. Procs. in the Chem. Ind.; Nancy (France), Bakish Materials Corp., Englewood (USA), 1988, 449.

[12] Kaschemekat, J., J.G.Wijmans, R.W.Baker, *Removal of organic solvent contaminants from industrial effluent streams by pervaporation*, Proc. 4th Int. Conf. on Perv. Procs. in the Chem. Ind.; Ft. Lauderdale (USA), Bakish Materials Corp., Englewood (USA), 1989, 321-343.

[13] Blume, I., J.G.Wijmans, R.W.Baker, *The separation of dissolved organics from water by pervaporation*, J.Membr.Sci., 49 (1990) 253.

[14] Garcia, M.E.F., A.C.Habert, R.Nobrega, L.A.Pires, *Use of PDMS and EVA membranes to remove ethanol during fermentation*, Proc. 5th Int. Conf. on Perv. Procs. in the Chem. Ind., Heidelberg (Germany), Bakish Materials Corp., Englewood (USA), 1991, 319-330.

[15] Bengtson, G., K.W.Böddeker, H.P.Hansen, I.Urbasch, *Recovery of 6-pentyl-α-pyrone from Trichoderma viride culture medium by pervaporation*, Biotechnol.Tech., 6 (1992) 23-36.

[16] Karlsson, H.O.E., G.Trägårdh, *Pervaporation of dilute organic-waters mixtures. A literature review on modeling studies and applications to aroma compound recovery*, J.Membr.Sci., 76 (1993) 121-146.

[17] Burger, B.V., W.J.G.Burger, I.Burger, *Trace determination of volatile organic compounds in water using permeation through a hollow fiber membrane and carrier gas stripping*, Journal of high resolution chromatography, 19 (1996) 571.

[18] Néel, J., *Pervaporation*, in: Noble, R.D., S.A.Stern, *Membrane separations technology, principles and applications*, Elsevier Science B.V., Amsterdam (NL), 1995.

[19] Blume, I., I.Pinnau, *Composite membrane, method of preparation and use*, USP 4,963,165 (1990).

[20] Böddeker, K.W., G.Bengtson, E.Bode, *Pervaporation of low volatility aromatics from water*, J.Membr.Sci., 53 (1990) 143-158.

[21] Nijhuis, H.H., M.H.V.Mulder, C.A.Smolders, *Selection of elastomeric membranes for the removal of volatile organics from water*, J.Appl.Polym.Sci., 47 (1993) 2227-2243.

[22] Bennett, M., B.J.Brisdon, R.England, R.W.Field, *Organophilic pervaporation using modified polysiloxane membranes*, in: Bowen, W.R., R.W.Field, J.A.Howell (eds), Proceedings of Euromembrane '95, Bath, Anthony Rowe Ltd, Chippenham (UK), 1995, I-323.

[23] Meuleman, E.E.B., J.H.A.Willemsen, M.H.V.Mulder, H.Strathmann, *EPDM as a barrier material for pervaporation*, Chapter 3 of this thesis, 1997.

[24] Lipski, C., P. Côté, *The use of pervaporation for the removal of organic contaminants from water*, Environmental Progress, 9 (1990) 254-261.

[25] Raghunath, B., S.-T.Hwang, *Effect of boundary layer mass transfer resistance in the pervaporation of dilute organics*, J.Membr.Sci., 65 (1992) 147-161.

[26] Ji, W., S.K.Sikdar, S.-T.Hwang, *Modeling of multicomponent pervaporation for removal of volatile organic compounds from water*, J.Membr.Sci., 93 (1994) 1-19.

[27] Borges, C.P., *Fibras ocas compostas para a remoçao de poluentes orgânicos de soluções aquosas pelo processo de pervaporação*, PhD-thesis, COPPE/UFRJ, Rio de Janeiro, 1993.
Borges, C.P., M.H.V.Mulder, C.A.Smolders, *Composite hollow fiber for removal of VOCs from water by pervaporation*, in: Bakish, R., (ed.), Proc.6th Int.Conf.Perv.Procs.Chem.Ind.; Ottawa (CND), Bakish Materials Corp., Englewood (USA), 1992, 207-222.

[28] Perreira, C.C., *Transferencia de massa na remoção de contaminates orgânicos da agua por pervaporação*, M.Sc.-Thesis, COPPE/UFRJ, Rio de Janiero (BRA), 1995.

[29] Meuleman, E.E.B., C.P.Plug, K.Bouma, M.H.V.Mulder, H.Strathmann, *Pervaporation via composite membranes: longitudinal and transverse flow modules*, Chapter 7 of this thesis, 1997g.

[30] Wijmans, J.G., R.W.Baker, A.L.Athayde, *Pervaporation: Removal of organics from water and organic/organic saparations*, in: Crespo, J.G., K.W.Böddeker (eds), *Membrane processes in separation and purification*, NATO ASI Series, Series E: Applied Sciences Vol 272, Kluwer academic

publishers, Dordrecht (NL), 1994.

[31] Blume, I., R.W.Baker, *Process for recovering organic components from liquid streams*, USP 5,030,356 (1991).

[32] Masuoka, T., K.Ogasawara, *Pervaporation system for in situ removal of volatile organic contaminations (VOCs) from water*, in: Bowen, W.R., R.W.Field, J.A.Howell (eds), Proceedings of Euromembane '95, Bath (UK), Antony Rowe Ltd., Chippenham, UK, 1995, II-228.

[33] Dotremont, C., S.Goethaert, C.Vandecasteele, *Pervaporation behaviour of chlorinated hydrocarbons through organophilic membranes*, Desalination, 91 (1993) 177-186.

[34] Yamaguchi, T., S.Yamahara, S.-I.Nakao, S.Kimura, *Preparation of pervaporation membranes for removal of dissolved organics from water by plasma-graft filling polymerization*, J.Membr.Sci., 95 (1994) 39-49.

[35] Scott, K., *Handbook of industrial membranes*, Elsevier Advanced Technology, 1995.

[36] Futselaar, H., *The transverse flow membrane module: application to pervaporation of volatile organic compounds*, in: Bowen, W.R., R.W.Field, J.A.Howell (eds), Proceedings of Euromembane '95, Bath (UK), Antony Rowe Ltd., Chippenham, UK, 1995, II-106.

[37] Hickey, P.J., C.H.Gooding, *The economic optimization of spiral wound membrane modules for the pervaporative removal of VOCs from water*, J.Membr.Sci., 97 (1994) 53-70.

[38] Futselaar, H., C.P.Borges, A.C.Habert, R.Nobrega, *Removal of volatile organic contaminants from ground and waste waters by pervaporation*, Final report of COPPE/UFRJ, CT-92-0081, Rio de Janeiro (BRA), 1996.

[39] Futselaar, H., I.G.Rácz, *Counter-current flow membrane module for liquid separations*, EP 0,464,945 A1 (1990).

[40] Côté, P.L., R.P.Maurion, C.J.Lipski, *Frameless array of hollow fiber membranes and module containing a stack of arrays*, USP 5104535, 1992.

[41] Meulen, ter, B.Ph., *Transfer device for the transfer of matter and/or heat from one medium flow to another medium flow*, WO 91/09668 (1991).

[42] Prasad, R., C.J.Runkle, *An improved hollow fiber module for mass transfer operations*, Proceedings of the NAMS, 6th, Breckenridge, Colorado (USA), 1994.

[43] Bessarabov, D.G., A.V.Vorobiev, E.P.Jacobs, R.D.Sanderon, S.F.Timashev, *Separation of olefin/paraffin gaseous mixtures by means of facilitated-transport membranes based on metal-containing perfluorinated carbon-chain copolymers*, in: Bowen, W.R., R.W.Field, J.A.Howell (eds), Proceedings of Euromembrane '95, Bath, Anthony Rowe Ltd, Chippenham (UK), 1995, II-186.

[44] Ji, W., A.Hilaly, S.K.Sikdar, S.-T.Hwang, *Optimization of multicomponent pervaporation for removal of volatile organic compounds from water*, J.Membr.Sci., 97 (1994b) 109-25.

[45] Wijmans, J.G., Kamaruddin, H.D., *Pervaporation process with reduced driving force*, WO 95/32,051 (1995).

3

EPDM

AS A BARRIER MATERIAL FOR PERVAPORATION

SUMMARY

Several ethylene-propylene-diene terpolymers (EPDM) and crosslinking procedures have been investigated using pervaporation, vapor sorption, liquid sorption and gas permeation experiments. The EPDM parameters that have been changed are ethylene content, molecular weight, choice of third monomer and type of branching. Various crosslinking procedures were carried out.

The permeability coefficients were determined from pervaporation experiments and were about 40,000 Barrer for toluene and 700 Barrer for water. From vapor sorption measurements a value of 22,000 Barrer for toluene was obtained which is similar to the value obtained from pervaporation experiments. This indicates that, indeed, the presence of water does not influence the toluene flow during pervaporation. Gas permeation experiments resulted in permeabilities for CO_2, O_2 and N_2 of 120, 24 and 11 Barrer, respectively.

No clear differences were found for both EPDM-variation and different crosslinking procedures.

3.1 SHORT INTRODUCTION TO EPDM

EPDM (ethylene-propylene-diene terpolymer) is a very commonly used elastomer in the rubber industry. Major applications are found in the car and building industry and appliances [1]. EPDM is a bulk polymer and is often chosen over other elastomers because of its ozone-resistancy and relatively good thermal stability. The chemical structure is shown in fig.1. The diene amount is about 1 mole procent and it is either ENB (5-ethylidene-2-norbornene) or DCPD (dicyclopentadiene). Many different types of EPDM are available with different properties. The ethylene amount ranges between 45 (amorphous types) to 55-60 wt-% (semi-crystalline types) and 70 wt-% (crystalline types). For EPDMs with an ethylene-percentage below 50 wt-% the crystalline fraction is zero, but, it can increase to 20% for EPDMs containing 80 wt-% ethylene [1]. Also the sequence length of an ethylene part may vary and the molecular weight (M_n) ranges from 30,000 to 150,000 g/mole. Apart from these intrinsic property-variations, properties can be altered by crosslinking or by the addition of fillers. Sulfur-vulcanisation is the most common crosslinking process. However, recently, an increasing interest for peroxide crosslinking was observed [2].

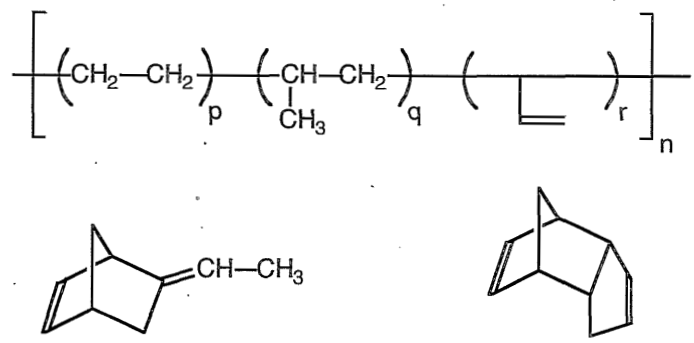

Figure 1 *Chemical formula of EPDM, ENB and DCPD, respectively.*

Nijhuis [3] investigated many elastomers for the removal of VOCs from water. EPDM showed the highest separation factor due to a low water permeability and a reasonable organic permeability.

In this paper the structure-performance relationship will be discussed of EPDM in relation to VOC removal.
Various EPDMs have been investigated and crystallinity, molecular weight, free volume and polarity are believed to be important parameters that affect the permeability.

The pervaporation properties of various EPDMs will be discussed. Furthermore, the sorption and diffusion behaviour of water and toluene in different EPDMs will be related to intrinsic pervaporation properties using the sorption-diffusion

model. Also, gas permeation experiments have been carried out to determine the intrinsic gas permeability coefficients which may give information as well on structural differences.

3.2 CHARACTERIZATION METHODS

3.2.1 Pervaporation

The performance of a pervaporation process may be described by the flux through the membrane and the separation factor. In the removal of volatile organic compounds (VOCs) from water, liquid boundary layer resistances to mass transfer occur at the feed side of the membrane [4]. The permeation of molecules from the bulk feed to the permeate side occurs in five consecutive steps:

- diffusion from the well mixed feed bulk through the laminar boundary layer to the membrane surface,
- selective sorption of molecules into the membrane at the feedside,
- selective diffusion through the membrane,
- desorption into a vapor phase at the permeate side,
- diffusion from the membrane surface to the permeate bulk.

The last step is usually neclected since mass transfer in the vapor phase is much higher than in the liquid phase. The flux equation of component i (J_i) may be described by eqn (1)

$$J_i = k'_{ov,i} \cdot \left(p_{f,i} - p_{p,i}\right) \quad , \tag{1}$$

where $k'_{ov,\,i}$ is the overal mass transfer coefficient [mol/m^2.s.Pa], which is also referred to as the pressure-normalized permeation flux [5]. The driving force is the partial pressure difference between feed ($p_{f,i}$) and permeate ($p_{p,i}$), respectively. Often, typically under lab-conditions, the permeate pressure can be taken zero, since the permeate flow is low due to a small membrane surface and liquid nitrogen is used as condensing medium. The partial pressure of component in the feed can be linked to the concentration. At thermodynamic equilibrium, the activity of each component in liquid and vapor phase are equal:

$$a_i = \gamma_i \cdot x_{f,i} = \frac{p_{f,i}}{p_i^o} \quad , \tag{2}$$

where $x_{f,i}$ is the mole fraction and γ is the activity coefficient. Combination of eqns (1) and (2) and assuming $p_{p,i} \to 0$ gives

$$J_i = k'_{ov,i} \cdot \gamma_i \cdot x_{f,i} \cdot p_i^o \ . \tag{3}$$

According to the resistance-in-series model the overall mass transfer coefficient equals the sum of the resistances of the liquid boundary layer ($1/k_L$ [s/m]) and the membrane phase ($1/k_M$ [s/m][1]), assuming that the resistance in the permeate phase is neglected [6]

$$\frac{1}{k_{ov,i}} = \frac{1}{k_{M,i}} + \frac{1}{k_{L,i}} \quad . \tag{4}$$

The transport process of component i through a dense membrane is commonly given by

$$J_i = \frac{P_i}{l} \cdot p_{f,i} \quad , \tag{5}$$

where P_i is the permeability of i and l the thickness of the selective top layer. With the conversion factor[2] $\gamma_i \cdot p^\circ_i / \rho_f$ for k_L to correct for the dimensions, where ρ_f is the molar density of the feed, eqn (4) becomes

$$\frac{1}{k'_{ov,i}} = \frac{l}{P_i} + \frac{\gamma_i \cdot p^o_i}{\rho_f \cdot k_{L,i}} \quad . \tag{6}$$

Eqns (3) through (6) lead to the following flux equation of component i permeating from the feed bulk into the permeate side

$$J_i = \left(\frac{l}{P_i} + \frac{\gamma_i \cdot p^o_i}{\rho_f \cdot k_{L,i}} \right)^{-1} \cdot \gamma_i \cdot x_{f,i} \cdot p^o_i \quad . \tag{7}$$

Introducing the Henry's law coefficient (H_i) of the VOC in an aqueous solution in molar density and pressure dimension, according to

$$H_i = \frac{\gamma_i \cdot p^o_i}{\rho_f} \quad , \tag{8}$$

leads to a more convenient description of the boundary layer resistance [5]

---

1 The resistances-in-series model for pervaporation is can be described with a concentration difference as the driving force and k is in [m/s]. The analogon with the partial pressure difference as the driving force results in a k' in [mol/m^2.s.Pa].

2 Commonly it is preferred to describe k in [m/s] and P is described in [Barrer]. Therefore, these units will be used when discussing these quantities. However, for calculations and in the equations the following units are preferably used: P in [mol.m/(m^2.s.Pa)], p in [Pa], ρ_f in [mol/m^3], x in [mol/mol] and J in [mol/(m^2.s)].

$$J_i = \left(\frac{l}{P_i} + \frac{H_i}{k_{L,i}} \right)^{-1} \cdot H_i \cdot \rho_f \cdot x_{f,i} \quad . \tag{9}$$

The separation performance is generally expressed by the separation factor (α) which is defined as

$$\alpha_{i,j} = \frac{y_i / y_j}{x_i / x_j} \quad , \tag{10}$$

where y is the concentration in the permeate of component i and j, respectively and x is the concentration in the feed. α can also be described by ratio of fluxes divided by the ratio of the feed concentration:

$$\alpha = \frac{J_{tol} / J_w}{x_{tol} / x_w} \quad . \tag{11}$$

When boundary layer resistances exist, α represents the overall separation factor and not just the membrane separation factor.

3.2.2 Permeability coefficient via vapor sorption experiments

The permeability coefficient (P_i) of a specific component in a particular polymer depends on the diffusivity and the solubility. From eqn (5) P_i can be given as

$$P_i = \frac{J_i \cdot l}{p_i} \tag{12}$$

P_i can be determined by a pervaporation experiment. Eqn (12) is derived from Fick's law and the permeability coefficient represents:

$$P_i = \frac{1}{p_i} \cdot \int_0^{c_m} D_i(c) \cdot \mathrm{d}\, c \quad , \tag{13}$$

where D_i is Fick's diffusion coefficient, c is the concentration of component i in the membrane at a certain place, c_m is the concentration in the membrane at the feed side, while the concentration at the permeate side is assumed to be zero and p_i the vapor pressure of component i in the feed. If the diffusion coefficient is independent of the concentration and if Henry's law applies, eqn (13) simplifies to the well known solution-diffusion equation:

$$P_i = \frac{c_m}{p_i} \cdot D_i = S_i \cdot D_i \quad , \tag{14}$$

where S_i is the solubility coefficient.

To solve eqn (13) the diffusion coefficient has to determined as a function of the concentration of sorbed permeant. With vapor-sorption experiments both the concentration of the sorbed permeant and the diffusion coefficient can be determined as a function of the activity of the permeant vapor. An emperical relationship for $D_i(c)$ can be obtained and eqn (13) can be solved. When comparing the P_i from vapor sorption with the P_i from pervaporation for a single component i, p_i and c_m equal the corresponding values as found in the pervaporation experiments. Then, p_i is the vapor pressure of component i in the feed at the membrane surface (indicated by $p_{m,i}$), which can be calculated via the resistances-in-series and the film theory model. At steady-state conditions the flux through the boundary layer equals the flux through the membrane and equals the total flux. Eqn (15) describes the flux through the stagnant boundary layer,

$$J_i = \frac{k_{L,i}}{H_i}\left(p_{f,i} - p_{m,i}\right) \quad , \tag{15}$$

where $p_{m,i}$ is the partial pressure of the feed adjacent to the membrane. In pervaporation it is assumed that the activity of component i in the membrane at the feed side is in thermodynamic equilibrium with the feed activity at the membrane surface. And $c_{m,i}$ can be calculated from a sorption isotherm in which the partial vapor pressure equals $p_{m,i}$.

*a. **Diffusion coefficient***

The penetration theory is used to calculate the diffusion coefficient from the sorption experiments. It is assumed that the film has an infinite thickness. It is assumed that thermodynamic equilibrium exists at the membrane interfaces [7]. Now the mass uptake (m_t) per time (t) is described by eqn (16) [8]

$$m_t = 2\,A\,(C_W - \bar{C})\sqrt{\frac{D\,t}{\pi}} \quad , \tag{16}$$

where A is the surface area, C_W is the concentration of the vapor at the wall and $\bar{C}$ the initial concentration in the film. The final weight increase at a certain vapor concentration is m_∞ and is described by

$$m_\infty = (C_W - \bar{C})\cdot V_f \quad , \tag{17}$$

where V_f is the volume of the film. Combining eqns (16) and (17) gives the relation for the relative sorption at time t

$$\frac{m_t}{m_\infty} = \frac{2\,A}{V_f}\sqrt{\frac{D\,t}{\pi}} \quad . \tag{18}$$

When the relative weight increase is plotted versus $\sqrt{t}$ then initially a constant

increase is observed whereafter the uptake flattens off to a maximum where m_t is m_∞. D can be calculated from the initial slope of that plot.

b. Sorption coefficient

The sorption coefficient at a certain vapor pressure can be calculated with eqn (19)

$$S_i = \frac{V_i\,(\mathrm{STP})}{V_{EPDM}} \cdot \frac{1}{p_i} \quad , \tag{19}$$

where V_i(STP) is the volume of the sorbed penetrant at STP-conditions, V_{EPDM} is the volume of the dry EPDM and p_i is the partial pressure of the penetrant.

3.2.3 Liquid sorption

Liquid sorption is a common technique to investigate the effect of crosslinking. The crosslink density can be determined from the Flory-Rehner eqn (20) [9], in which the molecular weight between two crosslinks (M_c) is a measure for the crosslink density,

$$\ln a_i = \ln \phi_i + \phi_2 + \chi_{i2} \cdot \phi_2^2 + \frac{V_i \cdot \rho_2}{M_c}\left(1 - 2\frac{M_c}{M_w}\right) \cdot \left(\phi_2^{0.33} - \frac{\phi_2}{2}\right) \quad . \tag{20}$$

The subscripts i and 2 refer to the penetrating molecule and the polymer, respectively, ϕ the volume fraction, χ is the interaction parameter between penetrant and polymer, V the molar volume, ρ the density of the crosslinked polymer and M_w the average molecular weight before crosslinking.

3.2.4 Gas permeation

Gas permeation experiments were carried out to determine the permeability coefficient of CO_2, O_2 and N_2 in EPDM. Structural changes such as crystallinity and crosslink density may then be related to difference in the permeability coefficient. P_i can be obtained from eqn (5). In gas permeation, the ideal selectivity (α_{id}) is given by eqn (21)

$$\alpha_{id,\,i/j} = \frac{P_i}{P_j} \quad , \tag{21}$$

where subscripts i and j refer to the components of the binary gas mixture.

3.3 METHODS AND MATERIALS

3.3.1 Materials

a. Chemicals

Various ethylene-propylene-diene terpolymer were very kindly supplied by

DSM-elastomers. n-Hexane, toluene and ethanol were purchased from *Merck*. The water was ultrafiltrated and demineralized (UF-demi). The crosslink initiator dicumyl peroxide (DCP 98%) was purchased from *Aldrich* and used without further purification. Helium, air, hydrogen, carbon dioxide, oxygen and nitrogen were purchased from *Hoekloos*.

b. Preparation of membrane films

EPDM was cut into little pieces and a 10 wt-% solution in n-hexane was prepared containing 5 phr[3] DCP. The polymer solution was filtered through a 40 μm filter and then casted with a thickness of 1 mm upon a Teflon plate. The hexane was allowed to evaporate during the night in a nitrogen atmosphere. Finally, crosslinking occured for 1 hour in an oven at 150° C in a nitrogen atmosphere. The resulting films had a thickness of about 120 μm as measured with a digital thickness meter (*Mitutoya*).

Some films were prepared and crosslinked in a press at 10 MPa. Both 5 phr DCP (1 hour, 150° C) and a sulfur blend (20 minutes, 160° C) were used as crosslink initiators. The sulfur blend consisted of: 1.5 phr sulfur, 5 phr zinkoxide, 1 phr stearic acid, 0.5 phr 2-mercaptobenzothiazole and 1.5 phr tetramethyl-thiuramdisulfide.

3.3.2 Pervaporation

A schematic drawing of the pervaporation set-up is given in fig.2. The cell contains an EPDM-film with an effective membrane surface area 47.8 cm^2. As feed mixture a solution of about 250 ppm toluene in UF-demi-water is used.

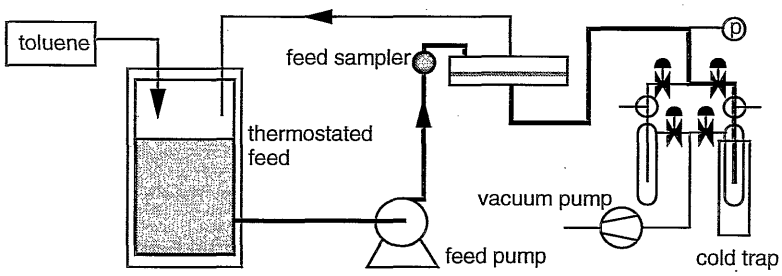

Figure 2 *Flow sheet of the pervaporation test set-up. The fat black line indicates the major toluene flow.*

A feed pump (*Iwaki*, Magnet Pump) establishes a constant flow over the membrane of 3.0 l/min. The feed temperature is kept constant at 26° C. At the permeate side a vacuum (< 1 mbar) is applied by an *Edwards* two stage high vacuum pump and measured with an *Edwards* absolute pressure pirani (PRM 10) and pressure indicator (Controller 1101). The permeate is condensed in a cold trap filled with liquid nitrogen (-196° C). The permeate could be collected alternately by one of two parallel cold traps. After a certain period of time an

[3] phr = gram per hundred gram of rubber.

experiment was taken by allowing nitrogen gas to enter the cold trap, which was closed with teflon sealed cups. Then a fixed amount of ethanol was added and a homogeneous system was obtained. The liquid permeate and feed compositions are determined by gas chromatography (*Varian* 3400, column: Hayesep Q) with a thermoconductivity detector and a flame ionization detector, respectively. Without decompressing the trap (no toluene loss) a sample of this homogeneous liquid mixture was analysed by GC. The permeate weight was calculated via a calibration curve knowing the exact amount of ethanol added. An additional advantage of adding ethanol to the frozen permeate is that the partial vapor pressure of toluene is much lower now.

Another problem is the exact determination of the amount of water permeating through the membrane. During the pervaporation experiment a small inevitable leakage of air introduces a certain amount of water vapor which is condensed in the trap as well. Also as a result of airation some water is introduced. This amount is very small but it is not negligible due to the very low water fluxes of EPDM films. To correct for this extra water, experiments have been carried out with an impermeable thick film (polyethylene of 2 mm) instead of the EPDM membrane. The amount of water collected in the cold trap has been determined against time. A linear relation was found between the amount of water and the time of the measurement, that is, the slope represents the water flux due to leakage and the extrapolated value to t=0 represents the water which condenses due to airation at the end of a measurement.

3.3.3 Vapor sorption

Vapor sorption experiments have been performed with the set-up as depicted schematically in fig.3. It contains a thermographic analysis microbalans (*Perkin-Elmer* TGS-2), a bubble-column and a vapor-gas ratio-flow tuner (*Brooks* 5898). A small piece of an EPDM-film (5 - 10 mg) is cut from the film. The thickness is determined with a digital thickness meter. Before the experiment the EPDM-film is degassed for at least two nights in a vacuum oven at 30° C. The weight increase was monitored when the activity of the toluene vapor was increased from 0 to 0.9 with steps of 0.1.

3.3.4 Liquid sorption

EPDM K578 was crosslinked in an oven in a nitrogen atmosphere and under a press at 10 MPa at a temperature of 150° C for 1 hour and with different concentrations of dicumylperoxide (DCP). A part of the crosslinked polymer (K578) is weighed and immersed in pure toluene. The weight increase of the polymer film was monitored for one week and equilibrium was reached after 4 days. The volume fraction ϕ_{tol} and ϕ_{EPDM} can be calculated from weighing the sample before and after the sorption. The interaction parameter $\chi_{tol,EPDM}$ was taken from literature. Boom [10] and Dudek [11] gave constant values for $\chi_{tol,EPDM}$ ranging from 0.45 to 0.51. But concentration dependent values are also found; $\chi_{tol,EPDM} = 0.42 + 0.2 \cdot \phi_{EPDM}$, [1]. Variation of this value had only a minor effect

on the value of the molecular weight between two crosslinks M_c. The film density ρ was determined by weighing films in ethanol and air. With Archimedes' law the density can be calculated. M_n was determined by GPC-meaurements and is about 48 kg/mol.

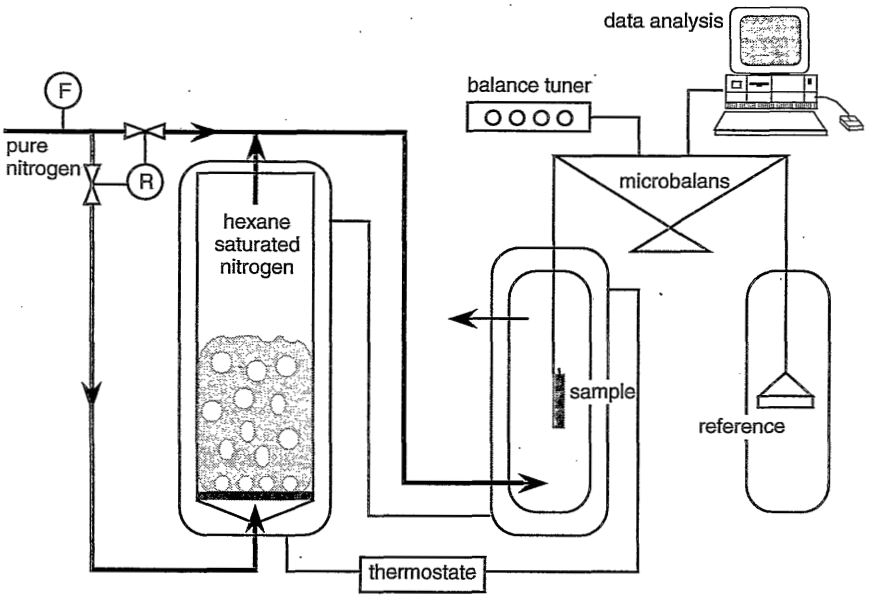

Figure 3 *Schematic drawing illustating the vapor sorption set-up. R and F indicate ratio and flow indicators, respectively.*

3.3.5 Gas permeation

The gas permeation set-up has been depicted schematically in fig.4. EPDM films were mounted into a flat cell. At the feed side an absolute pressure of 3.5 bar (p_f) was applied. At the permeate side a vacuum of less than 0.01 mbar was applied by means of an high vacuum pump (*Edwards*). The doubled wall membrane cell allows to adjust the temperature at 30° C and it has an effective area of 11.9 cm^2. At a certain time the valve to the vacuum pump was closed and the increase in pressure (Δp_p) is measured in a calibrated volume (V_c) as a function of time (Δt). Using the ideal gas law one can calculate the pressure normalized permeation rate (cm^3 (STP)/cm^2.s.cmHg).

$$\frac{P}{l} = \frac{\Delta p_p}{\Delta t\,(p_f - p_p)} \frac{V_{cp}}{R\,T\,A} V_m \quad , \tag{22}$$

where V_m is the molar volume, R the gas constant, T the temperature and A the membrane area. The set-up has been automized and an ALPPS (automatic low pressure permeation set-up) controls the measurement.

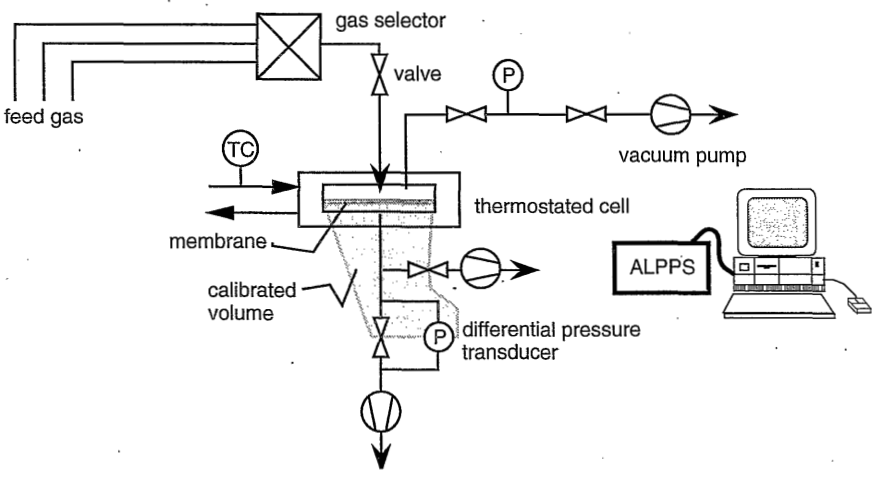

Figure 4 *Schematic drawing illustrating the gas permeation set-up. All valves and pressure indicators are connected to the ALPPS.*

3.4 RESULTS AND DISCUSSION

3.4.1 Properties of Keltan® EPDMs

Some characteristics of EPDM have been summarized in table 1. The main variations are the ethylene content, kind and amount of third monomer and the molecular weight. The content percentages in table 1 are taken from DSM-brochures. The molecular weights were obtained from Noordermeer [12] and determined as well by GPC/HPLC experiments in our laboratories. Despite of some deviations, the trends for the different EDPMs were the same. Differential scanning calometry (DSC) experiments have been carried out in our lab to determine the crystallization temperature and the heat of crystallization, which is a measure for the degree of crystallinity.

As expected, the crystallinity increases strongly with increasing ethylene content. Furthermore, it can be observed from table 1 that the Keltan-numbers starting with a 4 have a much lower M_w/M_n ratio implying a much smaller molecular weight distribution (M_n is the average number molecular weight). This generally results in better crosslinking, i.e., smaller chance to uncrosslinked chains.

Table 1 *Characteristics of several EPDMs [12].*

Keltan®	Et-% [wt-%]	ENB [wt-%]	DCPD [wt-%]	M_n [kg/mol]	M_w/M_n [-]	DSC [J/g]	DSC [° C]
variation of Ethylene content							
4802	**49**	4.5	0	69	2.8	4.7	-41
4778	**70**	4.8	1.3	65	2.7	28	31
712	**53**	4.5	2.1	36	6.0	7.3	-24
778	**65**	5.0	2.2	54	4.9	23	12
variation of molecular weight							
378	66	5.3	2.2	**41**	3.7	28	14
578	65	5.0	2.2	**48**	4.1	23	13
778	65	5.0	2.2	**54**	4.9	25	12
variation of third monomer content							
4802	49	**4.5**	0	69	2.8	4.7	-41
4703	45	**10**	0	44	4.8	1.5	-31
740	62	0	**1.2**	59	3.5	25	2
820	55	0	**4.9**	40	6.0	13	-25

3.4.2 Pervaporation

a. Mass transfer coefficient

A simple way to determine the mass transfer coefficient in the boundary layer is to use the resistances-in-series model (eqn (9)). Here, the film thickness is varied and the toluene flux is measured at a certain constant feed flow velocity and temperature. By plotting the reciprocal value of the pressure normalized flux versus the membrane thickness, a straight line will be found in which the slope represents the reciprocal permeability and the abscissa at l=0 represents the reciprocal mass transfer coefficient [3]. Fig.5 shows the result for Keltan 578 using a toluene concentration of 250 ppm. From this figure a k_L of $2.6 \cdot 10^{-5}$ m/s was found. In further calculations we assumed k_L to be constant, which holds as long as the temperature, feed flow velocity, membrane module, solute are kept constant and convectional fluxes stay negligible when compared to the diffusional fluxes. Fig.5 also shows that for a membrane thickness of 120 μm the resistance in the membrane is about one third of the total resistance.

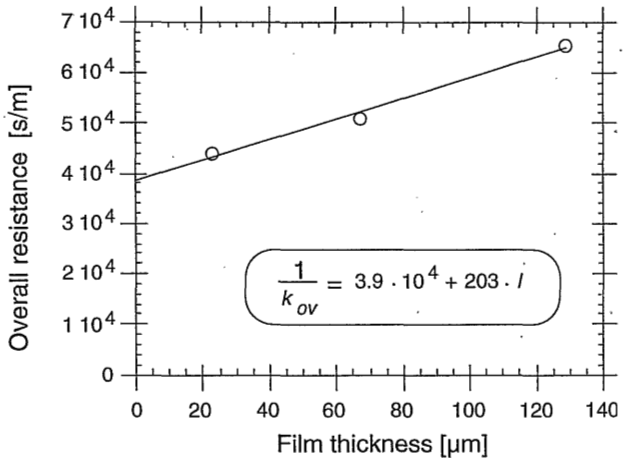

Figure 5 *Reciprocal flux as a function of the membrane thickness (l in µm) for K578; feed conditions: 250 ppm toluene in water, T=26° C and v=3 l/min.*

b. Variation of EPDM

Fig.6 shows the toluene permeability of several EPDMs. The absolute error in the determination of the permeability was quite high, because the effect of the error in k_L is high. However, k_L does not change for the different EPDMs and the relative error in the permeability between EPDMs is much smaller. This relative error is mainly caused by a deviation of about 15% in the thickness of one film, which could not be prevented during the preparation of the polymer films.

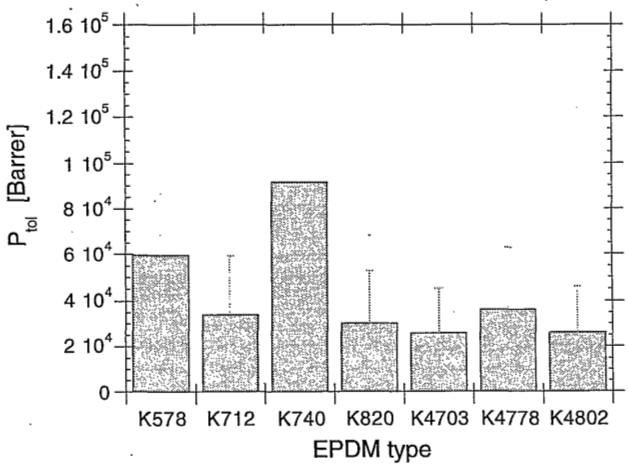

Figure 6 *Toluene permeability in different types of EPDM; feed solution: 250 ppm toluene in water, T=26° C and v=3 l/min.*

Because of these errors no clear conclusions can be drawn concerning the toluene permeability of different EPDMs. As an average of all EPDMs the intrinsic toluene permeability is about 40,000 Barrer. In literature [6] a value is found of $P_{tol} = 10^{-9}$

m^2/s at 25° C, which equals 5,000 Barrer ($\gamma_{tol} = 10^4$ [13]). This difference could not be explained at this point.

Fig.7 shows the water permeability coefficient of different EPDMs at 26° C from a 250 ppm toluene feed solution. The water flux is not affected by the boundary layer resistance and consequently the error in the permeability is much smaller than for toluene. As an average of all EPDMs the intrinsic water permeability is about 700 Barrer. The water flux across a 100 μm EPDM film at 26° C is 0.5 $g/m^2.h$ which is comparable to the values found in literature [3,14].

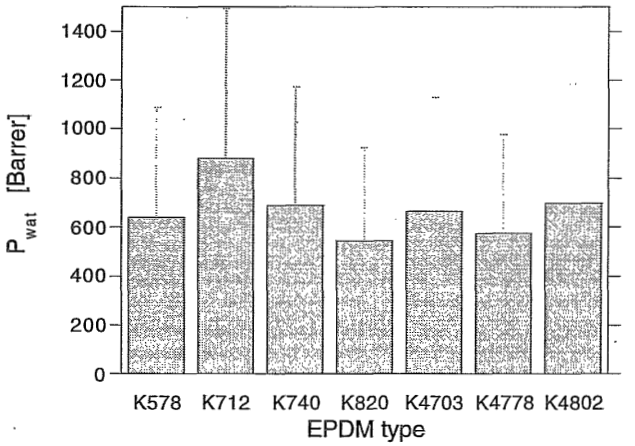

Figure 7 *Water permeability for different types of EPDM; feed solution: 250 ppm toluene in water, T=26° C and v=3 l/min.*

c. Variation of crosslink procedures

Fig.8 shows the effect of different crosslink procedures on the toluene permeability. Keltan®578 (K578) was used as standard material for these experiments since this type of EPDM has been described in literature [6, 15-17]. The columns represent non-crosslinked K578, K578 crosslinked with DCP as the initiator in an oven at 150° C in nitrogen atmosphere for 1 hour, K578 crosslinked with DCP as the initiator at high pressure (10 MPa), 150° C for 1 hour and K578 crosslinked with the sulfur blend at high pressure (10 MPa) and 160° C for 20 minutes, respectively.

It may be concluded that indeed crosslinking at high pressure is more efficient, when compared to crosslinking in the oven. Most probably this due to the impurity of the nitrogen atmosphere in the oven. This atmosphere may well contain a little oxygen which is enough to interfere with the reaction.

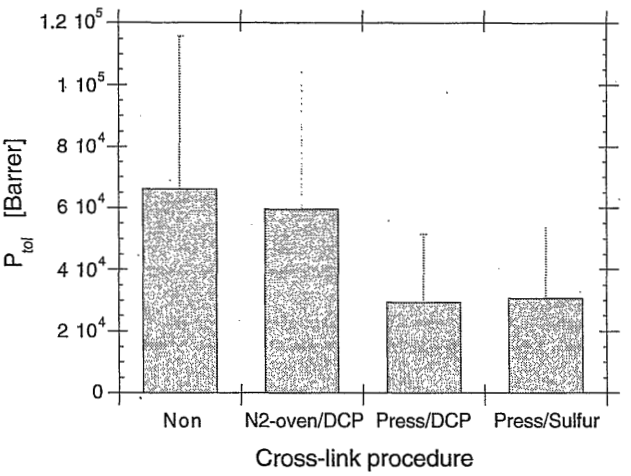

Figure 8 *Effect of crosslink procedure on toluene permeability in EPDM; feed solution: 250 ppm toluene in water, T=26° C and v=3 l/min.*

The effect of different crosslink procedures on the water permeability is shown in fig.9. This graph shows exactly the same trend as the toluene permeability. However, also here the error in the experiments is quite high and it is not possible to distinguish between various crosslink procedures.

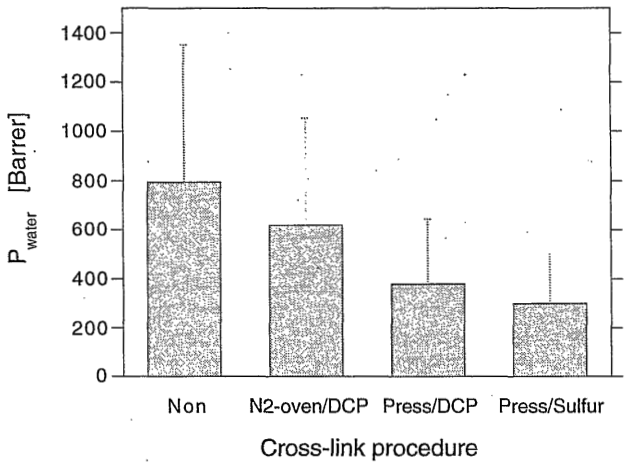

Figure 9 *Effect of crosslink procedure on water permeability in EPDM; feed solution: 250 ppm toluene in water, T=26° C and v=3 l/min.*

d. Coupling phenomena

Before a toluene containing feed is brought in contact with the membrane, pervaporation was carried out with pure water. This pure water flux is much lower than the water flux from a toluene containing feed. A reason could be that the toluene in the feed affects the water permeability. However, in literature it is often stated that the water flux is constant for different toluene concentrations in the feed. Ji et al. [18] show this nicely for the toluene removal from water with PDMS where the water flux was constant over the range from 140 to 520 ppm. However, they measured a small increase of the water flux with increasing toluene concentration for polyether-block-polyamide and polyurethane. Fig.10 shows the water and toluene flux across a EPDM film versus the toluene concentration in the feed. The toluene flux increases linearly with the concentration in the feed. For these very low toluene concentrations it may be assumed that the permeability coefficient remains constant and if the activity coefficient does not change so much then the flux increase is due to a linear increase in driving force. However, a clear increase of the water flux can be observed when the toluene concentration increases from 0 to 250 ppm. This phenomenon, called coupling, was also predicted for EPDM when modeling the pervaporative removal of toluene from water with pervaporation and sorption data from literature [19]. To explain the difference between EPDM and PDMS one should keep in mind that the same phenomenon may occur with PDMS but the small water flux increase is negligible due to the high water permeability of PDMS. For 250 ppm toluene in the feed the water flux for EPDM with a thickness of 163 μm is 0.25 $g/m^2.h$ and that for PDMS with a thickness of 140 μm is 45 $g/m^2.h$.

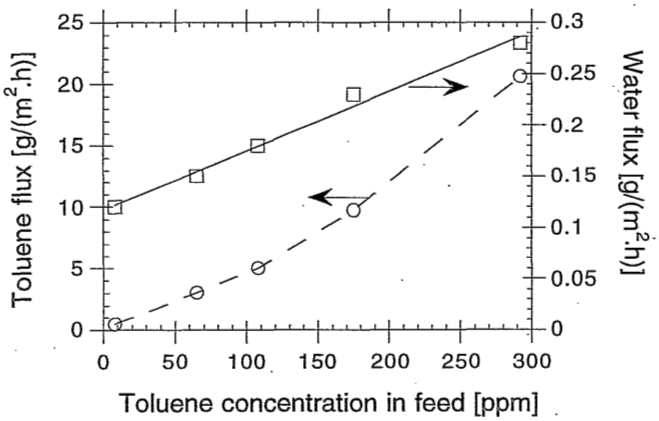

Figure 10 *The effect of coupling phenomena, water and toluene fluxes in EPDM (K578) as a function of toluene concentration in the feed; membrane thickness: 163 μm, Feed conditions: T=26° C and v=3 l/min.*

3.4.3 Vapor sorption

a. Sorption isotherms

Fig.11 shows a typical sorption-isotherm curve. The curve relates the absorbed volume of toluene (normalized to STP) per volume of dry EPDM as a function of the vapor pressure of toluene. The experimental values have been interpolated with a fourth polynomial relation. This relation is later used to calculate the permeability.

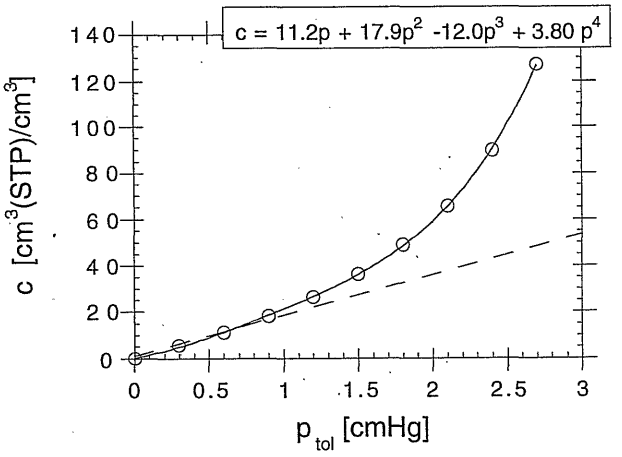

Figure 11 *Sorption-isotherm for toluene in EPDM (K578) in which the toluene concentration c (cm^3(STP)/cm^3 dry polymer) is given as a function of the toluene vapor pressure at T=25° C.*

The dashed line represents the initial slope of the graph, where a Henry-type of sorption may be assumed. From the slope a solubility coefficient of S = 19 cm^3(STP)/ (cm^3.cmHg) is found. The highest activity applied is 0.9 which equals a vapor pressure of 2.7 cmHg. Table 2 summarizes all experiments.

It can be concluded that the sorption-isotherms of the different EPDMs and different crosslink procedures hardly differ. The Henry's solubility coefficient of K4778, which is 15 cm^3(STP)/ (cm^3.cmHg) is significant lower than the value for the other EPDMs. This can be explained by the fact that K4778 has a higher content of crystallinity and it is the only EPDM with a T_m higher than the experimental temperature (T_m(K4778) = 31° C). However, $S_{0.9}$ of K4778 has the same value as the other EPDMs, which is about 49±3 cm^3(STP)/(cm^3.cmHg). Addition of toluene into the EPDM-matrix may well result in loss of crystalline parts and therefore comparable sorption to the other EPDMs. Presumably, this effect takes place for K4778 between an activity of a=0.4 and a=0.9 (the sorption increases linear with activity from a=0 to about a=0.4). No clear jump in the sorption isotherm was observed in this range, so the loss of crystallinity occurs gradually. In literature a value for S=86.5 cm^3(STP)/(cm^3.cmHg) was found at a=1 and 40° C [20] which is comparable to the results in this paper.

Only K578 crosslinked in the oven shows a much higher $S_{0.9}$ which is even higher than the $S_{0.9}$ of the non-treated film. This is another indication that during the heat-treatment in the oven parallel to crosslinking some degradation occurs (the film is crosslinked since it does not dissolve anymore). The crosslinking procedure with pressure seems much more reproducible. Liquid sorption experiments in §3.4.4 will strengthen this statement.

Table 2 *Henry's solubility coefficient (S at p→0) and the solubility coefficient (S) at a toluene activity of 0.9 for various types of EPDMs.*

EPDM / crosslink procedure	Henry's sorption coeffient [cm^3(STP)/(cm^3.cmHg)]	S (a_{tol} = 0.9) [cm^3(STP)/(cm^3.cmHg)]
K378 / press-DCP	19	46
K578 / press-DCP	18	48
K712 / press-DCP	18	47
K4703 / press-DCP	18	48
K4778 / press-DCP	15	49
K4802 / press-DCP	19	51
K578 / non	18	52
K578 / oven	18	58
K578 / press-DCP	19	49
K578 / press - sulfur	19	49

b. Diffusion coefficient

From the vapor sorption experiments the diffusion coefficients (D) can be calculated as a function of the applied vapor pressure. Plotting these values versus the toluene concentration absorbed by the polymer at the same vapor pressure results typically in a graph as shown in fig.12. First D increases with increasing sorption, but then it reaches a maximum and it decreases with still increasing sorption.

In literature this relation between the diffusion coefficient and the sorption have been found for sorption of vapors in rubbers [21,22]. With a higher amount of toluene in the polymer matrix the polymer chains will become more flexible, which is referred to as plasticization, and accordingly D increases. However, the decrease is not expected on forehand. It may be explained by the following effects as suggested by Blume et al. [21]:

- toluene molecules could form a cluster in the polymer matrix at high concentrations, hence D decreases due to the larger size of the penetrants,
- above a certain activity the activity coefficient increases more than linear with increasing concentration and as a result D decreases,
- due to swelling the film becomes thicker which has not been accounted for, consequently the calculated D is lower than the actual D,

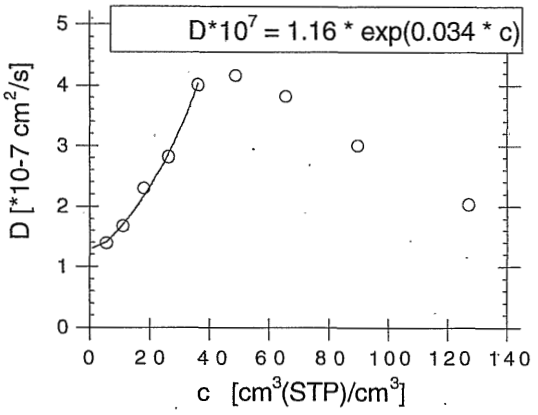

Figure 12 *Diffusion coefficient of toluene as a function of the concentration toluene in EPDM (K378); T=26° C, crosslinking: with DCP at 150° C and 10 MPa for 1hour.*

To calculate the permeability coefficient from vapor sorption experiments a relation of D as a function of the absorped concentration is needed. A fourth order polynomial relation interpolates the results quite good, but a high deviation is obtained at low concentrations. Because water and toluene hardly influence each other during pervaporation [6,18], it is possible to compare the toluene permeabilities of pervaporation and vapor sorption. Due to the boundary layer resistance in pervaporation the actual activity of toluene at the membrane surface is rather low ($a_{tol} < 0.2$ [19]). So, the interpolation, especially, below a is 0.3 should be very good. A relation as used by Mulder [7] (eqn (23)), where D_o is the diffusion coefficient at a=0 and τ a plasticizing variable,

$$D(c) = D_o \cdot exp(\tau \cdot c) \ , \qquad (23)$$

describes this initial part very well as can be observed in fig.12. For all EPDMs and crosslink procedures a D_o value of $(1.5 \pm 0.3) \cdot 10^{-11}$ m^2/s is found.

c. Permeability coefficient

The permeability coefficient can be calculated via vapor sorption measurements by solving eqn (13) which can be combined with eqn (23)

$$P_{tol} = \frac{D_o}{p_{tol}} \cdot \int_0^{c_m} e^{\tau \cdot c} \cdot d\,c = \qquad (24)$$

$$P_{tol} = \frac{D_o}{\tau \cdot p_{tol}} \cdot \left(e^{\tau \cdot c}\right)\Big|_0^{c_m} = \frac{D_o}{\tau \cdot p_{tol}} \cdot \left(e^{\tau \cdot c_m} - 1\right) \ , \qquad (25)$$

p_{tol} and c_m are directly related via the empirical relationship from the sorption-isotherm. For K378 the following eqn is obtained: $c_m = 11.15 \cdot p_{tol} + 20.31 \cdot p_{tol}^2$

$-14.11 \cdot p_{tol}^3$ $4.23 \cdot p_{tol}^4$. The feed vapor pressure at the membrane surface ($p_{m,i} = p_{tol}$) can be obtained from flux measurements of toluene (see §3.4.2 and eqn (15)). The toluene flux is typically 17 g/(m^2.h) which is equal to $5 \cdot 10^{-9}$ mol/(cm^2.s), k_L is $2.6 \cdot 10^{-5}$ m/s and H is 648 Pa.m^3/mol. The vapor pressure of the feed is related to the toluene concentration in the feed bulk which is 250 ppm (= $2.71 \cdot 10^{-6}$ mol/cm^3) by eqn (2) resulting in p_{tol} is 0.36 cmHg (≈ 5 mbar). From this value the permeability coefficient can be calculated and P_{tol} becomes $2.2 \cdot 10^4$ Barrer. Fig.13 summarizes the permeability coefficients for the different EPDMs and it can be seen clearly that no significant differences are observed. Only the permeability coefficient in K4703 is significantly lower compared to the others, which is due to a lower diffusion coefficient. This can not be explained from structural properties.

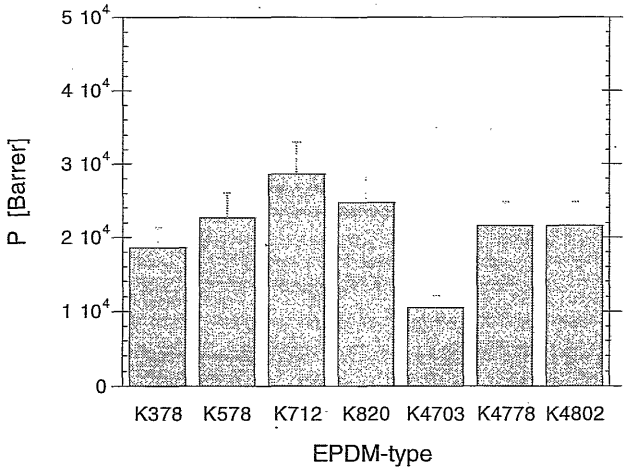

Figure 13 *Toluene permeability coefficient for different EPDMs as determined by vapor sorption experiments.*

In literature [20] a P_{tol} value of $9 \cdot 10^5$ Barrer was found from actual vapor permeation experiments through a 100 µm film EPDM at 25° C. This value is 40 times higher than the values we find from sorption measurements. This discrepancy can be described mainly to the fact that the permeation experiments of Blume et al. were performed at a toluene activity of 1, at which the swelling of the film is severe and much higher permeabilities will be found than in our case where the activity is below 0.2.

3.4.4 Liquid sorption

Liquid sorption experiments were carried out to investigate the crosslink efficiency. Fig.14 demonstrates the effect of different methods on the crosslink efficiency of EPDM K578. The M_c-value decreases with increasing DCP concentration as may be expected. However, the M_c value of the oven-treated film decreases much stronger than the pressurized crosslinked film. At 5 phr DCP the crosslinking seems to reach a maximum and addition of more DCP does not lead to a higher crosslink density. Furthermore, it is obvious that crosslinking at

high pressure give better results than crosslinking in the oven. At 5 phr the M_c-value is 2.5 kg/mol for the oven treated film and 1.1 kg/mol for the press-treated film.

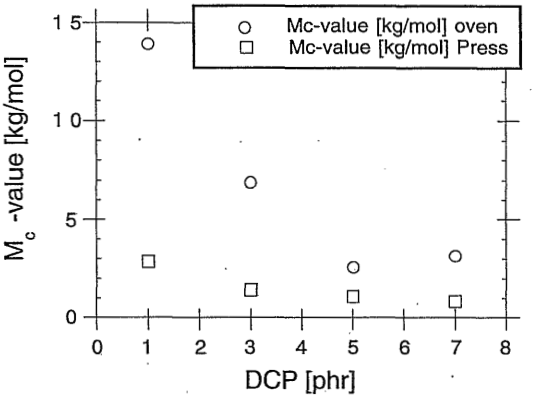

Figure 14 *M_c-values of crosslinked K578 films as a function of crosslink procedure and DCP concentration.*

3.4.5 Gas permeation

Gas permeation experiments were carried out to give additional insight in structural differences of EPDM and their effect on permeation behaviour of gases. Table 3 summarizes the gas permeation experiments for several EPDMs and various gases (CO_2, O_2, N_2). Permeability values have been calculated from flux and film thickness measurements. Ideal selectivities are also reported. Typical thicknesses were 50 µm.

Table 3 *Permeabilities and ideal selectivities for gases through different EPDMs at 30° C (oven-treated; 1 hour, 150° C, 5 phr DCP).*

EPDM	$P(N_2)$ [Barrer]	$P(O_2)$ [Barrer]	$P(CO_2)$ [Barrer]	$\alpha_{id}(CO_2 / N_2)$ [-]	$\alpha_{id}(O_2 / N_2)$ [-]	$\alpha_{id}(CO_2 / O_2)$ [-]
K578	7.7	-	110	14	2.8	-
K712	10	26	107	11	2.7	4.1
K740	8.4	22	-	-	2.6	-
K778	14	30	135	10	2.2	4.5
K4778	8.8	26	122	14	2.9	4.7
K578 [16]#			110	14		

non crosslinked

K4703 and K4802 could not be measured since the polymer films showed strong relaxation upon the applied pressure and defects occured after a certain period of time. No significant differences were found for the EPDMs. The error in the permeability measurements is about 10% mainly due to the deviation in the

membrane thickness. Therefore, it is better to compare the selectivities since the error in the thickness has no effect on this parameter. $\alpha_{id}(CO_2 / N_2)$ for K778 and K712 is lower than of the other EPDMs. $\alpha_{id}(O_2 / N_2)$ for K778 is lower but K712 is comparable with the other EPDMs. However, these differences could not be explained when discussed as a function of the various EPDM parameters.

3.5 CONCLUSION

Different ethylene-propylene-diene terpolymers (EPDM) and crosslinking procedures have been evaluated in relation to pervaporation, vapor sorption, liquid sorption and gas permeation experiments. EPDM various parameters that have been changed are ethylene content, molecular weight, third monomer and molecular weight distribution. In crosslinking experiments in an oven with nitrogen atmosphere, a heatable press and the use of dicumylperoxide or a sulfur blend as crosslink initiators were the variables. No clear differences were found for the various EPDMs nor for the different crosslink procedures.

Pervaporation experiments to remove toluene from an aqueous feed mixture have been performed with EPDM films of about 120 μm. Data have been normalized to a thickness of 100 μm and a feed concentration of 250 ppm toluene. The experimentally determined differences in permeability of toluene and water were too small for various types of EPDM and various crosslink procedures to comment on the effect of structural differences. The permeability from pervaporation experiments was about (40±30) kBarrer for toluene and (600±300) Barrer for water. The toluene flux ranges from 15 to 18 $g/m^2.h$. The mass transfer resistance of toluene in the stagnant boundary layer is about two third of the total resistance in case of 120 μm thick EPDM films. The water flux is about 0.5 $g/m^2.h$ and depends on the toluene concentration in the feed. The separation factor is about 200,000 for a 100 μm EPDM and an overall mass transfer coefficient of $2.6 \cdot 10^{-5}$ m/s.

Toluene permeability coefficients have been calculated from vapor sorption measurements. The reproducibility of these experiments was much better than that of pervaporation experiments. The sorption-isotherms were very reproducible. On the other hand, the diffusion coefficients, which were determined from the initial weight increase on increased vapor activity, were less accurate, because these kinetic measurements could only be measured at a very small time interval. Henry's solubility coefficient ($S_{p\to 0}$) of the EPDMs was 18.5±1 $cm^3(STP)/(cm^3(dry\ polymer).cmHg)$, except for K4778 which shows a value of 15 $cm^3(STP)/(cm^3.cmHg)$. The T_m of K4778 is the only one which is higher than the temperature of the experiment, resulting in less sorption due to presence of crystalline regions in K4778. The permeability for the EPDMs is about 22±10 kBarrer. This is in reasonable good agreement with results from the pervaporation experiments.

Gas permeation experiments resulted in permeabilities for CO_2, O_2 and N_2 which were 120±10, 24±2, 11±3 Barrer, respectively. The discrepancies in

permeabilities of a gas between the EPDMs could not be explained with structural differences of the EPDMs.

Liquid sorption measurements with pure toluene at 25° C proved that crosslinking in the oven is less efficient than with the press. At 5 phr the M_c-value is 2.5 kg/mol for the oven-crosslinked EPDM-film and 1.1 kg/mol for the press-crosslinked film.

ACKNOWLEDGEMENTS

Jeroen Willemsen is acknowledged for performing the experiments and the fruitful discussions related to this work. Betty Folkers is acknowledged for additional measurements. Prof. dr. ir. J.W.M. Noordermeer is kindly acknowledged for the enlightening discussions concerning EPDM.

LIST OF SYMBOLS

Roman

a	activity	[-]
A	membrane area	[m^2]
c	concentration (pervaporation)	[mol/m^3]
c	concentration (vapor sorption)	[cm^3/cm^3]
D	diffusion coefficient	[m^2/s]
H	Henry coefficient	[$Pa.m^3/mol$]
J	flux	[$mol/(m^2.s)$]
k	mass transfer coefficient	[m/s]
k'	modified mass transfer coefficient	[$mol/(m^2.s.Pa)$]
m	mass	[g]
M_c	molecular weight between two crosslinks	[g/mol]
M_n	number molecular weight	[g/mol]
M_w	molecular weight	[g/mol]
p	(partial) pressure	[Pa]
P	permeability	[cm^3(STP).cm/(cm^2.s.cmHg)]
P	permeability (pervaporation eqns)	[$mol/m^2.s.Pa$]
S	sorption coefficient	[cm^3(STP)/(cm^3.cmHg)]
STP	standard T=273.15 K and p=10^5 Pa	[-]
T	temperature	K
t	time	[s]
v	feed flow velocity	[l/min]
V	volume	[m^3]
x	mole fraction in liquid	[-]
y	mole fraction in vapor	[-]

Greek symbols

α	separation factor	[-]
α_{id}	ideal selectivity for gas separation	[-]
χ	Flory-Huggins interaction parameter	[-]
ϕ	volume fraction	[-]
γ	activity coefficient	[-]
ρ	density	[g/cm^3]
ρ_f	molar density of feed	[mol/m^3]
τ	plasticizing coefficient	[-]

subscripts

f	feed (side)
i	component i
L	stagnant liquid boundary layer
m	membrane
ov	overall
p	permeate (side)
tol	toluene
voc	volatile organic contaminant
w	water

superscript

'	pressure normalized units
°	saturated

REFERENCES

[1] Grünes Buch Nr. 39, *Beitrage zur Technologie des Kautschuks und verwandter Stoffe*, Elastomere auf Basis Äthylen-Propylen, Wirtschaftsverband der Deutchen Kautschukindustrie E.V., 1979.

[2] Dikland, H.G., *Coagents in peroxide vulcanisations of EP(D)M rubber*, PhD-Thesis, University of Twente, Enschede, NL , 1993.
Dikland, H.G., *Influence of chemical composition and molecular structure of EPDM on peroxide crosslinking efficiency*, Kautschuk Gummi Kunststoffe, 49 (1996) 413.

[3] Nijhuis, H.H., M.H.V.Mulder, C.A.Smolders, *Selection of elastomeric membranes for the removal of volatile organics from water*, J.Appl.Polym.Sci., 47 (1993) 2227-2243.

[4] Meuleman, E.E.B., Chapter 2 of this thesis, 1997.

[5] Wijmans, J.G., A.L.Athayde, R.Daniels, J.H.Ly, H.D.Kamaruddin, I.Pinnau, *The role of boundary layers in the removal of volatile organic compounds from water by pervaporation*, J.Membr.Sci., 109 (1996) 135.

[6] Nijhuis, H.H., *Removal of trace organics from water by pervaporation (a technical and economic analysis)*, PhD-Thesis, University of Twente, Enschede, The Netherlands, 1990.

[7] Mulder, M.H.V., *Thermodynamic Principles of Pervaporation*, in: R.Y.M.Huang (ed), *Pervaporation Membrane Separation Processes*, Membrane Science and Technology Series, 1991.

[8] Crank, J. G.S.Park, *Diffusion in polymers*, Academic Press, London (UK), 1968.

[9] Flory, P., *Principles of polymer chemistry,* Cornell university press, Itaca, New York (USA), 1953.
[10] Boom, J.P., *Transport through zeolite filled polymeric membranes,* Ph.D.-thesis, University of Twente, Enschede (NL), 1994.
[11] Dudek, T.J., *Behaviour of ethylene-propylene rubbers,* J.Polym.Sci., A2 (1962) 812.
[12] Noordermeer, J.W.M., DSM-elastomers, personal communication, 1995.
[13] Nielsen, F., E.Olsen, A.Fredenslund, *Henry's law constants and infinite dilution activity coefficients for volatile organic compounds in water by a validated batch air stripping method,* Environ. Sci. Technol., 28 (1994) 2133 - 2138.
[14] Rufino, J.R.M., *Recuperação de componentes de aromas por pervaporação,* M.Sc.-thesis, UFRJ/COPPE, Rio de Janeiro (BRA), 1996.
[15] Borges, C.P., M.H.V.Mulder, C.A.Smolders, *Composite hollow fiber for removal of VOCs from water by pervaporation,* in: Bakish, R., (ed.), Proc.6th Int.Conf.Perv.Procs.Chem.Ind.; Ottawa (CND), Bakish Materials Corp., Englewood (USA), 1992, 207-222.
[16] Duval, J.-M., *Absorbent filled polymeric membranes, application to pervaporation and gas separation,* PhD-Thesis, University of Twente, Enschede (NL), 1993.
[17] Meuleman, E.E.B., Chapter 6 of this thesis, 1997.
Meuleman, E.E.B., Chapter 7 of this thesis, 1997.
[18] Ji, W., S.K.Sikdar, S.-T.Hwang, *Modeling of multicomponent pervaporation for removal of volatile organic compounds from water,* J.Membr.Sci., 93 (1994) 1-19.
[19] Meuleman, E.E.B., Chapter 4 of this thesis, 1997d.
[20] Blume, I., A.Bos, P.J.F.Schwering, M.H.V.Mulder, C.A. Smolders, *On the transport of organic liquids through elastomeric films and membranes,* Membraantechnologie 6, 1991.
[21] Blume, I., E.Smit, M.Wessling, C.A.Smolders, *Diffusion through rubbery and glassy polymer membranes,* Makromol.Chem, Makromol.Symp., 45 (1991) 237.
[22] Aminabhavi, T.M., S.B.Harogoppad, R.H.Balundgi, *Swelling characteristics of polymer membranes in the presence of aromatic hydrocarbon liquids,* J.Appl.Pol.Sci., 44 (1992) 1687.

4

MODELING OF LIQUID/LIQUID SEPARATION BY PERVAPORATION - TOLUENE FROM WATER

SUMMARY

The resistances-in-series model, the modified solution-diffusion model, the Flory-Rehner theory and the film theory have been used to calculate the diffusion coefficients of two components of a liquid feed mixture which are separated by pervaporation. The toluene and water fluxes through EPDM membranes of various thicknesses have been modeled for different mass transfer coefficients in the feed boundary layer (k_L). Both the concentration dependent and concentration independent diffusion coefficients have been determined by numerical methods. Diffusion coefficients of $3.2 \cdot 10^{-12}$ m^2/s and $1.4 \cdot 10^{-11}$ m^2/s were found for toluene and water, respectively. The use of concentration dependent diffusion coefficients did not improve the results.

It is shown that the toluene flux depends strongly on the k_L. Furthermore, the membrane resistance has a significant effect on the toluene flux only for very high values of k_L ($>10^{-4}$ m/s). The water flux increases linearly with the reciprocal value of the membrane thickness and is not affected by the boundary layer resistance. The small increase of the water flux due to the toluene concentration increase in the feed, can adequately be described by the presented model.

4.1 INTRODUCTION

Pervaporation is a process in which a liquid feed mixture is separated by a dense homogeneous membrane. At the feed or upstream side a liquid is in contact with the membrane at atmospheric pressure while at the permeate or downstream side a low partial pressure is maintained by a vacuum pump or a sweeping gas. The permeate is removed as a vapor. The driving force for the process is the chemical potential difference or partial pressure difference across the membrane.

Ji et al. [1] modeled multicomponent pervaporation with the resistances-in-series model in which the film theory was incorporated for the transport through the liquid boundary layer and the solution-diffusion model with constant permeability coefficients. Their experiments with PDMS-membranes showed that the VOC flux increased linearly with VOC concentration in the feed. The water flux decreased linearly with increasing membrane thickness. Furthermore, the water flux increased about 10% with the toluene concentration in the feed being increased from 20 to 500 ppm. From these results Ji et al. [1] concluded that the process can be described satisfactory by a solution-diffusion model with constant permeabilility coefficients neglecting the small increase in water flux. In addition, they incorporated the effect of the permeate pressure (drop) in their modeling.

Michaels [2] used even more simplified equations for the different transport steps in the resistances-in-series model. He suggested a dimensionless parameter which could serve as a tool to predict the performance of a given pervaporation membrane and membrane module with a limited amount of experimental information. Michaels suggested that his proposed correlations together with Ji's [3] findings would be a reliable basis for the selection of membranes, membrane modules and process parameters. Before Michaels many researchers introduced closely related dimensionless parameters to show the polarization effect of the pervaporative removal of sparingly soluble VOCs from water [4-7].

The work described in this paper is based on earlier studies of Mulder [8] who described the transport through a dense membrane and the film theory to account for the mass transfer limitations in the boundary layer.

4.2 MASS TRANSFER

The transport mechanism in pervaporation through a homogeneous dense membrane can be described by five consecutive steps:

1. transfer of a component from the bulk of the feed to the membrane surface,
2. partition of a component between the liquid feed and the membrane,
3. transport of the component across the membrane,
4. desorption of the component as vapor on the permeate side of the membrane,
5. transfer of the component from the membrane surface to the permeate bulk.

This general transport mechanism can be applied for each component present in the liquid mixture. The treatment of the mass transfer in the membranes is based on the film theory, Fick's law, the thermodynamics of irreversible processes and the

Maxwell - Stefan equations. The Maxwell - Stefan equations will not be discussed in this work. It has already been done earlier by Heintz [9] and Wesselingh and Krishna [10].

4.2.1 Film theory and resistances-in-series model

The concentration profiles in volume fractions (ϕ) for a binary mixture according to the film theory and the resistances-in-series model at steady state are given in fig.1. The dashed line shows the concentration profile of the slower permeating component and the full line shows the concentration profile of the component which is permeating preferentially.

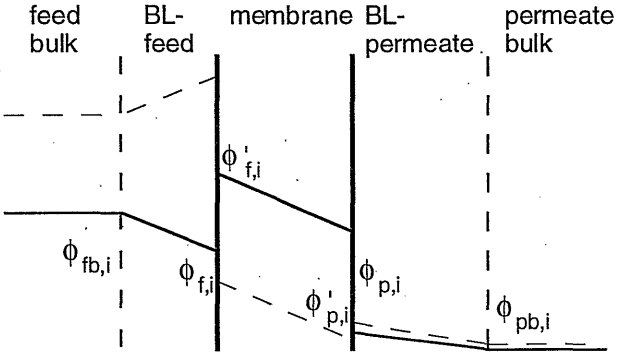

Figure 1 *Schematic drawing showing the concentration profiles at both sides of a membrane during pervaporation (according to the film theory). BL = boundary layer.*

The mass transfer across the boundary layer at the feed side of the membrane can be described with equation (1):

$$J_i = k_{L,i}(\phi_{fb,i} - \phi_{f,i}) \,, \qquad (1)$$

where $k_{L,i}$ is a mass transfer coefficient which can be obtained from a Sherwood relation. The mass transfer across the membrane is given by eqn (2)

$$J_i = k_{m,i}(\phi'_{f,i} - \phi'_{p,i}) \,, \qquad (2)$$

in which $k_{m,i}$ is the mass transfer coefficient in the membrane. Usually the mass transfer resistance of the permeate boundary layer is assumed to be negligible. The flux across the boundary layer at the permeate side of the membrane can be described by:

$$J_i = k_{p,i}(\phi_{p,i} - \phi_{pb,i}) \,, \qquad (3)$$

here $k_{p,i}$ is the mass transfer coefficient in the downstream side boundary layer. The following partition coefficients can be introduced for upstream side ($s_{f,i}$) and

downstream side ($s_{p,i}$), respectively,

$$s_{f,i} = \frac{\phi'_{f,i}}{\phi_{f,i}} \text{ and } s_{p,i} = \frac{\phi'_{p,i}}{\phi_{p,i}} \quad . \tag{4}$$

At steady-state the flux through each layer is the same and combination of equations (1), (2), (3) and (4) leads to an expression which describes the overall mass transfer:

$$J_i = \frac{\phi_{fb,i} - \frac{s_{p,i}}{s_{f,i}}\phi_{pb,i}}{\frac{1}{k_{L,i}} + \frac{1}{s_{f,i}k_{m,i}} + \frac{s_{p,i}}{s_{f,i}k_{p,i}}} \quad . \tag{5}$$

Generally, the mass transfer resistance and the concentration at the permeate side are neglected, which leads to:

$$J_i = \frac{\phi_{fb,i}}{\frac{1}{k_{L,i}} + \frac{1}{s_{f,i}k_{m,i}}} \quad . \tag{6}$$

Eqn (6) can be further modified by introducing an overall mass transfer coefficient (k_{ov})

$$J_i = \frac{\phi_{fb,i}}{\frac{1}{k_{L,i}} + \frac{1}{s_{f,i}k_{m,i}}} = k_{ov}\,\phi_{fb,i} \text{ in which } \frac{1}{k_{ov}} = \frac{1}{k_{L,i}} + \frac{1}{s_{f,i}k_{m,i}} \quad . \tag{7}$$

The overall mass transfer coefficient can be obtained from flux measurements at various feed concentrations.

4.2.2 Fick's law with concentration dependent diffusion coefficients

According to Fick's law the flux J of component i through a homogeneous membrane is proportional to its concentration gradiënt:

$$J_i = D_i \frac{d\phi'_i}{dx} \quad , \tag{8}$$

where D_i is the diffusion coefficient and ϕ'_i is concentration in the membrane of component i and x is the directional coordinate. The diffusion coefficient of low molecular components in polymers is concentration dependent. In pervaporation processes there are large concentration differences across the membrane. One of the most commonly used relation to describe this dependence is an exponential relation [11]:

$$D_i = D_{0,i} e^{\tau_i \phi'_i} \quad , \tag{9}$$

here is τ, the plasticizing coefficient, describing the interaction between permeating species and membrane and $D_{0,i}$ is the Fickian diffusion coefficient at infinite dilution of the permeant. Using eqn (9) in the Fick's eqn (8) with the following boundary conditions: $x = 0$, $\phi'_i = \phi'_{0,i}$ and $x = l$, $\phi'_i = 0$ leads to:

$$J_i = \frac{D_{0,i}}{l\,\tau_i}\left(e^{\tau_i \phi'_{0,i}} - 1\right) \quad . \tag{10}$$

Modeling multi-component pervaporation is more complex, because not only component-membrane but also component-component interactions have to be taken into account. A component in a mixture usually has a higher diffusivity in the membrane than it has as a single component. Greenlaw [12] used a linear relationship between the concentrations of components in the membrane and their diffusion coefficients. For ideal liquid mixtures (like heptane-hexane) this may be hold, but for non-ideal mixtures in which mutual interactions and polymer-component interactions have to be taken into account other relationships would give a better description of the experimental results.

$$D_i = D_{i,0} + f \cdot (\phi'_i + g\phi'_j)^h \quad . \tag{11}$$

The constants f and h depend on components i and the constant g on component j. Exponentially modified diffusion coefficients are also used [8,13]:

$$D_i = D_{0,i}\, e^{l\phi'_i + m\phi'_j} \quad , \tag{13}$$

where the constants l and m depend on components i and component j, respectively.

4.2.3 Solution-diffusion model

Pervaporation processes are usually described with a solution-diffusion model. If no external forces (like pressure difference) are present and if there is no coupling of flows, then the flux of component i is proportional to its chemical potential gradient ($d\mu_i/dx$) [14-16]:

$$J_i = -\frac{D_i^T}{R\,T} \cdot \phi_i \frac{d\mu_i}{dx} \quad , \tag{14}$$

where D_i^T is the thermodynamic diffusion coefficient and may depend on the concentration and therefore on the place in the membrane [8]. The chemical potential can be described as:

$$\mu_i = \mu_i^o + RT \ln a_i \quad . \tag{15}$$

Substitution of μ_i in eqn (14) gives:

$$J_i = -D_i^T \phi_i \frac{\mathrm{d} \ln a_i}{\mathrm{d}x} \quad . \tag{16}$$

Eqn (8) can be written as

$$J_i = -D_i \frac{\mathrm{d}\phi_i}{\mathrm{d} \ln a_i} \frac{\mathrm{d} \ln a_i}{\mathrm{d}x} \quad . \tag{17}$$

Combination of equations (16) and (17) leads to a relation between D_i and D_i^T:

$$D_i^T \phi_i = D_i \frac{\mathrm{d}\phi_i}{\mathrm{d} \ln a_i} \Leftrightarrow \quad D_i = D_i^T \frac{\mathrm{d} \ln a_i}{\mathrm{d} \ln \phi_i} \quad . \tag{18}$$

Lee [16] used a solution-diffusion model with a concentration independent diffusion coefficient and without considering a possible coupling of fluxes. In the case of liquid mixtures which hardly show any mutual interaction nor any interaction with the polymer, this assumption is valid, but with other non-ideal mixtures this approach is often too simple.

a. Membrane boundary conditions

To describe the mass transfer through the membrane the boundary conditions must be defined as follows:

1. Steady state conditions are assumed. The permeation rate is independent of time and no accumulation of components takes place in the membrane. The membrane undergoes no structural changes. The chemical potential of component i is a function of the volume fraction of all components present.
2. Mass transfer in the membrane and in the feed are taken into account. Mass transfer resistance in the permeate is neglected.
3. The concentrations of the components at the boundary of the membrane can be calculated from thermodynamic principles. At the membrane interface the thermodynamic potentials of the membrane and its adjacent phase are assumed to be equal [16]:

$$\mu_{f,i} = \mu'_{f,i} \text{ and } \mu_{p,i} = \mu'_{p,i} \quad . \tag{19}$$

The chemical potentials at the boundary of the membrane are:

$$\mu_{f,i} = \mu_o + RT \ln a_{f,i} \ , \tag{20}$$
$$\mu'_{f,i} = \mu_o + RT \ln a'_{f,i} \ , \tag{21}$$
$$\mu_{p,i} = \mu_o + RT \ln a_{p,i} \ , \tag{22}$$
$$\mu'_{p,i} = \mu_o + RT \ln a'_{p,i} \ . \tag{23}$$

Combining equations (19), (20) and (21) and equations (19), (22) and (23) leads to:

$$a'_{f,i} = a_{f,i} \quad , \tag{24}$$

$$a'_{p,i} = a_{p,i} \tag{25}$$

The activities on the outside of the membrane can be described by using activity coefficients (γ): $a_i = \gamma_i \phi_i$.

4. The chemical potential inside the membrane is described with the Flory - Rehner theory. Therefore, in the following a short description is given of this theory.

b. Solubility aspects, Flory-Huggins theory

Nijhuis [17] showed that the Flory-Rehner theory [18] describes the sorption of penetrants (toluene, trichloro-ethylene and water) well in a crosslinked film (various elastomers such as: ethylene-propylene terpolymer, polydimethylsiloxane, etc.). Eqns (26) and (27) give the expressions for the activities (a) in ternary systems, in which the index 1 denotes an organic component, 2 water and 3 the polymer:

$$\ln a_1 = \ln \phi_1 + (1-\phi_1) - \phi_2 \frac{V_1}{V_2} - \phi_3 \frac{V_1}{V_3} + (\chi_{12}\phi_2 + \chi_{13}\phi_3)(\phi_2 + \phi_3) - \chi_{23}\frac{V_1}{V_2}\phi_2\phi_3 + \frac{V_1\rho_3}{M_c}\left(1 - \frac{2M_c}{M}\right)\left(\phi_3^{1/3} - \frac{1}{2}\phi_3\right) \quad , \tag{26}$$

$$\ln a_2 = \ln \phi_2 + (1-\phi_2) - \phi_1 \frac{V_2}{V_1} - \phi_3 \frac{V_2}{V_3} + (\chi_{12}\phi_1\frac{V_2}{V_1} + \chi_{23}\phi_3)(\phi_1 + \phi_3) - \chi_{13}\frac{V_2}{V_1}\phi_1\phi_3 + \frac{V_2\rho_3}{M_c}\left(1 - \frac{2M_c}{M}\right)\left(\phi_3^{1/3} - \frac{1}{2}\phi_3\right) \quad , \tag{27}$$

where V is the molar volume, χ_{ij} is a binary interaction parameter between components i and j, ρ is the density, M is the molecular weight and M_c is molecular weight between two crosslinks. The first 4 terms on the right hand side describe the entropy of mixing, the fifth and the sixth term the enthalpy of mixing and the last term is an elastic term. This elactic term is necessary since by swelling the chain between the crosslink points will be elongated and this causes a force exerted by the network. In the original Flory-Huggins theory the interaction parameters are constant. In practice, these parameters are taken to be concentration dependent.

4.3 COMPUTATIONS WITH THE SOLUTION-DIFFUSION MODEL

Flux equations for component 1 and 2 can be written with eqn (14) as:

$$J_1 = -\phi_1 D_1 \frac{\mathrm{d} \ln a_1}{\mathrm{d}x} = -\phi_1 D_1 \left(b_{11}\frac{\mathrm{d}\phi_1}{\mathrm{d}x} + b_{12}\frac{\mathrm{d}\phi_2}{\mathrm{d}x} \right) \quad , \tag{28}$$

$$J_2 = - \phi_2 D_2 \frac{d \ln a_2}{d x} = - \phi_2 D_2 \left(b_{21} \frac{d\phi_1}{dx} + b_{22} \frac{d\phi_2}{dx} \right) , \qquad (29)$$

in which: $b_{11} = \frac{\partial \ln a_1}{\partial \phi_1}$, $b_{12} = \frac{\partial \ln a_1}{\partial \phi_2}$, $b_{21} = \frac{\partial \ln a_2}{\partial \phi_1}$ and $b_{22} = \frac{\partial \ln a_2}{\partial \phi_2}$.

Expressions for b can be obtained by differentiation of the Flory-Huggins (eqns (26) and (27)) and are given by Mulder and Smolders [8]. If the membrane is subdivided in m layers with thickness Δx the volume fractions ϕ_i can be calculated on each place n on the membrane. The discrete analogon of (28) and (29) are:

$$J_1 \Delta x = - \phi_1(n\text{-}1)\, D_1 \,(b_{11}(n\text{-}1)(\phi_1(n) - \phi_1(n\text{-}1)) + b_{12}(n\text{-}1)(\phi_2(n) - \phi_2(n\text{-}1)) , \qquad (30)$$

$$J_2 \Delta x = - \phi_2(n\text{-}1)\, D_2 \,(b_{21}(n\text{-}1)(\phi_1(n) - \phi_1(n\text{-}1)) + b_{22}(n\text{-}1)(\phi_2(n) - \phi_2(n\text{-}1)) . \qquad (31)$$

With equations (30) and (31) all $\phi_i(n)$ can now be calculated for n = 1 to m. It is not necessary to first differentiate eqns (30) and (31) to ϕ_1 and ϕ_2 as was done previously [8], but the discrete analogon can be presented as:

$$J_1 = - \phi_1 D_1 \frac{d \ln a_1}{dx} \approx - \phi_1 D_1 \frac{\Delta(\ln a_1)}{\Delta x} , \qquad (32)$$

$$J_2 = - \phi_2 D_2 \frac{d \ln a_2}{dx} \approx - \phi_2 D_2 \frac{\Delta(\ln a_2)}{\Delta x} . \qquad (33)$$

Values of $\ln a_1$ and $\ln a_2$ at place n of the membrane can now be calculated with the values of $\ln a_1$ and $\ln a_2$ on place (n-1): (In which: $\Delta \ln a_i = \ln a_i(n) - \ln a_i(n\text{-}1)$).

$$\ln a_1(n) = \ln a_1(n\text{-}1) - \frac{J_1}{\phi_1(n\text{-}1)\, D_1} , \qquad (34)$$

$$\ln a_2(n) = \ln a_2(n\text{-}1) - \frac{J_2}{\phi_2(n\text{-}1)\, D_2} . \qquad (35)$$

The values of $\phi_1(n)$ and $\phi_2(n)$ must be calculated from the values of $\ln a_1(n)$ and $\ln a_2(n)$ with the Flory-Huggins equations in an iterative way. Two advantages might be given to calculate the volume fractions in this way over the calculations via differentiation to ϕ_1 and ϕ_2 performed by Mulder [8]:

1. b_{ij} is not differentiated anymore. The differentiated terms b_{ij} were calculated at place (n-1), therefore, accuracy was reduced.
2. Parameters like χ are assumed to be constant. However, if they are considered to be dependent on the volume fractions or other parameters in the model it will be much easier to incorporate them in a computer program.

The fluxes through EPDM membranes for the removal of toluene from water were measured by Nijhuis [17] at different membrane thicknesses. Some results are given below.

Table 1 *Toluene and water fluxes as determined by Nijhuis [17]*

membrane thickness [μm]	J_1 (water) [$\cdot 10^{-10}$ m/s]	J_2 (toluene) [$\cdot 10^{-9}$ m/s]	J_2/J_1 [-]
40	2.5	2.78	11.1
72	1.6	1.98	12.4
120	0.83	1.76	21.2
200	0.50	1.15	23

Because the toluene flux and concentration ($\phi_{fb,2}$) are known the concentration at the membrane interface ($\phi_{f,2}$) can be calculated with equation (1):

$$J_i = k_{L,i}(\phi_{fb,i} - \phi_{f,i}) \ , \qquad (1)$$

$\phi_{fb,2} = 2.9 \cdot 10^{-4}$ m^3/m^3, which is 250 ppm. A $k_{L,i}$-value of $1.3 \cdot 10^{-5}$ (m/s), which was determined by Nijhuis was used in the calculations. The concentration at the interface ($\phi_{f,i}$) is used to calculate the activity. Therefore, an activity coefficient was used from literature. Some values from literature are listed below.

Table 2 *Toluene activity coefficient in water (0-500 ppm)*

T °C	γ^*	γ^{**}	ref.
12.5	7100	1390	[19]
20.0	4500	880	[20]
22.0	9700	1890	[21]
23.0	10400	2040	[22]

* When mole fractions are used

** When volume fractions are used

From these values it is not very clear which activity coefficient should be used in the calculations. An averaged value of 1500 (based on volume fractions) was used. The activity of water was assumed to be 1. With equations (34) and (35) the activities were calculated through the membrane using a Runge-Kutta procedure. On each step n the volume fractions ϕ_1 and ϕ_2 were iterated with Secant's method [23]. On the permeate side the activities are assumed to be equal to their partial pressures, since at very low reduced pressures ($p_r = p/p_c$) the activity coefficients are 1. The critical pressures (p_c) are 217.7 and 40.5 atm for water and toluene, respectively [24] and the total pressure on the permeate side is assumed to be 0.001 atm, so the activity coefficient is 1. Therefore, the activities of the components are:

$$a_{p,i} = p_p y_{p,i} = p_p \frac{J_i}{J_1 + J_2} \quad . \tag{36}$$

The (vapor) volume fractions (y) are assumed to be proportional to their fluxes. The pressure at the membrane interface at the vapor side is assumed to be p_p, so the activities at the membrane surface are equal to those in the vapor phase:

$$a'_{p,i} = a_{p,i} \quad . \tag{25}$$

The activities at the surface of the membrane ($a'_{p,i}$) are calculated with the Flory-Huggins equations (26) and (27). There is only one set of volume fractions of water and toluene which give the right activity values. The following values are used in the equations:

$V_1 = 1.07 \cdot 10^{-4}$	$\chi_{12} = 12.2$	$\rho_1 = 0.87$	$\gamma_1 = 1500$
$V_2 = 1.8 \cdot 10^{-5}$	$\chi_{13} = 0.3$	$\rho_2 = 1.00$	$\phi_{fb,1} = 2.9 \cdot 10^{-4}$
$V_3 = 0.116$	$\chi_{23} = 6.3$	$\rho_3 = 0.86$	$a_{f,2} = 0.99975$
			$k_{L,1} = 1.3 \cdot 10^{-5}$

Values of V, χ, ρ, $\phi_{fb,1}$ and $k_{L,1}$ are obtained from Nijhuis [17]. The only parameters which are not known are the diffusion coefficients. These coefficients were assumed to be constant (which means: not a function of volume fractions) in the first runs and fitted on the experimental results. Therefore, a computer program was written which calculated volume fraction profiles. Calculations were carried out from the permeate side to the feed side. $\phi_1(1)$ and $\phi_2(1)$ can be calculated from the Flory-Huggins equations. $\phi_3(1)$ can be calculated from: $\phi_1 + \phi_2 + \phi_3 = 1$. The initial activities were given by equation (36).

The activity of toluene in the liquid can be calculated with: $a_i = \gamma_i \phi_i$. This activity must be equal to the activity at the membranes surface (eqns (24) and (25)). Sets of diffusion coefficients were solved with a simplex method until a minimum between the sum of the actual activity values and the calculated values was obtained. The set of water and toluene diffusion coefficients were used to calculate volume fraction profiles at membrane thicknesses of 40, 72, 120 and 200 mm. A diffusion coefficient for toluene (D_1) was found of $3.2 \cdot 10^{-12}$ m^2/s and for water (D_2) of $1.4 \cdot 10^{-11}$ m^2/s. The mean difference between the calculated and real toluene and water activities on the permeate side was about 10 %.

Some concentration dependent diffusion coefficients were also calculated. First, it was tried to find a minimum with linear descriptions:

$$D_1 = D_{0,1}(1 + \kappa_{11}\phi_1 + \lambda_{12}\phi_2) \quad , \tag{37}$$

$$D_2 = D_{0,2}(1 + \kappa_{21}\phi_1 + \lambda_{22}\phi_2) \quad . \tag{38}$$

where κ and λ are fitting constants. It was not possible to give a better description of Nijhuis' experiments with these diffusion coefficients. The relative mean difference

between the calculated and real toluene and water activities were the same as with constant diffusion coefficients. The same can be said about the exponential relationships (39) and (40):

$$D_1 = D_{0,1} \exp(l_{11}\phi_1 + m_{12}\phi_2) \ , \qquad (39)$$

$$D_2 = D_{0,2} \exp(l_{21}\phi_1 + m_{22}\phi_2) \ . \qquad (40)$$

where κ and λ are the fitting constants.

With the diffusion coefficients (for toluene $D_1 = 3.2 \cdot 10^{-12}$ m^2/s and for water $D_2 = 1.4 \cdot 10^{-11}$ m^2/s) it is possible to calculate the fluxes at different membrane thicknesses. This must be done in an iterative way. With a simplex method the two fluxes J_1 and J_2 were solved numerically until the right activities on the feed side were obtained ($a_{f,1} = \gamma \phi_{f,1}$, $a_{f,2} = 0.99975$). These results will be discussed in the next paragraph.

4.4 RESULTS AND DISCUSSION

In this paragraph the numerical results will be given for the removal of toluene from water through EPDM with pervaporation as a function of the membrane thickness. Also the mass transfer coefficient in the feed and the feed concentration has been varied. Standard conditions are a mass transfer coefficient of $1.3 \cdot 10^{-5}$ m/s and a toluene concentration of 250 ppm in the feed. Fluxes have been reported in m/s. These values may be multiplied by approximately $36 \cdot 10^8$ for toluene and $7.0 \cdot 10^8$ for water to get g/m^2.h as a unit.

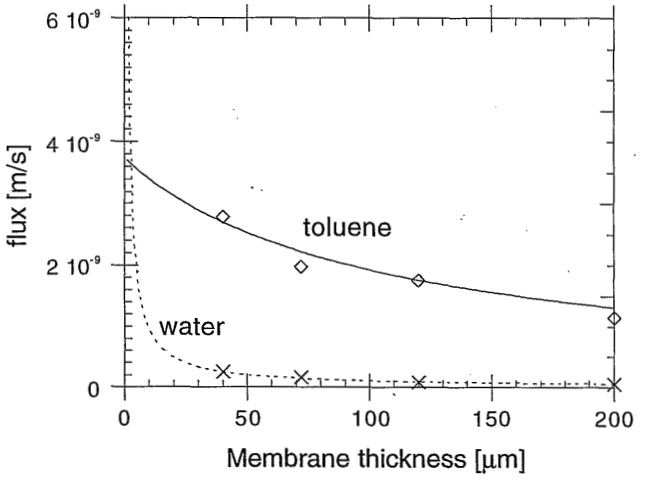

Figure 2 *Experimental flux (◊ for toluene and x for water) and simulated flux (line) as a function of the membrane thickness (feed toluene concentration = 250 ppm and $k_L = 1.3 \cdot 10^{-5}$ m/s)*

Fig.2 shows the experimental toluene and water fluxes and the simulated curves as a

function of the membrane thickness. The most important conclusion which can be drawn from these results is that a further decrease in membrane thickness is not very effective since the water flux will increase strongly and the toluene flux only a little.

Fig.3 is basically the same as fig.2 and shows the toluene and water flux as a function of the reciprocal thickness. Furthermore, the fluxes have been calculated for higher and lower mass transfer coefficients. Various values were taken which might be characteristic for a simple plate-and-frame module $k_L = 1.3 \cdot 10^{-6}$ m/s, for a very well stirred flat membrane module or inside flow capillary module $k_L = 1.3 \cdot 10^{-5}$ m/s and for well spacered spiral wound and transverse flow modules $k_L = 1.3 \cdot 10^{-4}$ m/s.

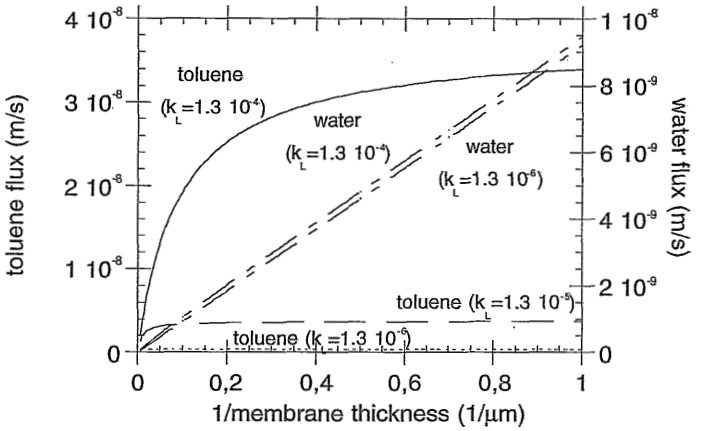

Figure 3 *Fluxes versus the reciprocal membrane thickness for various values of* k_L.

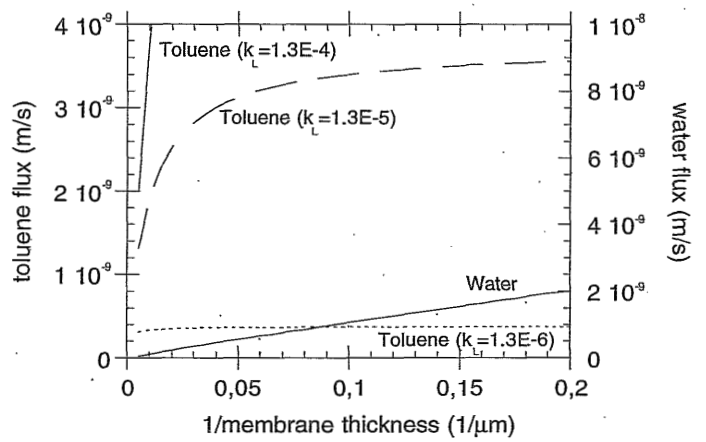

Figure 4 *Magnification of figure 3.*

Fig.3 shows how the toluene flux depends strongly on the mass transfer in the feed. The toluene flux for a 20 μm thick (= 0.05 μm^{-1}) membrane changes approximately linearly with the mass tranfer coefficient. On the other hand, the water flux increases linear with the reciprocal value of the membrane thickness as may be expected. This

latter parameter depends hardly on k_L. With a higher value of k_L the toluene concentration in the membrane film increases, consequently the swelling increases a little and the water flux might increase slightly. The influence of the toluene concentration on the water flux is clearly demonstrated by fig.5 and 6. In fig.5 a 10 thick μm membrane has been simulated and in fig.6 a 200 μm thick membrane. For the thinner membrane the water flux increases roughly 5 % while for the thicker membrane an increase of roughly 50 % can be observed when the toluene concentration increases from 0 to 500 ppm. This may be ascribed to the effect of swelling which results in an increase in diffusion coefficient and which is more pronounced for thicker membranes. Ji et al. [1] show in their results indeed a water flux increase of about 10 % when the concentration of toluene in the feedis increased from 120 to 500 ppm for a 27 μm polyether-block-polyamide membrane. In Chapter 3 of this thesis a water flux increase of 100% is found when the toluene concentration increases from 0 to 300 ppm for a 163 μm EPDM film.

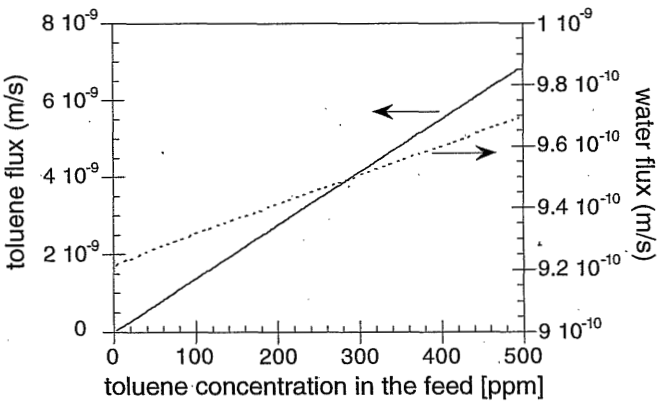

Figure 5 *Water flux and toluene flux versus the toluene feed concentration for a 10 μm thick membrane ($k_L = 1.3 \cdot 10^{-5}$ m/s).*

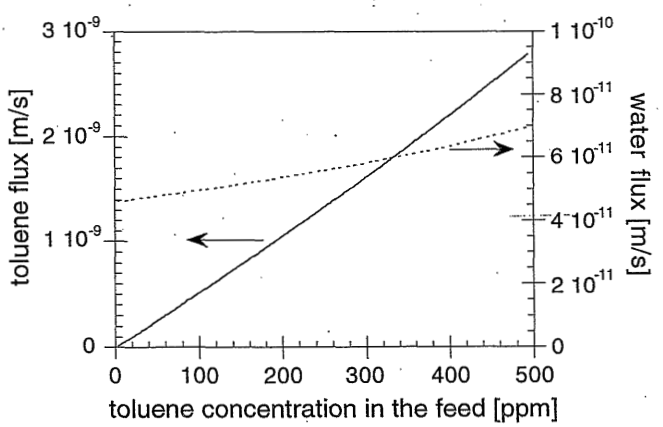

Figure 6 *Water flux and toluene flux versus the feed toluene concentration for a 200 μm thick membrane ($k_L = 1.3 \cdot 10^{-5}$ m/s).*

On the other hand, the toluene flux increases linearly with the toluene concentration. Fig.7 shows the relative difference in water flux from the film model (J^{FM}) and the solution-diffusion model (J^{SD}) (= $(J^{SD}-J^{FM})/J^{SD}$). In the film model the water diffusion coefficient does not depend on the toluene present. In the SD-model the toluene concentration dependence has been incorporated by the Flory-Huggins interaction parameter. The maximum difference with the film theory is about 25 % which is caused by interaction effects (ranged by the maximum amount of water which can be present with toluene and EPDM). Finally, fig.8 represents the selectivity as a function of the membrane thickness and k_L value. It is clear that even for the highest mass tranfer coefficient the selectivity drops steep for membranes thinner than 20 μm.

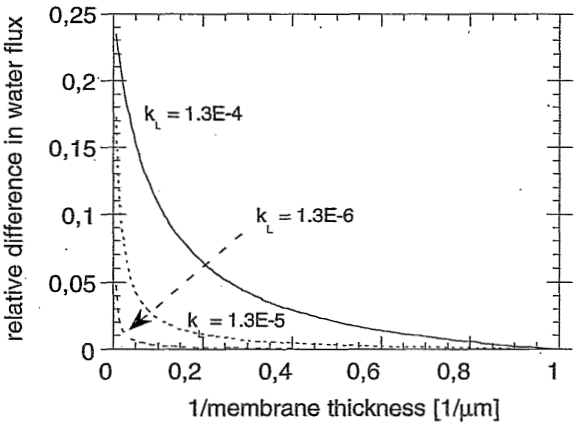

Figure 7 *Difference in water fluxes when film model and SD-model are compared versus the membrane thickness and k_L in m/s.*

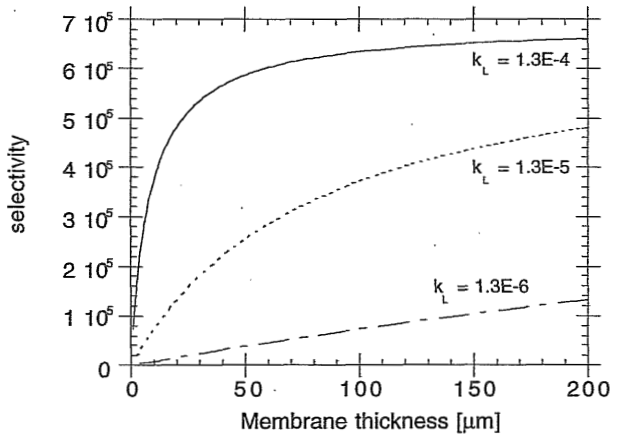

Figure 8 *Overall selectivity versus the membrane thickness and k_L in m/s.*

4.5 CONCLUSION

The resistances-in-series model with a modified solution-diffusion model, the Flory-Rehner theory and the film theory incorporated have been used to calculate the diffusion coefficients of two components in a liquid feed which are separated by pervaporation. To predict the behaviour of the pervaporative removal of toluene from water by EPDM some basic data were used from literature [17]. The Flory-Rehner theory was used to calculate the activity. Both concentration dependent and independent diffusion coefficients have been determined by numerical methods. The difference between these coefficients was less than 1%, so it was decided to use a concentration independent diffusion coefficient. A diffusion coefficient for toluene (D_1) was found of $3.2 \cdot 10^{-12}$ m^2/s and for water (D_2) of $1.4 \cdot 10^{-11}$ m^2/s. Concentration dependent diffusion coefficients did not improve the results.

These values have been used to calculate the toluene and water fluxes in case of a membrane thickness between 200 μm and 1 μm. Furthermore, the mass transfer coefficient (k_L) has been changed. It has been shown that the toluene flux depends strongly on k_L. The toluene flux depends only on the membrane thickness for very high values of k_L ($> 10^{-4}$ m/s). It may be concluded that $k_L = 10^{-5}$ m/s is too small since the toluene can increase strongly at higher k_L.

The water flux increases (almost) linear with the reciprocal value of the membrane thickness. It hardly changes for different k_L. This small difference for different feed toluene concentration was found in Chapter 3 of this thesis to actually occur. A simple film model is sufficient to describe the water flux.

ACKNOWLEDGEMENTS

Bert Bosch is kindly acknowledged for the programming of the numerical procedure.

LIST OF SYMBOLS

Roman symbols

a	= activity	[-]
D	= diffusion coefficient	[m^2/s]
f,g,h	= constants	[-]
J	= flux	[$m^3/m^2 s$]
k	= mass transfer coefficient	[m/s]
l	= thickness of membrane	[m]
l,m	= constants as used in equation (32)	[-]
M	= molecular weight	[gram/mol]
m	= number of layers, in which the membrane is subdivided	[-]
n	= place on membrane in discrete analogon	[-]
p	= pressure	[N/m^2]

P	= permeability	[m^2/s]
R	= gas constant	[Joule/mol K]
s	= partition coefficient	[-]
T	= temperature	[K]
V	= molar volume	[m^3 /mol]
W	= weight fraction	[-]
x	= place in membrane	[m]

Greek symbols

α	= separation factor	[-]
β	= enrichment factor	[-]
γ	= activity coefficient	[-]
μ	= thermodynamic potential	[Joule/mol]
ρ	= density	[kg/m^3]
τ	= plasticizing coefficient	[m^3 /mol]
ϕ	= volume fraction (concentration)	[-]
χ	= interaction parameter	[-]

Subscripts

b	= bulk
c	= crosslinking
f	= feed side
i	= component
j	= component
m	= membrane
p	= permeate side

Superscripts

'	= inside the membrane

REFERENCES

[1] Ji, W., S.K.Sikdar, S.-T.Hwang, *Modeling of multicomponent pervaporation for removal of volatile organic compounds from water*, J.Membr.Sci., 93 (1994) 1-19.

[2] Michaels, A.S., *Effects of feed-side solute polarization on pervaporative stripping of volatile organic solutes from dilute aqueous solution: a generalized analytical treatment*, J.Membr.Sci., 101 (1995) 117-126.

[3] Ji, W., A.Hilaly, S.K.Sikdar, S.-T.Hwang, *Optimization of multicomponent pervaporation for removal of volatile organic compounds from water*, J.Membr.Sci., 97 (1994) 109-25.

[4] Gooding, C.H., P.J.Hickey, P.Dettenberg, J.Cobb, *Mass transfer and permeate pressure effects in the pervaporation of VOCs from water*, in: R.Bakish (ed), Proc.6th Int.Conf.Perv.Procs. Chem.Ind.; Ottawa (CND), Bakish Materials Corp., Englewood, USA, 1992.

[5] Raghunath, B., S.T.Hwang, *General treatment of liquid phase boundary layer resistance in the pervaporation of dilute aqueous organics through tubular membranes*, J.Membr.Sci., 75 (1992) 29-46.

[6] Wijmans, J.G, R.W.Baker, *A simple predictive treatment of the permeation process in pervaporation,*

J.Membr.Sci., 79 (1993) 101.

[7] Feng, X., R.Y.M.Huang, *Concentration polarization in pervaporation separation processes,* J.Membr.Sci., 92 (1994) 201-208.

[8] Mulder, M.H.V., C.A.Smolders, *On the Mechanism of Separation of Ethanol/Water Mixtures by Pervaporation. I. Calculation of Concentration Profiles,* J.Membr.Sci., 17 (1984) 289-307.

[9] Heintz, A. W.Stephan, *A generalized solution-diffusion model of the pervaporation process through composite membranes.- Part II. Concentration polarization, coupled diffusion and the influence of the porous support layer,* J.Membr.Sci., 89 (1994) 153-169.

[10] Wesselingh, J.P., R.Krishna, *Mass transfer,* Ellis Horwood limited, 1990.

[11] Mulder, M.H.V., *Thermodynamic Principles of Pervaporation,* in: R.Y.M.Huang (ed), *Pervaporation Membrane Separation Processes,* Membrane Science and Technology Series, 1991.

[12] Greenlaw, F.W., R.A.Shelden, E.V.Thompson, *Dependence of Diffusive Permeation Rates on Upstream and Downstream Pressures. II. Two Component Permeant,* J.Membr.Sci., 2 (1977) 333-348.

[13] Long, R.B., *Liquid permeation through plastic films,* Ind.Eng.Chem.Fundam., 4 (1965) 445-451.

[14] Merten, U, *Transport Properties of Osmotic Membranes, Desalination by Reverse Osmosis,* The M.I.T. Press, Cambridge, 1966.

[15] Londsdale, H.K., U.Merten, R.L.Riley, *Cellulose Acetate Osmotic Membranes,* J.Appl.Polym.Sci., 9 (1965) 1341.

[16] Lee, C.H., *Theory of Reverse Osmosis and Some Other Membrane Permeation Operations,* J.Applied Polym.Sci., 19 (1975) 83-95.

[17] Nijhuis, H, *Removal of Trace Organics from Water by Pervaporation,* PhD-thesis, University of Twente (NL), 1990.

[18] Flory, P.J., *Principles of Polymer Chemistry,* Cornell University Press, Ithaca, New York, 1953.

[19] Karger, B.L., P.A.Sewell, R.C.Castells, J. Colloid Interface Science, 35 (1971) 328.

[20] Thomas, E.R., B.A.Newman, T.C.Long, D.A.Wood, C.A.Eckert, J.Chem.Eng.Data, 27 (1982) 399.

[21] Economou, I.G., P.Vimalchaud, M.D.Donohue, Fluid Phase Equilibria, 68 (1991) 131.

[22] Nielsen, F., E.Olsen, A.Fredenslund, *Henry's law constants and infinite dilution activity coefficients for volatile organic compounds in water by a validated batch air stripping method,* Environ. Sci. Technol., 28 (1994) 2133 - 2138.

[23] Press, W.H., B.P.Flannery, S.A.Teukolsky, W.T.Vetterling, *Numerical recipes in Pascal,* Press Syndicate of the university of Cambridge, Cambridge, 1990.

[24] Vargaftik, N.B., *Handbook of Physical Properties of Liquids and Gases, Pure Substances and Mixtures,* second edition (1975).

5

PREPARATION AND CHARACTERIZATION OF POROUS SUPPORT MATERIALS

SUMMARY

Poly(ether imide) and poly(ether sulfone) capillaries were spun by a dry-wet spinning technique with 1-methyl-5-pyrrolidone as the solvent and water as the nonsolvent. Several high and low molecular additives were added to the polymer solution; poly(vinyl pyrrolidone), lithium nitrate, water and diethylene glycol. Characterization has been performed by gas permeation, liquid-liquid displacement and scanning electron microscopy. Several porous ultrafiltration membranes were selected as support for composite membranes. A whole range of pore sizes and pressure-normalized gas fluxes were covered. The support with the lowest overall porosity had a P/l-value of 0.03 cm^3(STP)/ (cm^2.s.cmHg) and a narrow pore radius distribution of 6 to 10 nm with a maximum pore radius of 20 nm. The support with the highest porosity had a P/l-value of 0.8 cm^3(STP)/ (cm^2.s.cmHg) and a maximum surface pore radius of 0.6 μm.

5.1 INTRODUCTION

In this chapter the preparation of porous membranes of poly(ether imide) (PEI) or poly(ether sulfone) (PES) will be discussed. Some of these membranes will be used as support materials for composite membranes The most important properties of such materials are a high mechanical and thermal stability and a low resistance to mass transfer. A pressure-normalized gas flux (or P/l-value) of at least 0.01 $cm^3/(cm^2.s.cmHg)$ was used as a criterion. In this way the contribution of the support resistance is less than 0.1% of the overall resistance since a typical P/l-value for a composite membrane is less than 10^{-5} cm^3 (STP)/(cm^2.s.cmHg). Previous studies by Borges [1] showed that the pore size of the support is very important in the coating procedure, because many coating-steps were necessary to obtain defect-free membranes. On the other hand, small pores usually mean a low porosity. To study the effect of penetration several support membranes with sharp pore size distributions in the range of 5 to 500 nm were developed.

5.2 SHORT INTRODUCTION ON HOLLOW FIBER SPINNING

Phase inversion membranes can be prepared as flat sheets or hollow fibers. There are various ways to spin hollow fibers and in this project the dry-wet technique was used. Immersion precipitation is a widely used membrane forming process [2-6]. In this technique a polymer solution is pumped through a spinneret, together with a bore liquid. Before entering the outer coagulation bath, the nascent fiber is in contact with an air gap containing a defined water vapor pressure. Complete precipitation will occur after immersion in the coagulation bath. Spinning parameters are, i.e.:

- composition of the polymer solution (additives) and the bore liquid
- flow rate of polymer solution and bore liquid from the spinneret
- residence time, temperature and composition of the air gap
- coagulation bath temperature and composition.

The membrane morphology can be adjusted by changing these variables. In general, a more open structure is obtained when the polymer concentration in the polymer solution decreases, the water vapor concentration in the air gap increases and the residence time in the air gap increases when the solvent is non-volatile. If a volatile solvent is used then evaporation will occur in the air gap and the polymer concentration at the surface increases and a denser structure will be obtained.

The pore size at the inner surface of the capillary can be changed by the composition of the lumen solution. The higher the content of solvent in the lumen the bigger the pores will be.

Two different spinning systems have been used to prepare capillary supports for the composite membranes; poly(ether sulfone) (PES) as the membrane forming polymer and poly(vinyl pyrrolidone) (PVP) as the additive and poly(ether imide) (PEI) with lithium nitrate ($LiNO_3$), diethylene glycol (DEG)

or water as the additive. 1-Methyl-2-pyrrolidone (NMP) was used as the solvent for both systems and water as the coagulant.

The effect of PVP as an additive on the properties of microfiltration and ultrafiltration membanes has been described well in literature [3,7-9]. Due to PVP the viscosity of the polymer solution increases and the pore interconnectivity in the final membrane increase. However, an important drawback is pore blockage due to swelling of PVP in aqueous feed solutions and in humid atmospheres, which leads to a higher transmembrane resistance. A hypochlorite treatment is used to remove the excessive PVP [3]. The hypochlorite reacts with the PVP chain after which it can be flushed out with water [10]. However, the membranes become quite brittle upon this post-treatment.

$LiNO_3$ as an additive has been investigated by Borges [1]. This salt increases the viscosity of the spinning solution as well. It was shown that promising supports could be formed without the use of PVP. Water is an interesting additive and allows to locate the initial solution composition very close to the binodal at low polymer concentration. This favours the formation of membranes with many small pores [11]. However, the viscosity is not increased and as a consequence spinning is difficult. Di(ethylene glycol) has been chosen as an additive for its well known viscosity enhancing properties [3].

5.3 MATERIALS AND METHODS

5.3.1 Materials

For the spinning experiments poly(ether sulfone) (PES) was purchased from *BASF* (Ultrason) and poly(ether imide) (PEI) was kindly supplied by *GEP* (Ultem 1000). The solvent 1-methyl-2-pyrrolidone (NMP) was purchased from *Merck* (synthesis grade). The additives were poly(vinyl pyrrolidone) (*Janssen Chimica*, K90), lithium nitrate (*Merck*), diethylene-glycol (*Merck*, synthesis grade) and ultrafiltrated-demineralized (UF-demi) water. This water was also used for the coagulation bath. Prior to use PES and PEI were kept in a nitrogen atmosphere at 150° C for four hours. After spinning the capillaries were dried via a subsequent ethanol-hexane step (synthesis grade, *Merck*). Both solvents were used without further purification.

For the liquid-liquid displacement experiments UF-demi water and iso-butanol (analysis grade, *Merck*) were used.

For the gas permeation experiments nitrogen and carbon dioxide were used (*Hoekloos*).

5.3.2 The spinning process

The polymer solution was filtered through a 40 μm stainless steel filter and degassed overnight at 50° C prior to spinning. The spinning set-up is schematically depicted in fig.1. During the spinning process the polymer solution is extruded through a tube-in-orifice spinneret. The bore liquid is fed by an HPLC-pump pumped via a pulse-damper through the inner orifice of the spinneret. The extruded polymer solution goes through an air gap into the thermostated

coagulation bath (UF-demi water). After coagulation the fibers were rinsed with warm tap water and then cut in pieces of about 40 cm. Finally, these cut fibers were rinsed with warm tap water (50° C) for 24 hours.

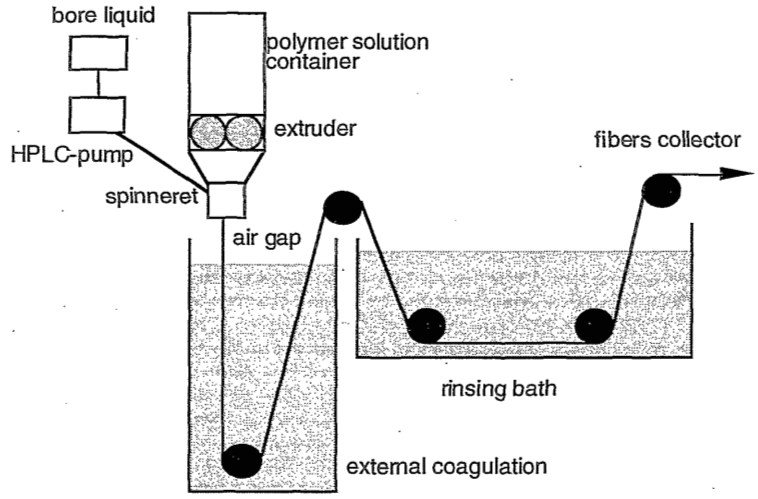

Figure 1 *Schematic drawing of the spinning set-up.*

The membranes have been dried via an ethanol-hexane procedure [12]. The capillaries have been characterized by scanning electron microscopy (SEM), gas permeation, Coulter®-porometry and liquid-liquid displacement experiments.

a. PES-capillaries

The spinning solution contained PES, PVP and NMP. The coagulation bath contained UF-demi water. For the preparation of the PES fibers a number of parameters have been varied and these are summarized in table 1.

Table 1 *Preparation of PES capillaries.*

Polymer solution composition	13 wt-% PES; 13 or 17 wt-% PVP; NMP
Bore liquid composition	20/80, 30/70, 40/60 or 50/50 wt-% H_2O/NMP mixture
Residence time in the air gap	0.5, 0.8, 1.7 and 2.5 seconds
Spinning temperature	50° C
Coagulation bath temperature	70° C

After preparation the fibers were exposed to a post-treatment with 4000 ppm hypochlorite for 48 hours and then rinsed with warm water for 24 hours.

b. PEI-capillaries

Also for the system PEI /NMP /H_2O with $LiNO_3$, H_2O or diethylene glycol (DEG) as an additive various spinning parameters have been changed systematically and these have been summarized in table 2.

Table 2 *Preparation of PEI capillaries.*

Polymer solution composition	13, 15, 16 or 18 wt-% PEI; 6 wt-% LiNO3 or H_2O or 20 wt-% DEG; NMP
Bore liquid composition	0/100, 3/97, 5/95 10/90, 15/85, 20/80, 40/60, 60/40, 80/20 and 100/0 wt-% H_2O/NMP mixture
Residence time in the air gap	0, 0.7, 1.1, 1.3, 2.5 and 2.7 seconds
Spinning temperature	25° and 50° C.
Coagulation bath temperature	25, 41, 55, 70 and 73° C.

All membranes have been flushed with warm water for 48 hours and dried to air via an ethanol-hexane procedure before they were characterized with SEM, gas permeation and liquid-liquid displacement (LLD).

5.3.3 Scanning electron microscopy

With the SEM (*Jeol* T-220A) a good impression of the morphology of the membrane can be obtained. Typically magnifications of 35,000X are possible and structures with pores of 0.05 μm can be observed. The samples have been prepared by breaking the fibers after immersion in liquid nitrogen to get a clear cross-section. The samples were then covered with a thin gold layer, to improve the conductivity and to prevent burning in the SEM. Typically, pictures are taken from the cross-section (wall thickness and skin layer thickness) and from the surface to look for defects or irregularities and to estimate the surface pore size.

5.3.4 Gas permeation

A capillary is mounted into a simple module. An absolute pressure of 1.5 bar was applied on the outside. The permeate was led through Brooks mass flow meters at 1 bar. Via calibration curves the permeation rate could be calculated. Nitrogen and carbon dioxide were used as gases.

5.3.5 Liquid-liquid displacement

For an extensive describtion of this technique the reader is referred to Wienk [5]. Here only the basics will be discussed.

The fibers were mounted into the same modules as used with the gas permeation. For 16 hours the fibers were immersed in the better wetting liquid which was an iso-butanol (i-BuOH) phase saturated with UF-demi water. The displacing phase was water saturated with i-BuOH. Prior to use the liquids were degassed ultrasonically for one hour.

The displacing liquid was applied from the outside of the membrane. The inside was freely connected to air (1 bar). The pressure generated at the outside was measured as a function of a constant flux which was applied by an HPLC-pump (*Waters* 590). When the flux is adjusted the pressure will increase until the first pores open. Then the pressure will decrease until a constant pressure is obtained. At the maximum the radius of the pores which open at that specific

pressure can be calculated using the Laplace equation:

$$\Delta p = \frac{2\gamma}{r}\cos\theta \quad , \qquad (1)$$

in which Δp is the pressure difference applied over the membrane [Pa], γ the interfacial tension of the two liquids [N/m], r is the radius of a pore [m] and θ is contact angle between the displacing liquid and the pore wall. It is assumed that complete wetting occurs, i.e. $\cos\theta$ is 1. From the constant value of the pressure at a certain flux the number of pores at a certain radius can be calculated by the Poiseuille equation:

$$J = \frac{\pi \sum_i n_i r_i^4}{8\,\eta\,\tau\,l}\Delta p \quad , \qquad (3)$$

in which J is the flux [m/s], Δp the pressure difference across the membrane [Pa], r_i the pore radius [m], n_i the number of pores of radius r_i per unit of cross section [m^{-2}], η the viscosity of the permeating fluid [Pa.s], l the toplayer thickness [m] and τ the tortuosity factor [-].

5.4 RESULTS AND DISCUSSION

5.4.1 PES-capillaries

a. Air gap

The most effective results in terms of P/l value and outer surface pore radius were obtained by changing the residence time in the air gap. With the SEM it was observed that the pore size at the outer skin surface increased (0.2-0.5 μm) and the P/l-values increased (0.4 - 0.8 cm^3 (STP)/ (cm^2.s.cmHg)) with increasing the air gap residence time (0.2 - 2.5 s). This trend was expected and was found in literature [9].

b. PVP concentration

Membranes were spun from solutions containing PES/PVP-ratio's of 13/13 and 13/17. Based on SEM image analysis it can be concluded that the surface pore size increases from 0.3 to 0.5 μm with increasing PVP-content with a constant air gap residence time of 2.5 seconds.

Furthermore, it was possible to spin membranes with a ratio of PES/PVP of 0.76. Boom et al. reasoned that no PES-matrix would be formed below the critical line, as derived from thermodynamics of quaternary systems. This critical ratio of PES/PVP is about 1 in the case of PES-PVP-NMP [13]. Therefore, based on our results their conclusion should be considered premature.

c. Solvent concentration in lumen

The NMP concentration in the lumen was changed from 50 to 70 wt-%. The pore

size at the inner surface increased considerably from 2 to 20 μm. No influence on the P/l-values were found, which implies that the resistant is, indeed, at the outer skin of the membrane.

d. Supports

PES-capillaries were spun with characteristics as listed in table 3.

Table 3 *Range of characterization results of PES-capillaries.*

P/l [cm^3 (STP)/(cm^2.s.cmHg)]	0.1 - 0.8
Maximum pore radius (SEM) [μm]	0.2 - 0.6

Two porous microfiltration membranes were chosen as substructures for composite membranes. The first one (referred to as CP1 in this thesis) has a P/l-value of 0.2 cm^3/ (cm^2.s.cmHg) and a maximum pore size at the surface of about 0.2 μm as observed by SEM. SEM-pictures of the cross-section, outer and inner surface of this membrane are depicted in fig.2. The second substructure (CP2) has a P/l-value of 0.15 cm^3/ (cm^2.s.cmHg) and a maximum pore size at the surface of about 0.1 μm as observed by SEM.

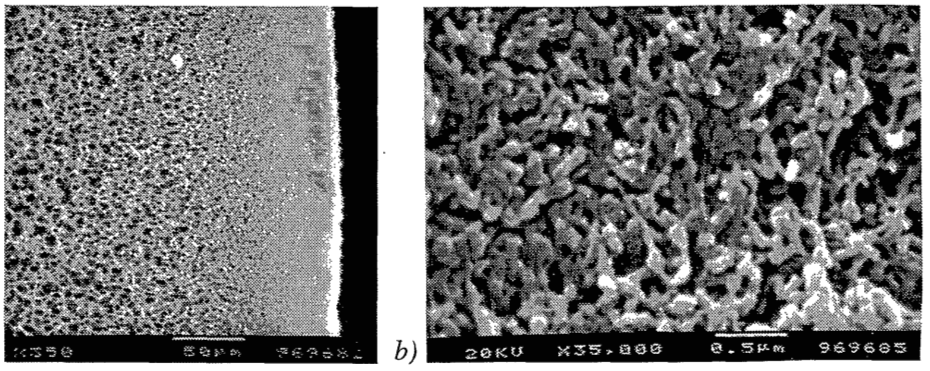

Figure 2 *SEM photographs of PES-capillary (CP1), cross-section, outer and inner surface, respectively.*

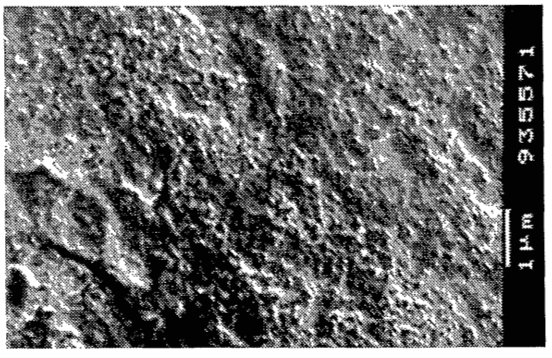

Figure 3 *SEM photograph of PES-capillary (CP2) of the outer surface.*

5.4.2 PEI-capillaries

a. Air gap and polymer concentration

The change of the pore radius and the P/l-values for the PEI-capillaries with different air gap residence times or polymer concentrations showed the same trend as those of the PES-capillaries. Many PEI-capillaries show a very low surface pore size as observed by SEM. These capillaries were characterized by liquid-liquid displacement. The pore size and the P/l-value increase when the residence time increases. Further, the pore size and the P/l-value increase also when the PEI concentration decreases. Also, for PEI-capillaries these trends were found and explained in literature [3]. The range of values of the pore size and the P/l-values was broader due to variation of the polymer concentration (13-18 wt-% PEI) in the polymer solution while for the PES-capillaries the PES-concentration was constant (13 wt-% PES).

b. Coagulation bath temperature

The gas permeability and the outer skin pore size increase when the outer coagulation bath temperature increases. For instance, for a 15 wt-% PEI with $LiNO_3$ as the additive the P/l increases from 0.04 to 0.1 cm^3 (STP)/ (cm^2.s.cmHg) when the coagulation bath temperature increases from 25° to 70° C.

c. Bore side composition

At a lumen concentration of less than 95 wt-% NMP an extra skin was formed at the inside of the membranes as observed by SEM, resulting in a higher resistance as observed by gas permeation measurements.

d. Additives

It could not be predicted on forehand which of the additives would lead to the higher P/l values and larger pore sizes. Because of the different concentrations of additives (6 % H_2O or 6 % $LiNO_3$ or 20 % DEG) in the polymer solution and due to the complexity of the spinning process it is also difficult to make any comparison and no clear conclusion could be drawn.

e. Supports

Table 4 shows the range of results obtained from the spinning experiments with PEI.

Table 4 *Range of characterization results of PEI-capillaries.*

P/l [cm^3 (STP)/(cm^2.s.cmHg)]	5.10^{-3} - 0.1
Maximum pore radius (SEM) [μm]	<0.03 - 0.5
Maximum pore size (liquid-liquid displacement*) [μm]	0.007 - 0.060

* Not all fibers have been characterized by this method

For instance, one capillary (referred to as JQ1 in this thesis) has a P/l-value of 0.06 $cm^3/(cm^2.s.cmHg)$. The morphology of these capillaries are depicted in fig.4. The cross-section and the inner surface pictures show that the macrovoids grow through to the bore side. The maximum pore size at the outer surface seems less than 50 nm as no clear pores have been observed by SEM at a magnification of 35.000X. Liquid-liquid displacement experiments have been carried out (fig.5), which reveals a pore diameter of 10 to 50 nm with a maximum of 70 nm.

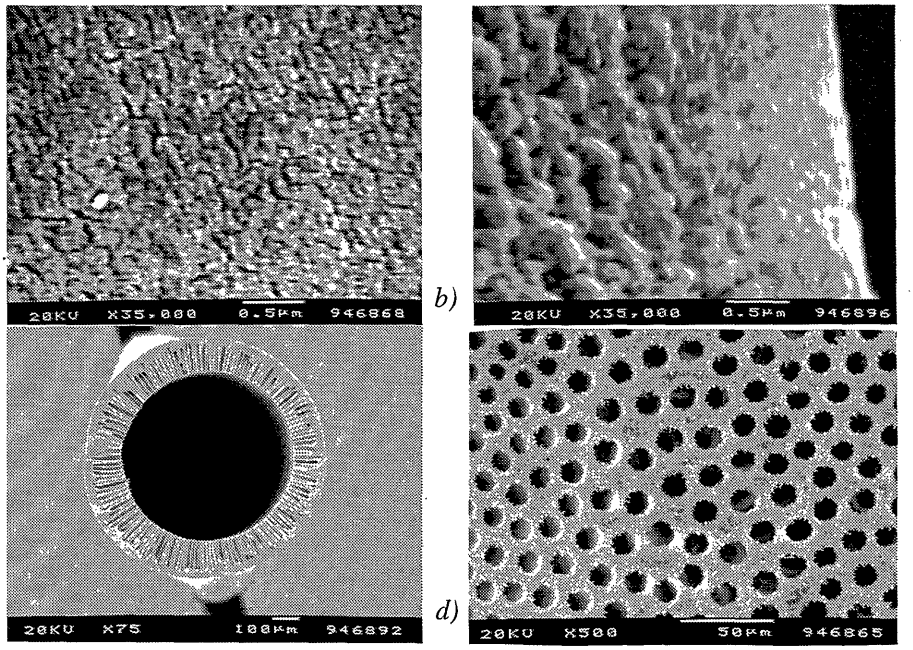

Figure 4 *SEM photographs of a PEI-capillary (JQ1). a) surface, b) cross section of outside skin, c) cross section of the capillary, d) surface of lumen.*

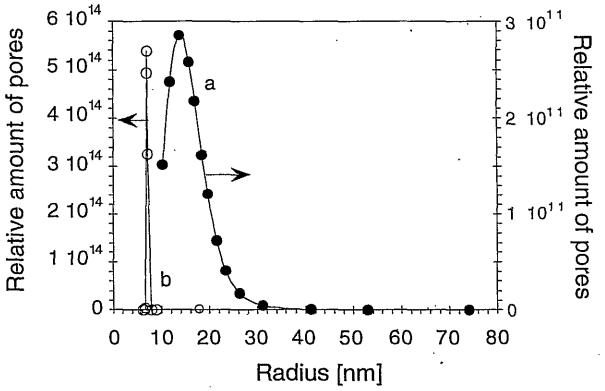

Figure 5 *Pore size distribution of PEI-capillaries as obtained from LLD.*
a) JQ1: PEI/$LiNO_3$/H_2O/NMP = 13/0.25/4.25/82.5
b) JQ2: PEI/DEG/NMP = 18/20/62.

Another capillary (JQ2) has a P/l-value of 0.03 $cm^3/cm^2.s.cmHg$ and the pore radius ranges from 6 to 10 nm with a maximum pore size of 18 nm (fig.5).

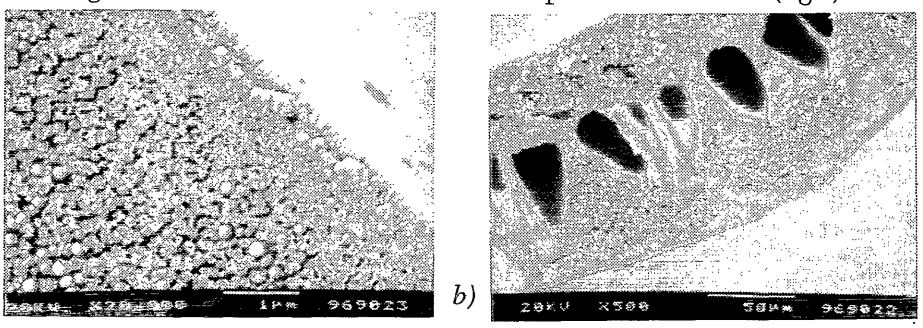

Figure 6 *SEM images of a PEI-capillary (JQ2). a) cross section of outside skin, b) cross section of the capillary.*

5.5 CONCLUSION

Many different support membranes have been prepared with respect to their gas permeation rates, morphologies and pore size distributions. Main spinning parameters investigated were the polymer and the additive concentration in the spinning dope, concentration of solvent in the bore liquid, residence time in the air gap and the spinning temperature. The trends of the obtained results were as expected from literature. A wide range of P/l-values (0.005 - 0.8 $cm^3/(cm^2.s.cmHg)$) and surface pore radii (10 - 500 nm) were obtained.

ACKNOWLEDGEMENTS

Kees Plug and Jianjun Qin are kindly acknowledge for the spinning and characterization of most of the PES- and PEI-supports.

REFERENCES

[1] Borges, C.P., M.H.V.Mulder, C.A.Smolders, *Support effect of composite hollow fiber for removal of VOC's from water by pervaporation*, in: Habert, C., E.Drioli (eds), *Workshop CEE-Brazil on membrane separation processes*, Rio de Janeiro (BRA), 1992.

[2] Hof, J.A.van 't, *Wet spinning of asymmetric hollow fibre membranes for gas separation*, PhD-thesis, University of Twente, Enschede (NL), 1988.

[3] Roesink, H.D.W., *Microfiltration - membrane development and module design*, PhD-thesis, University of Twente, Enschede (NL), 1988.

[4] Koops, G.-H., *Dehydration of acetic acid by pervaporation; material science aspects*, PhD-Thesis, University of Twente, Enschede (NL), 1992.

[5] Wienk, I.M., *Ultrafiltration membranes from a polymer blend, Hollow fiber prepartion and characterization*, PhD-Thesis, University of Twente, Enschede (NL), 1993.

[6] Li, S.-G., *Preparation of hollow fiber membranes for gas separation*, PhD-Thesis, University of

Twente, Enschede (NL), 1994.

[7] Cabasso, I., E.Klein, J.K.Smith, *Polysulfone hollow fibers. II. Morphology*, J.Appl.Pol.Sci., 21 (1977) 165.

[8] Miao, X., S.Sourirajan, W.W.Y.Lau, *Production of polyethersulfone hollow fiber ultrafiltration membranes. II. Effects of fiber extrusion pressure and PVP concentration in the spinning solution*, Sep.Sci.Technol., 31 (1996) 327-348.

[9] Wienk, I.M., F.H.A.OldeScholtenhuis, *Spinning of hollow fiber ultrafiltration membranes from a polymer blend*, J.Membr.Sci., 106 (1995) 233-243.

[10] Wienk, I.M., E.E.B.Meuleman, Z.Borneman, A.vandenBoomgaard, C.A.Smolders, *Chemical treatment of membranes of a polymer blend: mechanism of the reaction of hypochlorite with poly(vinyl pyrrolidone)*, J.Polym.Sci.: part A: Polymer Chemistry, 33 (1995) 49-54.

[11] Altena, F.W., *Phase separation phenomena in cellulose acetate solutions in relation to asymmetric membrane formation*, PhD-Thesis, University of Twente, Enschede (NL), 1982.

[12] Beerlage, M.A.M., *Polyimide ultrafiltration membranes for non-aqueous systems*, PhD-thesis, University of Twente, Enschede (NL), 1994.

[13] Boom, R.M., *Membrane formation by immersion precipitation: The role of a polymeric additive*, PhD-Thesis, University of Twente, Enschede (NL), 1992.

6

PREPARATION OF COMPOSITE MEMBRANES

SUMMARY

Composite membranes were prepared by a dip-coating technique with a polymer solution which contains ethylene-propylene terpolymer (EPDM) in an appropriate solvent. One of the main problems is the penetration of the coating-solution into the pores of the support material. Investigations were performed to prevent penetration. Prior to coating, some capillaries were pre-filled with different liquids, such as hexane, water and a thermo-reversible gel to prevent penetration. It was concluded that water and hexane gave the better results, however, penetration could not be prevented completely. With a coating-solution of 5 wt-% EPDM in hexane, 4 coating steps were needed to obtain defect-free membranes. This was concluded from gas permeation measurements, in which the composite membrane showed the same or higher selectivity than the intrinsic selectivity of the pure EPDM. Only one step was needed when a 10 wt-% EPDM solution was used. However, for these membranes the theoretical toplayer thickness is still higher than the toplayer thickness observed by scanning electron microscopy. Further, the gas selectivities are in between the intrinsic selectivity of the toplayer and the porous support material. This implicates that intrusion of the toplayer material occurs into the pores of the support.

The best properties are obtained with the relatively high porous PES-supports. In this case, the selectivity of the composite membrane is nearly equal to the intrinsic selectivity of the toplayer material and the effective thickness as determined from CO_2 permeation is close to the observed thickness as determined from scanning electron microscopy.

6.1 INTRODUCTION

In this chapter the preparation of composite membranes with poly(ether imide) (PEI) or poly(ether sulfone) (PES) as support and ethylene-propylene terpolymer (EPDM) as toplayer material will be discussed. For any composite membrane the support layer should have a low resistance and provide the mechanical strength for the toplayer. Many methods can be employed to apply the thin toplayer upon the support, i.e., dip-coating, spin-coating, interfacial polymerization, Langmuir-Blodgett technique and plasma polymerization. In this research work dip-coating was used as the coating technique where a support is immersed into a polymer solution which contains the toplayer material. Then either the support is pulled out of the solution or the solution is flowing out. One of the main problems in the preparation of composite membranes by dip-coating is penetration of the toplayer material into the porous support. Various methods have been investigated to prevent this as much as possible, i.e., highly porous support with relatively small pores, pre-filling of support or high polymer concentration.

6.2 BACKGROUND

Pore penetration of the coating solution may lead to defects in the toplayer. Furthermore, pore penetration implies pore-blocking and as a consequence the support layer may have a dominating effect on the separation process. Several methods can be used to prevent penetration. The pores may be (ir)reversely blocked prior to the actual coating experiment. This pre-filling of the pores with a liquid, which is either a nonsolvent or a solvent for the polymer or a gel has already been published [1,2]. Another method is to apply a highly permeable intermediate layer as a 'gutter-layer' between support and toplayer (most commonly used are poly(dimethyl siloxane) or one of its derivates) [3-9].

Also, by varying the coating procedure itself, the penetration can be reduced. Important parameters are the viscosity and the size of the polymer coil in the coating solution. These can be changed by the molecular weight of the polymer, the concentration, the solvent and the temperature. Furthermore, the pore size distribution in the support material is important. Rezac [10] found a direct relation between the radius of gyration of a polymer in a solution, the support layer pore size and the penetration. A better solvent results into a higher radius of gyration and when the pore radii were smaller than this radius defect-free composites could be prepared. The radius of gyration of the EPDM's used is about 6 to 10 nm (see Appendix A to this chapter). Rezac and Koros showed that if the polymer in solution is larger than the pore size of the support the polymer cannot penetrate.

As a post-treatment step a solvent or a swelling vapor or liquid is used to repair defects [11-15]. Due to the high swelling of the polymer, the polymer chains can 'move' and a small defect may be 'repaired'.

A higher polymer concentration in the coating solution causes an

increased viscosity which reduces the ability to penetrate the pores of the support, since the rate of penetration will be inversely proportional to the viscosity [16]. On the other hand, a higher polymer concentration in the coating-solution results in an increase in toplayer thickness of the composite membrane. In most patents on gas separation composite membranes low polymer concentrations in the coating-solution are used to reduce the toplayer thickness as much as possible. However, in the case of the pervaporative removal of organics from water the boundary layer resistance may become very high. Consequently, the toplayer does not have to be 'ultrathin' for these applications and a higher polymer concentration in the coating-solution resulting in a thicker toplayer is allowed and even preferable as less penetration occurs.

Influence of coating parameters on toplayer thickness

Many parameters can be changed effecting the thickness of the coated layer. A dip-coating set-up is illustrated in fig.2 in the experimental section. Fig.1 shows the boundary between the stagnant support and the coating solution which has a certain velocity.

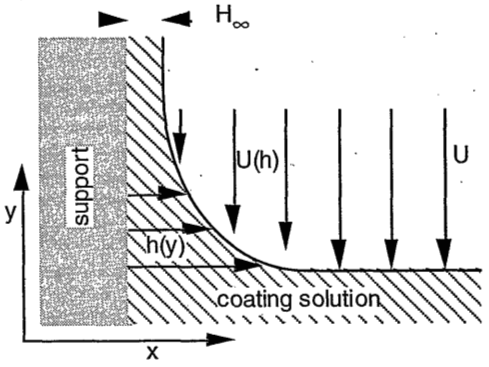

Figure 1 *Schematical illustration of the boundary between the stagnant support and the coating solution. See text for explanation of symbols.*

A relationship, which relates various parameters to the thickness of the coated layer, has been derived for flat surfaces [17]

$$H_\infty = \frac{2}{3}\sqrt{\frac{\eta U}{\rho g}} \quad , \tag{1}$$

where H_∞ is the final toplayer thickness (before drying) [m], U is the coating velocity [m/s], η is the viscosity [Pa.s], ρ is the density [kg/m^3] and g is the gravity acceleration [m/s^2].

Another relation has been derived for the case that a rod-like support material is moved perpendicular to the liquid surface [17]:

$$H_\infty = \frac{k\cdot(\eta\cdot U)^{2/3}}{(\rho\cdot g)^{0.5}\cdot\sigma^{1/6}}\cdot\left(1-\frac{k^2}{3}\cdot\left(\frac{\eta\cdot U}{\sigma}\right)^{1/3}\right) \quad , \tag{2}$$

where σ is the liquid surface tension [N/m] and k is an iteration constant to the height of liquid film (h), the distance from the support (x) and the velocity of the solution level. Both eqn (1) and (2) show that the toplayer thickness increases with increased U and viscosity and it decreases with increasing liquid density. The thickness also depends on the surface tension for curved surfaces (eqn (2)). These calculated film layer thicknesses are of the wet layer. After drying the final toplayer thickness is formed.

6.3 TRANSPORT THROUGH COMPOSITE MEMBRANES

After the composite membranes have been prepared and dried they were characterized by gas permeation. The gas flux is given by

$$J_i = \frac{P_i}{l} \cdot \Delta p_i \ , \qquad (3)$$

where J_i is the flux of component i, P_i is the permeability coefficient of component i, l is the membrane thickness and Δp_i is the pressure difference between the membrane feed and permeate side. P_i/l is also referred to as the pressure-normalized flux. For composite membranes not only the toplayer but also the sublayer may contribute to the membrane resistance. The effect of the sublayer resistance on the separation performance is discussed in Appendix B. The effective thickness of a composite membrane, the ideal selectivity as calculated from gas permeation experiments and the toplayer thickness as observed from SEM (l_{SEM}) are important characteristics to describe the performance of a composite membrane. The ideal selectivity (α) of CO_2 and N_2 for a composite membrane is

$$\alpha = \frac{(P/l)_{CO_2}}{(P/l)_{N_2}} \ . \qquad (4)$$

If α equals the intrinsic selectivity of the support polymer than the resistance in the toplayer material is negligible. If α equals the intrinsic selectivity of the toplayer then the influence of gas transport through the support polymer material is negligible. However, the support may still have a resistance due to low porosity and penetration. Eqn (1) can be rearranged to calculate the effective thickness (l_{eff}):

$$l_{eff} = \left(\frac{\Delta p_{CO_2}}{J_{CO_2}} \right) \cdot P_{CO_2}^{EPDM} \ , \qquad (5)$$

where $P_{CO_2}^{EPDM}$ is the permeability of CO_2 through EPDM. Comparison of l_{eff} and l_{SEM} gives a good first impression of the composite membrane.

Table 1 lists the permeabilities of several gases in various polymers which have been used in this research work.

Table 1 *Gas permeability properties of various polymer materials*

Polymer material	P (N_2) [Barrer]*	P (O_2) [Barrer]*	P (CO_2) [Barrer]*	$\alpha(CO_2/N_2)$ [-]
PES [Kimmerle, 1991; Sanders, 1988]	0.16	1.4	3.4	36
PEI (Ultem 1000) [Bos, 1996]	0.052	0.4	1.3	25
EPDM (25°C, K578) [Duval, 1993]	5.6	17	85	15

* 1 Barrer = 10^{-10} cm^3 (STP).cm / (cm^2.s.cmHg)

6.4 MATERIALS AND METHODS

a. Materials

Ethylene-propylene terpolymer (EPDM) was kindly supplied by *DSM* chemicals (Keltan 578) and was cut into little pieces. n-Hexane was purchased from *Merck* (analysis grade). The crosslink initiator dicumyl peroxide (DCP 98%, *Aldrich*) was used without further purification. Furthermore, ultrafiltrated-demineralized (UF-demi) water has been used. The properties of the supports are summarized in tables 2 and 3.

Table 2 *Properties of PES-capillaries.*

code	P/l [cm^3/cm^2.s.cmHg]	r_{SEM}* [nm]	ε** [%]
CP1	0.19	200	20
CP2	0.15	100	8

* r is the pore radius determined by scanning electron microsopy (SEM)
** ε is porosity determined by SEM-image analysis

Table 3 *Properties of PEI-capillaries.*

code	P/l [cm^3/cm^2.s.cmHg]	r_{SEM} [nm]	r_{peak}* [nm]	r_{max}* [nm]	ε [%]
JQ1	0.06	<30	10 - 30	70	≤1
JQ2	0.03	<30	6 - 10	20	<1

* determined with liquid - liquid displacement

b. Gas permeation

The gas permeation set-up and procedure has been described in Chapter 3. Composite hollow fibers were mounted into a simple module. An absolute pressure of 3.5 bar was applied at the outside of the composite membrane and at the inside a vacuum was maintained of less than 10 Pa.

c. Dip-coating technique

The dip-coating technique has been used to deposit a thin layer of EPDM upon a support. The capillaries are immersed into a pre-filler solution to fill the pores of the support. Then the actual coating occurs in a set-up which is shown schematically in fig.2. A 5 or 10 wt-% EPDM with 5 phr[1] dicumyl peroxide (DCP) in hexane solution is withdrawn with constant velocity by opening a tap at the bottom of the set-up. A thin film has now been applied onto the support. The solvent evaporates in a nitrogen atmosphere and the polymer is crosslinked at 150° C under N_2 atmosphere for one hour in an oven. This procedure can be repeated as many times as necessary. After the first step the impregnation time was 30 seconds. The following parameters were varied:

- pre-filling material used in the pores of the support (none, water, hexane and a water soluble thermo-reversible gel)
- number of coating-steps (1 - 6 times)
- coating-velocity
- pressurized nitrogen atmosphere
- polymer concentration.

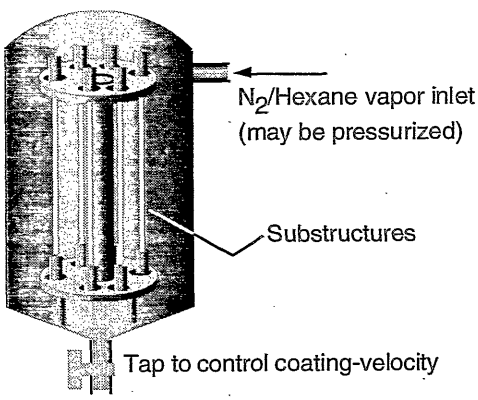

Figure 2 Coating set-up.

For all composites the permeability of CO_2, O_2 and N_2 have been measured at 3.5 bar absolute pressure. The composite membranes will be considered to be defect-free when the observed selectivity is about equal to the intrinsic ideal selectivity of EPDM. Scanning electron microscopy (SEM) was applied to compare the effect of the coating parameters on the coating-thickness and intrusion depth.

[1] phr = gram per hundred gram of rubber

d. Scanning electron microscopy

The preparation of SEM-samples has been described in Chapter 5. With this technique the observed toplayer thickness (l_{SEM}) can be determined. Of a certain fiber two different cross-sections are prepared and the l_{SEM} is the average of these two observed thicknesses.

6.5 RESULTS AND DISCUSSION

6.5.1 Prevention of pore penetration

a. Impregnation

The perfect pre-filler fills the pores of the support, remains during the coating step and can easily be withdrawn from the pores after the drying step. As pre-filler agents a thermo-reversible water soluble gel, hexane and water were used. Prior to coating experiments the pores in the supports were filled with this pre-filler. The hydrophobic PEI-supports were pre-filled with water via hexane and ethanol exchange. Table 4 summarizes the results.

Table 4 *Effect of different pre-fillers on P/l and selectivity, 5 wt-% K578 in hexane.*

Support	Pre-filler	steps*	P/l (CO_2) [$cm^3/(cm^2.s.cmHg)$]	α [-]	l_{eff} [μm]	l_{SEM} [μm]
CP1	none	6		<10		
CP1	hexane**	4	$4.4 \cdot 10^{-6}$	19	19	3.4
CP1	water**	4	$4.3 \cdot 10^{-6}$	18	19	3.9
CP1	gel	1	$9.1 \cdot 10^{-7}$	17	89	-
JQ2	none	3/4	$2.0 \cdot 10^{-6}$	10	43	-
JQ2	hexane	4	$2.0 \cdot 10^{-6}$	18	43	1
JQ2	water**	4	$4.8\ 10^{-6}$	18	17	4

* only first step with pre-filler

** one coating step involves: coating, drying, crosslinking at 150° C.

Results obtained with CP1-supports

4 to 6 coating steps are necessary to obtain a defect-free composite membrane. For the non-pre-filled composite defects still occurred after 6 steps. The membranes pre-filled with hexane and water became defect-free. Their fluxes and selectivities are very much comparable. After one step the P/l-value of the hexane pre-filled composite was 10^{-4} cm^3(STP).cm/(cm^2.s.cmHg) whereas the water pre-filled one was 10^{-3} cm^3(STP).cm/(cm^2.s.cmHg) However, in the next steps they became comparable.

The red coloured thermo-reversible gel was forced into the pores by a vacuum applied on the bore side, at 50° C. Excessive liquid at the surface was

wiped of with a tissue. At 35° C this liquid becomes gelly. After coating with a 5 wt-% EPDM in hexane at ambient conditions and drying of the toplayer, the bore side of the composite was flushed with hot water (70° C) until the red colour disappeared. Gas permeation proved that the membrane was defect-free but the resistance to mass transfer was very high. Obviously, the gel could not be flushed out completely.

Results obtained with JQ2 supports

Table 4 clearly shows the positive effect of water as pre-filler with this support layer. The effective thickness is much lower than without impregnation and with hexane. Without impregnation no defect-free membrane could be obtained. The membranes impregnated with hexane showed a relatively large membrane thickness. This may be caused by diffusion of EPDM into the pores. The coating procedure lasts about 3 minutes. It can be estimated by Einstein's law, which states that the mean square distance is given by $\langle x^2 \rangle = 2D \cdot t$ where D is the diffusion coefficient of a free EPDM-coil in hexane (10^{-7} cm^2/s) and t is the time (200 seconds). The distance a molecule can diffuse (x) in this time is about 63 µm.

Another phenomenon that occurs is that some of the impregnated hexane is removed from the support during the five seconds transport from the impregnation vessel to the coating vessel. A simple experiment was carried out in which the evaporation rate of hexane from the pre-filled capillary was monitored. Within 1 minute 50 wt-% of the hexane was evaporated. Then the transport corresponds to an evaporated hexane layer of about 4 µm. However, theoretically the smaller pores at the skin of the porous support material will remain filled since evaporation first occurs from the larger pores.

b. Different pore size

Table 4 also shows that for this research the kind of support material does not effect the amount of coating steps necessary to obtain defect-free membranes. Both the CP1 membrane with maximum pore radii of about 0.35 µm and the JQ2 membrane with maximum pore radii of about 10 nm had to be coated 4 times. The selectivity is higher than 15 and the effective thickness is much higher than the thickness observed by SEM. This indicates that in both cases pore penetration occurs.

c. Different solvents and EPDM's

The radius of gyration of K4778 in hexane is about 8.3 nm (see Appendix A). This value is about 0.5 nm lower in toluene and about 1 nm higher in cyclohexane. The JQ2 membrane shows a sharp pore size distribution with a peak from 6 to 10 nm and 20 nm as the maximum pore radius. This is in the range of the random coil size. However, table 5 shows that cyclohexane is not better than hexane for the JQ2 capillaries. Obviously, the pores were still not small enough.

Table 5 *Influence of different solvents on penetration. 8 wt-% K4778, 1 step without impregnation.*

Type	P/l (CO_2) [$cm^3/cm^2.s.cmHg$]	α (CO_2/N_2) [-]	l_{eff} [μm]	l_{SEM} [μm]
JQ2/cyclohexane	$2.7\ 10^{-6}$	19.9	34	8-15
JQ2/hexane	$3.0\ 10^{-6}$	19.7	30	7
CP2/cyclohexane	$1\ 10^{-3}$	1	0	3 (†)
CP2/hexane	$3.6\ 10^{-6}$	16.0	24	12

† defects visible

The CP2 membranes have much higher pore radii which are in the range of 0.5 μm compared to a coil radius of 8 to 10 nm. Reproducible defective membranes were obtained with the CP2 coated supports with cyclohexane as the solvent. The EPDM/cyclohexane solution obviously penetrated the support and defects (0.5 μm) could be observed with the SEM.

d. Polymer concentration

A higher polymer concentration proved to be the best way to prepare defect-free composite membranes. With a 10 wt-% solution of K578 in hexane defect-free membranes could be made in one step, whereas for a 5 wt-% K578 solution at least 4 steps were required. Even large pores of 0.5 μm can be bridged in one step in case of the 10 wt-% coating solution. With an 0.5 wt-% K578 solution defect-free composites have not been obtained within 6 steps.

6.5.2 Effects of coating-parameters

a. Number of coating steps

The number of coating steps is crucial with coating-solutions of 5 wt-% EPDM in hexane. Table 6 shows how the gas permeability and selectivity has been changed with increasing number of coating steps. It is clear that the P/l-values show a dramatic decrease after the third coating step, which indicates that most of the pores become blocked. Although one additional step is necessary to prepare defect-free composite membranes with this PES support (CP1), the P/l does not change so much anymore.

Table 6 *Gas selectivity and permeability versus the number of coating steps for a 5 wt-% solution. Support: PES (CP1).*

Coating step	0	1	2	3	4
α (CO_2/N_2)	0.81	0.81	0.9	3.0	15
P/l [cm^3 (STP)/(cm^2.s.cmHg)]	$6 \cdot 10^{-2}$	$4 \cdot 10^{-2}$	$2 \cdot 10^{-3}$	$16 \cdot 10^{-6}$	$4.3 \cdot 10^{-6}$

One coating step is enough to obtain defect-free membranes with a 10 wt-% coating-solution. More steps do increase the toplayer thickness.

b. Pressurizing of coating solution

JQ2 capillaries were put in a 10 wt-% polymer solution and a nitrogen pressure was applied upon the coating-solution ranging from 1.05 to 1.2 bar. It was expected that no pressure difference over the membrane would occur because the inside of the membranes were in contact with this pressure as well. Characterization results obtained from gas permeation have been summarized in table 7.

Table 7 *Gas permeability and selectivity versus the pressure during coating, JQ2, 10 wt-% K578, without impregnation.*

Pressure [bar]	Coating-velocity [cm/min]	P/l (CO_2) [cm^3/cm^2.s.cmHg]	α (CO_2/N_2) [-]	l_{eff} [μm]	l_{SEM} [μm]
1.05	0.75	$6.8\ 10^{-6}$	18	12	2
1.1	1.1	$3.1\ 10^{-6}$	22	26	5
1.2	2.2	$1.6\ 10^{-6}$	22	50	15

At increasing pressure the coating-velocity increases and consequently, the coated layer becomes thicker and the permeation rate reduces. The effective thickness increases and also the toplayer thickness as characterized by SEM increases. However, it is remarkable that the toplayer thickness, as seen by SEM, increases almost linear which is more than one would expect from eqn (1) or (2).

It is also remarkable that the selectivity increases with the increase in coating pressure. This means that the contribution of the support material increases which is caused by a higher penetration as can be seen from the effective thickness (table 7). Table 8 shows the results of the calculations from the Henis and Tripodi model (see Appendix B). This resistance model describes the measured effects remarkably well. The toplayer thickness l_1 equals the l_{SEM} quite good. Furthermore, l_2 increases with higher coating-pressures. In the Henis and Tripodi model this l_2 stands for the resistance in the pores of the support, the thickness of the skin of the support material and the penetration depth of the toplayer material into the support. With increased coating-pressure the first two remain constant and only the penetration depth changed.

Table 8 *Calculated toplayer thickness (l_1) and penetration depth (l_2) versus the coating-pressure.*

Pressure [bar]	l_{eff} [μm]	l_{SEM} [μm]	l_1 [μm]	l_2 [μm]
1.05	12	2	2.4	0.3
1.1	26	5	5.2	0.7
1.2	50	15	10	1.4

c. Coating velocity

CP2 supports were coated with a 10 wt-% EPDM in hexane solution. The coating velocity was varied from 0.04 cm/s to 0.8 cm/s. Even higher velocities resulted in inhomogeneous coating thicknesses. Fig.3 demonstrates that the coating thickness indeed increases with the coating velocity. It is clear that the coating thickness does not follow the square root of the velocity as it is obtained for flat non-porous surfaces (eqn (1)). It should be realized that the effective thickness is in fact not a good parameter to consider since the coating relation (eqns (1) and (2)) refer to the thickness of the coating layer on a non-porous surface.

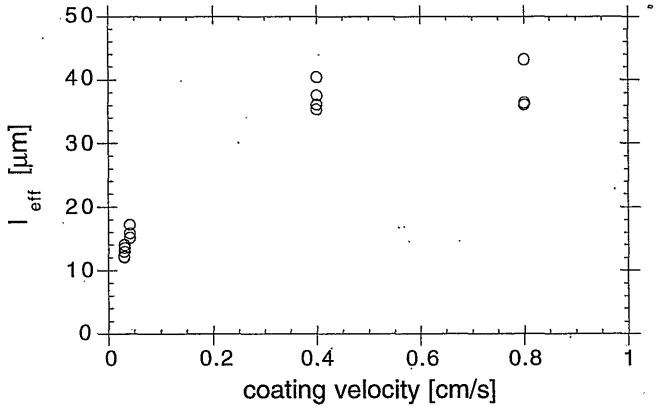

Figure 3 *The effective thickness versus the coating velocity. Coating conditions; 10 wt-% K578, 1 step without impregnation.*

6.5.3 Post-treatment with a solvent vapor

A solvent vapor post-treatment proved to be very useful to repair defect composite membranes with JQ-capillaries as support. After the removal of the coating-solution the coated capillaries were dried for one hour in nitrogen and characterized by gas permeation. Then the same membranes were exposed to a hexane saturated nitrogen atmosphere for four hours after which the capillaries were slowly dried overnight, subsequently further dried for one hour in a nitrogen atmosphere and again characterized.

After one coating step with the JQ1 supports about 40-50% of the membranes is defect-free. After the post-treatment the selectivity was increased

reproducibly to above 17 for about 80% of the fibers.

After one coating-step with CP2 supports typically 70% have the intrinsic selectivity of EPDM of 15.5±0.5. These composite membranes were not affected by the post-treatment.

6.5.4 Effect of the support material

Most results of the gas permeation experiments have been summarized in fig.4 in which the selectivity is depicted as a function of the effective thickness. The composite membranes with a highly porous (8-20%) PES-support show separation properties close to the intrinsic properties of EPDM. However, for the less porous (0.5-1%) PEI-supports selectivities were found between the intrinsic selectivities of the support and toplayer material.

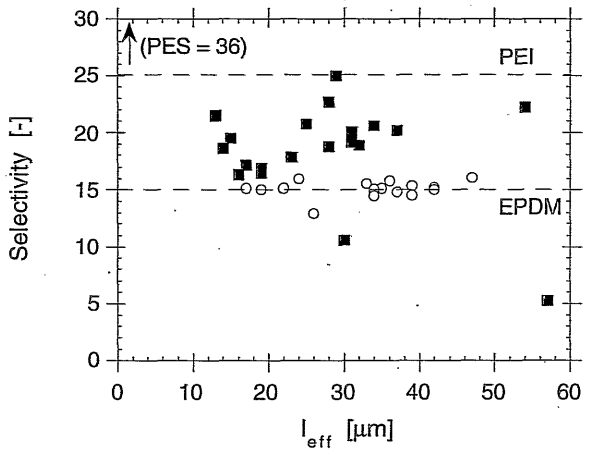

Figure 4 *Ideal selectivity (CO_2/N_2) of composite membrane versus the effective thickness. (o) represent PES-based composites and (■) represent PEI-based composites with EPDM as toplayer.*

Also fig.5 demonstrates that the PES-based composites are much less affected by the support than the PEI-based composites. Fig.6 shows a CP1 composite with a thick EPDM layer. The border can be clearly observed. Although gas permeation experiments show little effect of the support it must be concluded from SEM-images that still some penetration occurs.

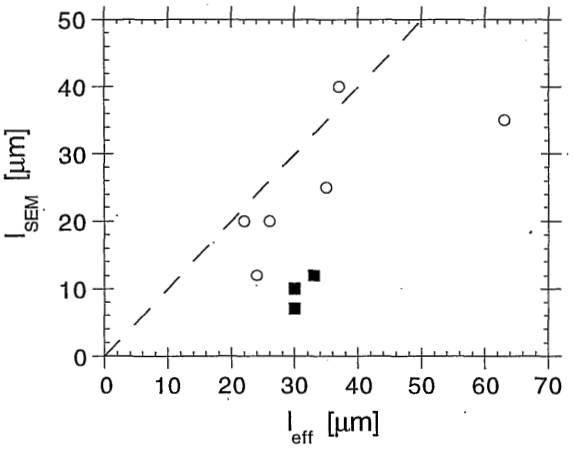

Figure 5 *The observed thickness of composites versus the effective thickness. (o) represent PES-based composites and (■) represent PEI-based composites. – – – represents $l_{SEM} = l_{eff}$. Coating conditions: 10 wt-% EPDM, no impregnation, 1 coating step. Selectivity of every composite is above 14.*

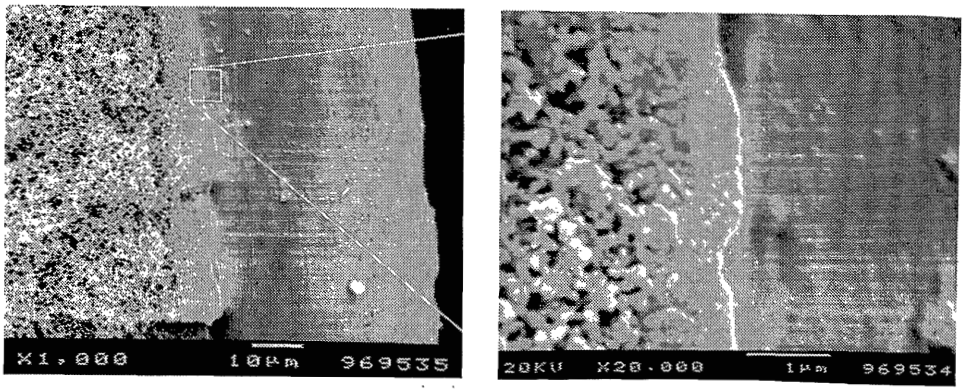

Figure 6 *Composite membrane; left: toplayer thickness, right: magnification of border. Coating conditions: CP1, 10 wt-% EPDM, no impregnation, 1 coating step at 0.4 cm/s.*

6.6 CONCLUSION

Poly(ether sulfone) and poly(ether imide) support membranes were successfully coated with EPDM. Several coating solutions were used for the dip-coating at different coating parameters such as polymer concentration, coating velocity, number of coating-steps and solvent type.

A 5 wt-% EPDM (Keltan 578) in n-hexane has been used as a coating-solution. The effect of different impregnation solvents to prevent penetration has been investigated. Composite membranes without penetration were not obtained. Without impregnation no defect-free membranes have been obtained with 6

coating steps. Defect-free membranes have been obtained after 4 coating steps with water or hexane as impregnating liquid. The P/l-value for CO_2 is about (1-10)·10^{-6} cm^3/ (cm^2.s.cmHg).

With a 10 wt-% of K578 in hexane coating-solution and no impregnation defect-free membranes could be made in one coating step, although penetration still occurs. P/l-values for CO_2 ranged typically from (2 to 8)·10^{-6} cm^3/ (cm^2.s.cmHg).

The toplayer thickness can be changed by varying the number of coating steps and the coating velocity. Penetration could not be completely prevented with impregnation.

The composite membranes with highly porous (5-10%) PES-membranes (CP1 and CP2) with pore radii of about 0.35 μm as the support, showed separation properties close to the intrinsic properties of EPDM. Moreover, the effective thickness was less than one third higher than the actually toplayer thickness as observed by SEM. It may be concluded for these PES-capillaries that penetration occurs but it does hardly effect the separation properties of EPDM.

The PEI-supports had small pore radii (10 nm) but penetration still occurred. As a consequence of low porosity and penetration selectivities were found between the intrinsic selectivities of the support and toplayer material. Furthermore, the effective thickness of these membranes were much higher than the observed toplayer thickness.

ACKNOWLEDGEMENTS

Kees Plug and Krista Bouma are acknowledged for developing the coating technique. Also, they are acknowledged for the discussions concerning this topics. Lydia Versteeg is acknowledged for performing many coating experiments and characterization of the composite membranes.

REFERENCES

[1] Williams, S.C., B.Bikson, J.K.Nelson, *Composite membranes for enhanced fluid separation*, EP 0,286,091.
Williams, S.C., B.Bikson, J.K.Nelson, R.D.Burchesky, *Methods for preparing composite membranes for enhanced gas separation*, U.S.Patent 4,840,819.

[2] Kafchinsky, E.R., T.Chung, *Asymmetric fluoropolymer-coated polyolefine hollow-fibers*, U.S.Patent 5,213,689.

[3] Riley, R.L., *Thin film separation membranes and processes for making the same*, U.S.Patent 3,648,845.

[4] Scheer, A. v.d., *Composite dense membranes*, U.S.Patent 4,581,043.

[5] Cabasso, I., K.A.Lundy, *Method for making composite membranes for gas separation*, U.S.Patent 4,602,922.
Lundy, K.A., I.Cabasso, *Analysis and construction of multilayer membranes for the separation of gas mixtures*, Ind.Eng.Chem.Res., 28 (1989) 742-756.

[6] Pinnau, I., *Ultrathin ethylcellulose/poly(4-methylpentene-1) permselective membranes*, U.S.Patent

4,871,378.

[7] Blume, I., I.Pinnau, *Composite membranes, method of preparation and use*, U.S.Patent 4,963,165.

[8] Gouchanour, C.R., *Gas separation membranes with ultrathin layers*, U.S.Patent 5,160,353.

[9] Chiou, J.J., *Composite gas separation membrane having a gutter layer comprising a crosslinked polar phenyl-containing organopolysiloxane, and method for making the same*, U.S.Patent 5,286,280.

[10] Rezac, M.E., W.J.Koros, *Preparation of polymer-ceramic composite membranes with thin defect-free separating layers*, J.Appl.Polym.Sci., 46 (1992) 1927-1938.

[11] Bikson, B., S.Gaglia, G.Kharas, *Composite separation membranes and the preparation and the use thereof*, U.S.Patent 4,767,422.

[12] Pinnau, I., J.Wind, *Process for increasing the selectivity of asymmetric membranes*, U.S.Patent 5,007,944.

[13] Hayes, R.A., *Surfactant treatment of aromatic polyimide gas separation membranes*, U.S.Patent 5,034,024.

Hayes, R.A., *Surfactant treatment of polyaramide gas separation membranes*, U.S.Patent 5,032,149.

[14] Rezac, M.E., J.D.LeRoux, H.Chen, D.R.Paul, W.J.Koros, *Effect of mild solvent post-treatment on the gas transport properties of glassy polymer membranes*, J.Membr.Sci., 90 (1994) 213-229.

[15] Ebert, K., *Thin film composite membranes of glassy polymers for gas separation - preparation and characterization*, PhD-Thesis, University of Twente, Enschede (NL), 1995.

[16] Pinnau, I., *Skin formation of integral asymmetric gas separation membranes made by dry/wet phase inversion*, PhD-thesis, University of Texas, Austin (USA), 1993.

[17] Deryagin, B.M., S.M.Levi, *Film coating theory*, The Focal Press, New York (USA), 1964.

[18] Kimmerle, K., T.Hofmann, H.Strathmann, *Analysis of gas permeation through composite membranes*, J.Membr.Sci., 61 (1991) 1-17.

[19] Sanders, E.S., *Penetrant induced plasticization and gas permeation in glassy polymers*, J.Membr.Sci., 37 (1988) 63-80.

[20] Bos, A., *High pressure CO_2/CH_4 separation with glassy polymer membranes - Aspects of CO_2-induced plasticization*, PhD-thesis, University of Twente, Enschede (NL), 1996.

[21] Duval, J.-M., *Adsorbent filled polymeric membranes; application to pervaporation and gas separation*, PhD-Thesis, University of Twente, Enschede (NL), 1993.

APPENDIX A TO CHAPTER 6

-

EPDM IN SOLUTION

INTRODUCTION

In this appendix the solution behaviour of the ethylene-propylene terpolymers (EPDM) in different solvents was studied with viscosimetry and gel permeation chromatography. From these experiments the radius of gyration can be determined. This parameters is a measure for the dimension of the polymer coil and it depends on the molecular weight of the polymer and the interaction between the solvent and the polymer. It allows in combination with the pore size of the porous support layer to discriminate whether pore penetration might occur [1,2]. In relation to this, it is important that a polymer has a narrow molecular weight distribution. Otherwise the smaller molecular weight fraction will still penetrate.

BRIEF THEORETICAL BACKGROUND

The radius of gyration $\langle R_g^2 \rangle^{1/2}$ is related to the root-mean-square-end-to-end distance $\langle h^2 \rangle^{1/2}$ as shown in eqn (1) [3],

$$\langle R_g^2 \rangle^{1/2} = \frac{\langle h^2 \rangle^{1/2}}{6} \quad . \qquad (1)$$

The value of $\langle h^2 \rangle^{1/2}$ can be obtained from eqn (2) which is valid for molecular weights higher than 10 kg/mol [4],

$$[\eta]\, M = \Phi \langle h^2 \rangle^{3/2} \quad , \qquad (2)$$

where $[\eta]$ is the intrinsic viscosity of the polymer in a certain solvent, M is the

molecular weight of the polymer and Φ is the universal constant ($2.84 \cdot 10^{23}$) [5].

EXPERIMENTAL

Viscosimetry

Different EPDMs were kindly supplied by *DSM-elastomers* and used without further purification. Toluene, hexane and cyclohexane (*Merck*, analysis grade) were used as solvent. Dilute polymer solutions were prepared ranging from 0.5 to 5 g/l and used in the viscosimetry experiments.

For all experiments the EPDM was cut from a block and the solutions were prepared overnight. The outer part (0.5 cm) of an EPDM block was not used. Only the samples in hexane were not completely dissolved, but after a 5 minutes ultrasonic treatment they finally dissolve. After a long period of time EPDM dissolves in hexane but no difference was found in the viscosity experiments with and without ultrasonic treatment.

Gel permeation chromatography

The GPC experiments have been performed with a μstyragel as the column material ($10^5+10^4+10^3+10^6$ Å + guard column). Calibration curves of polystyrene in the corresponding solvent were used.

RESULTS AND DISCUSSION

The reproducibility of the viscosimetry experiments is very good with an error less then 1% for the intrinsic viscosity values. From table 1 it is obvious that cyclohexane is the best solvent. The radii of gyration (R_g) in cyclohexane are typically 1 nm larger than in hexane or toluene for all EPDM-types. For K4802 the radius is 10.3 nm in cyclohexane, 9.16 nm in hexane and 8.70 for toluene. The effect of different molecular weights is larger. In cyclohexane the radii increase with the polymer weight of the EPDM from 7.16 nm for K378 to 10.3 nm for K4802.

Table 1 *Molecular weights and radii of gyration of several EPDMs in different solvents.*

		cyclohexane		hexane		toluene	
polymer Keltan®	M_w* [kg/mol]	[η] [l/g]	R_g [nm]	[η] [l/g]	R_g [nm]	[η] [l/g]	R_g [nm]
378	111	0.203	7.16	0.119	5.99	0.117	5.97
578	134	0.218	7.81	0.140	6.74	0.131	6.59
778	225	0.244	9.64	0.144	8.08	0.134	7.89
4778	200	0.240	9.21	0.173	8.27	0.147	7.83
4802	240	0.281	10.3	0.197	9.16	0.168	8.70

* typical values from DSM-elastomers [6]

For coating experiments high R_g are preferred, thus K4802 would be chosen. But, K4802 has very weak mechanical properties as a thin film (Chapter 3 of this thesis [7]). K778 and K4778 have comparable R_g's, but because K4778 has a much narrower molecular weight distribution than 778 [7], K4778 is the most interesting EPDM for coating procedures.

CONCLUSION

It can be concluded that the radius of gyration varies between 6 and 10 nm and it strongly depends on the EPDM type and the solvent. K4778 is the most interesting EPDM to apply as a toplayer on basis of mechanical and physical properties.

ACKNOWLEDGEMENTS

Frank Huys is acknowledged for performing the experiments and the fruitful discussions related to this work.

REFERENCES

[1] Rezac, M.E., W.J.Koros, *Preparation of polymer-ceramic composite membranes with thin defect-free separation layers*, J.Appl.Polym.Sci., 46 (1992) 1927-1938.

[2] Ebert, K., *Thin film composite membraens of glassy polymers for gas separtion - preparation and characterization*, PhD-Thesis, University of Twente, Enschede (NL), 1995.

[3] Heimenz, P.C., *Polymer chemistry*, Marcel Dekker Inc., New York (USA), 1984.

[4] Flory P.J., *Principles of polymer chemistry*, Cornell University Press, New York (USA), 1953.

[5] Bodor, G., *Structural investigations of polymers*, Ellis Horwood, New York (USA), 1991.

[6] Noordermeer, J.W.M., personal communication, typical values for EPDM of DSM-elastomers, 1995.

[7] Meuleman, E.E.B., J.H.A. Willemsen, M.H.V.Mulder, H.Strathmann, *EPDM as a barrier material for pervaporation*, PhD-Thesis, University of Twente, Enschede (NL), 1997.

APPENDIX B TO CHAPTER 6

-

RESISTANCE MODELS

INTRODUCTION

Gas permeation experiments can be used to characterize composite membranes. From the permeation rates of sublayer and toplayer material and composite membrane information can be obtained about the contribution of the various resistances. The effect of the support material on the total transport can be demonstrated by the resistance model as introduced by Henis and Tripodi [1]. In this paper several modifications of this model will be discussed. In addition, the results of a new model will be presented which is a small modification to the Henis and Tripodi model.

THEORETICAL BACKGROUND

The flux (J) through a dense polymer membrane can be described by the following equation

$$J_i = \frac{P_i}{l} \cdot \Delta p_i \ , \qquad (1)$$

where P is the permeability [Barrer], l is the polymer layer thickness [cm] and Δp is the partial pressure difference [cmHg] and subscribt i indicates component i. For porous supports and composite membranes the total flux can be measured but the P and l are not known and only the ratio, the pressure normalized flux $(P/l)_i$ can be calculated. However, the 'so-called' effective thickness (l_{eff}) is given by:

$$l_{eff} = \frac{\Delta p_i}{J_i} \cdot P_i \quad . \qquad (2)$$

Comparison of l_{eff} and the toplayer thickness as observed by scanning electron microscopy (l_{SEM}) gives a good first impression of the composite membrane [2].

Resistance model 1: Henis and Tripodi

The first resistance model was introduced by Henis and Tripodi and is shown schematically in fig.1.

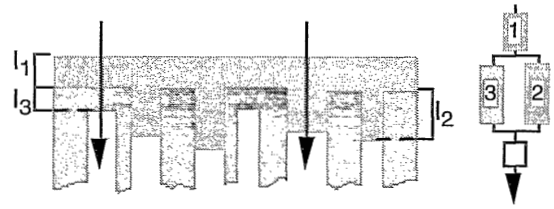

Figure 1 *Schematical representation of possible molecule pathways through a composite membrane (resistance in pores neglected) [1].*

In this model, it is assumed that the penetration depth (l_2) equals the toplayer thickness of the support (l_3). Eqn (3) can be derived:

$$J_i = \left\{ \frac{l_1}{P_{1,i}} + \frac{l_2}{\varepsilon P_{1,i} + (1-\varepsilon) P_{2,i}} \right\}^{-1} \cdot \Delta p_i \quad . \qquad (3)$$

where ε is the porosity. In eqn (3) l_1 and l_2 are the only two variables when the flux at a certain pressure is measured, since the porosity which has been determined by surface image analysis or the Poiseuille equation and the permeabilities are known. These thicknesses can be calculated when the permeation rates of two gases are determined. On the other hand, it is also possible to estimate the flux and selectivity as a function of porosity (ε) and the toplayer thickness of the support, which is equal to the penetration depth (l_2).

Both Kimmerle for gas separation [3] and Gudernatsch for pervaporation [4] discussed this Henis and Tripodi model for several limiting cases in which only two resistances were considered.

Resistance model 2: variable penetration depth

Since the exact penetration depth (l_2) is unknown and of great importance for the composite membrane performance, this should be taken into account. In fact, it is almost the same model as presented by Henis and Tripodi, but with a variable penetration depth l_2, which is of course not 'a priori' equal to the thickness of the toplayer of the support. The flux of component i is given as:

$$J_i = \left\{ \frac{l_1}{P_{1,i}} + \left(\frac{\varepsilon P_{1,i}}{l_2} + \frac{(1-\varepsilon) P_{2,i}}{l_3} \right)^{-1} \right\}^{-1} \cdot \Delta p_i \ . \qquad (4)$$

When the permeation rates of three gases have been measured and the porosity is known then the penetration depth of the coating material (l_2), the thickness of the toplayer of the support material (l_3) and the coating layer thickness (l_1) can be calculated independently. Then eqn (4) has to be solved for three different gases and this can be done numerically.

On the other hand, it is possible as well to estimate flux and selectivity as a function of porosity (ε), penetration depth (l_2) and toplayer thickness of support (l_3). The thickness of the toplayer (l_1) can be fairly well determined by scanning electron microscopy.

EXPERIMENTAL

Composite membranes have been prepared and characterized as has been described in Chapter 6. The effective thickness could be easily calculated from the permeation experiments. To calculate the two thicknesses from eqn (3) for two gases for one composite the equations were solved analytically with Mathcad 6. To solve the three thicknesses from eqn (4) for three gases for one composite Maple 5.3 was used.

The permeabilities of the various materials and gases, which have been used in this research, have been summarized in table 1.

Table 1 *Gas permeability properties of various polymer materials*

Polymer material	P (N_2) [Barrer]*	P (O_2) [Barrer]*	P (CO_2) [Barrer]*	α (CO_2/N_2) [-]
PES [3, 5]	0.16	1.4	3.6	36
PEI (Ultem 1000) [6,7]	0.052	0.4	1.3	25
EPDM (25°C, K578) [8,9]	5.6	17	85	15

* 1 Barrer = 10^{-10} cm.cm^3 (STP) / (cm^2.s.cmHg)

RESULTS AND DISCUSSION

The first composite membrane applied has a poly(ether sulfone) support with a porosity of about 5-10 % and pore radii of about 0.5 μm. EPDM is used as coating layer. Table 2 shows the pressure normalized fluxes of several gases for this composite membrane.

Table 2 *Pressure normalized fluxes of composite membranes with PES* supports.*

P/l (N_2) [GPU]	P/l (O_2) [GPU]	P/l (CO_2) [GPU]	α_{id} (CO_2/N_2) [-]	l_{eff} [μm]
0.227	0.772	3.63	16	24

* porosity 5%
1 GPU = 10^{-6} cm^3 (STP) / (cm^2.s.cmHg)

From eqn (1) an effective thickness of 24 μm is calculated. With scanning electron microscopy a coating layer thickness of 12 μm was found.

With resistance model 1 two unknowns can be solved from eqn (3) with two resistance equations. Table 2 gives the results when the thickness of the coating layer (l_1) as observed by the SEM is put in the model and ε and l_2 are the unknowns. It is also possible to use the porosity as observed with SEM as a known parameter in the model with l_1 and l_2 as the unknowns. Both l_1 and ε were the input variables because the l_1 from the SEM is only one small part of the total fiber. The l_1 from the SEM should be used as an indication. On the other hand, ε can be determined with the Poiseuille equation or via analysis of a SEM image. However, in case of the same support the porosity should remain constant.

Table 3 *Numerical calculations with model 1, for a highly porous support.*

	l_1 [μm]	ε [-]	l_2 [μm]
l_1 from SEM	***12***	0.042	0.66
ε from image analysis	10	***0.050***	0.87

bold represents input variable

When these calculations are performed on a different couple of gas-fluxes, e.g. CO_2 and O_2, the same values are obtained with a maximum difference of 5 % compared with the values in table 3.

In table 4 the results of the calculations with model 2 are summarized. With this modified Henis and Tripodi model one may find a coating layer thickness which is independent of the porosity. This should be correct since a certain flux and selectivity should give only one coating layer resistance. The difference in selectivity between the intrinsic coating layer material and the composite membrane is totally determined by the layer beneath this coating layer, that is, the penetration depth (l_2), the porosity (ε) and the thickness of the toplayer of the support (l_3). The fluxes through this layer must have a certain value in order to account for the change in selectivity. The higher the porosity the

thinner the toplayer of the support has to be to maintain the same effect on the fluxes. Furthermore, the higher the porosity, the greater the penetration depth (l_2).

Table 4 also shows that the thickness of the toplayer of the support is very small, 1.4 nm (at ε is 5% by SEM), and hardly changes with the porosity. In general, toplayer thicknesses of the support are at least 10 times higher.

Table 4 *Calculations with model 2, with variable penetration depth using a highly porous support.*

ε [-]	l_1 [μm]	l_2 [μm]	l_3 [nm]
0.0001	20.3	0.03	1.52
0.05	20.3	1.67	1.41
0.1	20.3	3.3	1.36
0.3	20.3	10	1.10

The results of model 1 and model 2 are in rather good agreement with each other for these porous supports, except for the fact that for model 2 the estimated value for the toplayer of the support (l_3) is too low. However, with another composite which has a larger resistance in the support the results with model 2 were rather poor. This composite with poly(ether imide) (PEI) as the support material has a porosity of about 0.007 and pore radii of about 6 to 10 nm. Table 5 shows the experimental results of the gas permeation experiments of the composite membrane with pure gases. It is clear that the reproduciblity is very good and it might be expected that from analysis of the morphology via resistance models comparable results would be obtained. Furthermore, table 5 shows the l_{eff} of the three composites and indeed they are quite the same.

Table 5 *Pressure normalized fluxes of composite membranes with PEI supports*.*

id	P/l (CO_2) [GPU]	P/l (O_2) [GPU]	P/l (N_2) [GPU]	α_{id} (CO_2/N_2) [-]	α_{id} (CO_2/O_2) [-]	l_{eff} [μm]
a	3.02	0.76	0.161	18.8	4.0	28
b	2.77	0.58	0.144	19.2	4.8	31
c	2.63	0.49	0.139	18.9	5.3	32

* porosity 0.007

1 GPU = 10^{-6} cm^3 (STP) / (cm^2.s.cmHg)

Table 6 *Numerical calculations with model 1 using low porous supports.*

	id	l_1 [μm]	ε [-]	l_2 [μm]
l_1 constant from SEM	a	***10***	0.0069	0.40
	b	***10***	0.0057	0.44
	c	***10***	0.0073	0.51
ε constant	a	10	***0.007***	0.40
	b	8.9	***0.007***	0.44
	c	10.3	***0.007***	0.51

Table 6 shows that the results with resistance model 1 give comparable results as well. But when these calculations are performed with CO_2 and O_2 fluxes then the results are quite different.

Table 7 *Numerical calculations with model 1 using low porous supports, from CO_2 and O_2 flux measurements.*

	id	l_1 [μm]	ε [-]	l_2 [μm]
l_1 constant from SEM	a	***10***	-0.0032	0.25
	b	***10***	0.10	2.4
	c	***10***	-0.07	-1.2
ε constant	a	-0.50	***0.007***	0.7
	b	26	***0.007***	0.1
	c	4.4	***0.007***	-0.3

From this table 7 it can be concluded that the best values are obtained for composite membrane **b**, although the values for the porosity and the penetration depth are quite high. For the other two composite membranes negative values are found, which is of course not realistic. This will be discussed later on.

The results with model 2 gave no good agreement at all (table 8). These values may be correct mathematically, but physically they have no meaning. In no case thicknesses can be negative.

Another attempt was made in which the area of the pores (= ε) and the area of the permeable skin of the sub layer (≠ 1-ε) were independent. In this way the area could be more or less than 1, which physically could be explained by the rough shape of the toplayer. However, no improvement was made. Obviously, the analytical solution of model 2 is too sensitive in relation to the values of the gas fluxes.

Table 8 *Numerical calculations with model 2 using low porous supports.*

id	ε [-]	l_1 [μm]	l_2 [μm]	l_3 [nm]
a	***0.0001***	0.16	0.00	8.7
	0.007	0.16	0.39	8.6
	0.018	0.16	1.0	8.5
b	***0.0001***	28	-0.31	220
	0.007	28	-21	219
	0.018	28	-55	217
c	***0.0001***	35	0.10	-114
	0.007	35	7.0	-113
	0.018	35	18	-111

It is also possible to estimate flux and selectivity as a function of porosity (ε), penetration depth (l_2) and toplayer thickness of support (l_3). In this approach several reasonable values of the penetration depth and the toplayer thickness of the support (between 0.2 and 1 μm) were put into eqn (4) of model 2. Now the component flux can be calculated as a function of the porosity. The toplayer thickness is 10 μm (from SEM). Fig.2 shows the result of this approach where l_2 is 0.2 μm and l_3 is 1 μm. The solid horizontal lines represent the actual P/l-values of composite membrane **b**. The curved lines represent the theoretical P/l-values,

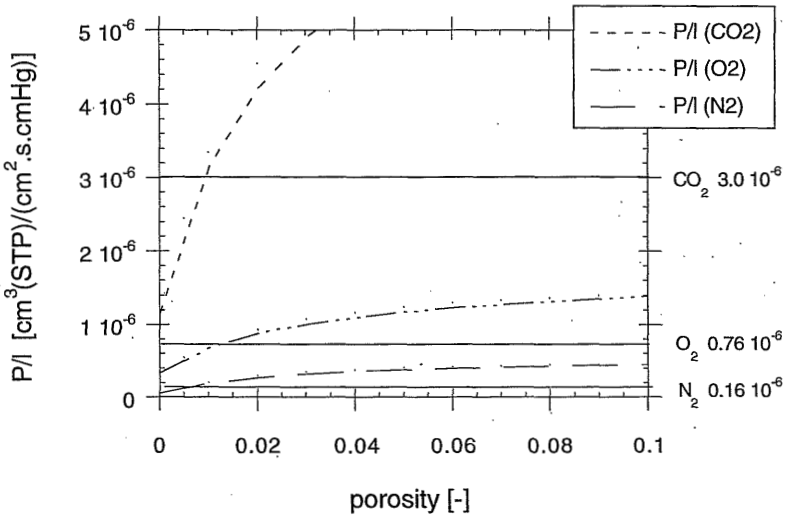

Figure 2 *Theoretical P/l values as a function of the theoretical porosity as a result of solving model 2 (eqn (4)) with l_1 is 10 μm (SEM), l_2 is 0.2 μm and l_3 is 1 μm. The horizontal solid lines are the experimentally determined values.*

calculated from eqn (4). This figures shows that the values of the theorectical and the actual line for a certain gas cross at about the same porosity. According to this approach the porosity is between 0.008 (N_2) and 0.015 (O_2) for this composite. These values for the porosity compare well with the porosity as determined from flux mearements of the porous support, which was 0.005 to 0.01.

When different values for the thicknesses are taken, then the variation in the porosity, where the theoretical and the actual gas flux of the different gases cross, is much higher. In conclusion, with this iteration method acceptable values for the thicknesses and the porosity can be obtained by allowing a small error in the gas fluxes.

CONCLUSION

The simple resistance model as proposed by Henis and Tripodi (model 1) results in values with which the different aspects of composite membranes can be evaluated very well. The variable penetration model with three parameters (model 2) as introduced in this work did result in a good description of the morphology of a composite with a highly porous support. However, for composites with low porous supports, this model proved to be very sensitive to small changes in the measured fluxes. The model then results in an unrealistic result, such as negative thicknesses and much too low coating layer thicknesses. It must be concluded that model 1 is more suitable than the physically more correct model 2 or in other words, model 2 cannot be applied to obtain the important parameters (l_2, l_3 and ε) based on gas fluxes.

On the other hand, in a different approach where model 2 is used as an iteration method, in which a small error in the measured gas fluxes is allowed, acceptable values for the thicknesses can be obtained.

REFERENCES

[1] Henis, J.M.S., M.K.Tripodi, *Composite hollow fiber membranes for gas separation: the resistance model approach*, J.Membr.Sci., 8 (1981) 233-246.

[2] Pinnau, I., J.G.Wijmans, I.Blume, T.Kuroda, K.-V.Peinemann, *Gas permeation through composite membranes*, J.Membr.Sci., 37 (1988) 81-88.

[3] Kimmerle, K., T.Hofmann, H.Strathmann, *Analysis of gas permeation through composite membranes*, J.Membr.Sci., 61 (1991) 1-17.

[4] Gudernatsch, W., Th.Menzel, H.Strathmann, *Influence of composite membrane structure on pervaporation*, J.Membr.Sci., 61 (1991) 19-30.

[5] Sanders, E.S., *Penetrant induced plasticization and gas permeation in glassy polymers*, J.Membr.Sci., 37 (1988) 63-80.

[6] Barbari, T.A., W.J.Koros, D.R.Paul, *Polymeric membranes based on bisphenol-A for gas separations*, J.Membr.Sci., 42 (1989) 69-86.

[7] Bos, A., *High pressure CO_2/CH_4 separation with glassy polymer membranes - Aspects of CO_2-induced plasticization*, PhD-thesis, University of Twente, Enschede (NL), 1996.

[8] Meuleman, E.E.B., J.H.A.Willemsen, M.H.V.Mulder, H.Strathmann, *EPDM as a barrier material*, Chapter 3 of this thesis, University of Twente, Enschede (NL), 1997.

[9] Duval, J.-M., *Absorbent filled polymeric membranes, application to pervaporation and gas separation*, PhD-Thesis, University of Twente, Enschede (NL), 1993.

7

PERVAPORATION WITH COMPOSITE MEMBRANES: OUTSIDE LONGITUDINAL AND TRANSVERSE FLOW MODULES

SUMMARY

Composite membranes with poly(ether sulfone) (PES) or poly(ether imide) (PEI) as porous support layer and with ethylene-propylene terpolymer (EPDM) as toplayer were used in removal of volatile organic contaminants (VOCs) by pervaporation. The toluene flux through the membrane was between 5 and 50 g/m^2.h at a toluene concentration in the feed of 250 ppm. The toluene flux was mainly affected by the toplayer thickness and the feed flow velocity. The water flux decreased with increasing toplayer thickness and ranged from 1.5 to 12 g/m^2.h. The separation factor ranges between 5,000 and 90,000 and increases with toplayer thickness and feed flow velocity. Composite membranes with a highly porous PES support showed a better performance than membranes with a less porous PEI support.

The composite membranes were built in transverse flow modules (TFM) and longitudinal outside flow modules (LOM) and pervaporation experiments were carried out with these modules. From the velocity-variation method and the resistances-in-series model a value for the mass transfer coefficient in the liquid boundary layer (k_L) was determined. At a Reynolds number of 2,400 the TFM had a k_L of $6.7 \cdot 10^{-5}$ m/s. For the LOM a k_L value of $5.7 \cdot 10^{-5}$ m/s was found at extreme high Reynolds numbers of 11,000.

7.1 INTRODUCTION

In this paper the pervaporation results will be discussed of the transverse flow module (TFM) and longitudinal outside flow module (LOM) containing composite membranes. Both the composite membrane resistance and the boundary layer resistance have been investigated in relation to the toplayer thickness, kind of porous support, the feed flow velocity and type of module.

7.2 THEORETICAL BACKGROUND

7.2.1. Mass transfer in the liquid boundary layer

In the removal of volatile organic compounds (VOCs) from water boundary layer resistances may become very dominant. This resistance can be decreased by better hydrodynamic conditions in the feed, which commonly is achieved by a higher feed flow velocity or by a different module or configuration of the membranes in a module.

Semi-emperical relationships exist which relate the feed flow velocity to the mass transfer coefficient. These so-called Sherwood relations are generally given by eqn (1)

$$Sh = p\, Re^{q}\, Sc^{r} \left(\frac{d_h}{L}\right)^{s} \quad , \qquad (1)$$

where Sh is the Sherwood number, Re is the Reynolds number, Sc is the Schmidt number, d_h is the hydraulic diameter [m], L is the length of the module [m] and p, q, r and s are constants. Sh, Re, and Sc are defined as

$$Sh = \frac{k_L \cdot d_h}{D_i} \quad , \; Re = \frac{v \cdot d_h}{\nu} \text{ and } Sc = \frac{\nu}{D_i} \quad , \qquad (2)$$

where k_L is the mass transfer coefficient [m/s], D_i is the diffusion coefficient of component i [m^2/s], v is the feed flow velocity [m/s] and ν is the kinematic viscosity [m^2/s].

For various flow regimes, module configurations or type of modules, different Sherwood relations are available in literature. In general, three flow regimes exist: laminar flow at low feed flow velocities, turbulent flow at high velocities and a mixed flow in the intermediate region.

7.2.2 Transverse flow membrane module

In Chapter 2 several membrane modules were depicted schematically. For flat membranes plate-and-frame and spiral wound modules are the most common module configurations. Hollow fiber or capillary membranes can be packed in an inside or outside longitudinal flow module or a transverse flow module. Important parameters which determine the choice of a certain membrane

module are: membrane and module prize, availability of the membrane material, investment costs and operation costs.

A similarity exists between heat transfer and mass transfer. In heat transfer, transverse flow modules are known for quite a time. The first transverse flow membrane module was patented in 1964 [1] and some more patents were assigned until the middle 80's. Then starting in the late 80's a numerous of researchers designed and patented all kinds of TFMs [2-7]. These TFMs may be found in all applications with mass or heat transfer limitations. In the case of microfiltration and ultrafiltration the TFMs are used because of the relative high shear stress generates at the membrane surface by which fouling can be decreased and as a consequence fluxes increase. For pervaporation and dialysis the TFMs are very promising because high mass transfer coefficients can be obtained at relative low feed pressure drop. Fig.1 shows the schematical drawings of patented TFMs which have been applied in pervaporation. The first one is assigned to TNO (NL) [5] and the second to Zenon (CND) [3].

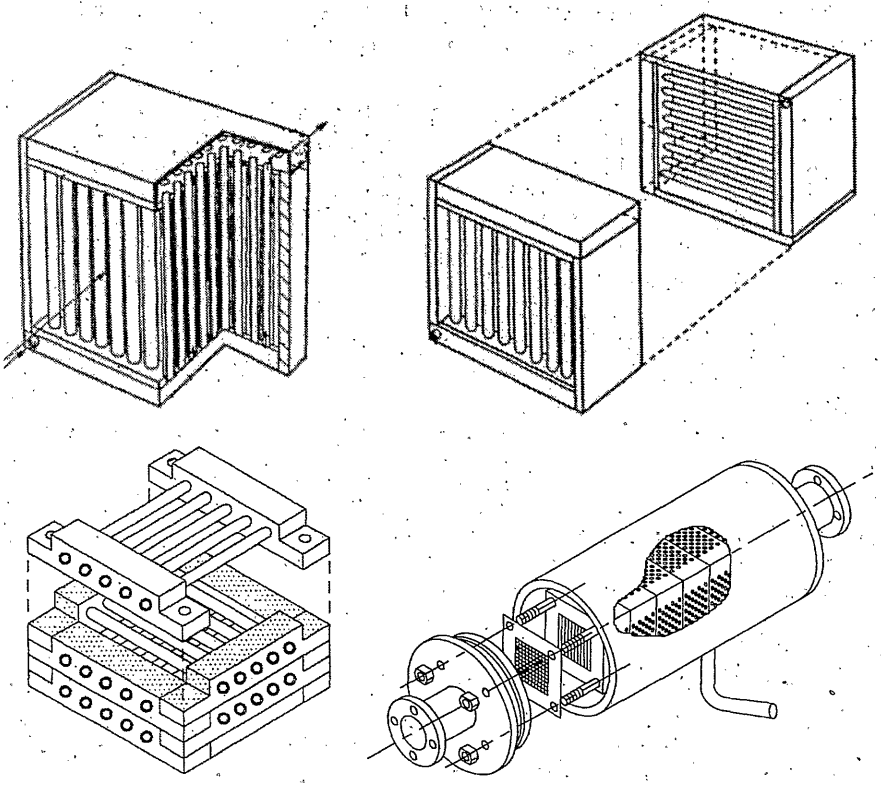

Figure 1 *Transverse flow membrane modules which have been used in pervaporation: a) ter Meulen [5] , b) Côté et al. [3].*

Fig.2 shows two TFMs for which Sherwood relations were measured [2,6] for transverse flow.

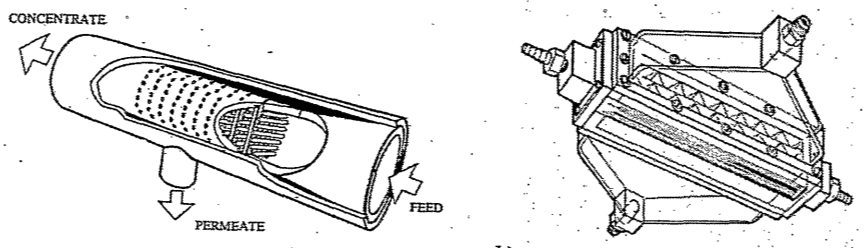

a) b)

Figure 2 *Transverse flow membrane modules for which Sherwood relations exist: a) Futselaar [2] , b) Yang [6].*

The major difference between the Yang module and the Futselaar module is that Yang has his fibers parallel behind each other, whereas Futselaar has his fibers crossed packed, which means that every grid of fibers is positioned 90° with respect to the neighboring grid. The main reason for the latter concept to provide mechanical strength. Futselaar published Sherwood relations for many different configurations [8] based on staggered or on in-line (fig.3).

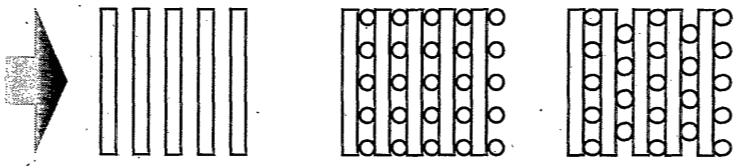

Figure 3 *Several configurations for transverse flow modules. Arrow indicates feed flow direction.*

Table 1 presents the values of the constants of eqn (1) as obtained by Yang and Futselaar.

Table 1 *Mass transfer correlations for transverse flow modules.*

Sherwood relation*	Validity range*	Reference	Remarks
$Sh = 0.90\ Re^{0.40}\ Sc^{0.33}$	$Re < 25$	[6]	Single fiber
$Sh = 1.38\ Re^{0.34}\ Sc^{0.33}$	$Re < 25$	[6]	Bundle of fibers
$Sh = 1.17\ Re^{0.34}\ Sc^{1/3}\ b^{1.32}$	$Re \leq 20$	[8]	Crossed in-line
$Sh = 0.72\ Re^{0.52}\ Sc^{1/3}\ b^{1.34}$	$20 < Re \leq 1000$	[8]	Crossed in-line
$Sh = 1.78\ Re^{0.31}\ Sc^{1/3}\ b^{0.79}$	$Re \leq 20$	[8]	Crossed staggered
$Sh = 1.11\ Re^{0.49}\ Sc^{1/3}\ b^{0.90}$	$20 < Re \leq 1000$	[8]	Crossed staggered

* The d_h in these relations is the external membrane diameter.

Yang et al. [6] derived their relations from experiments in which in water

dissolved oxygen diffusing to the membrane surface is the rate determining step. Futselaar [8] performed his experiments in an aqueous solution in which diffusion of ions from the feed bulk to the 'membrane' surface was the rate determining step. For VOC removal from water a mass transfer coefficient of 10^{-4} m/s was found in literature for spiral wound and transverse flow modules, which is about one order of magnitude higher than for other modules [6,9]. The advantage of hollow fiber modules over other modules is their much higher packing density. Consequently, the transverse flow module (TFM) combines a high k_L with a high packing density. Another advantage of a TFM is the relative short fiber length, which results in a rather low permeate side pressure drop.

7.2.3 Feed velocity-variation method

In Chapter 3 eqn (3) has been derived[1] which describes the pervaporation process in which both the membrane resistance and the boundary layer resistance were combined. The flux of component i (J_i) is related to the partial pressure difference which equals the partial pressure in the feed (p_i) if the partial pressure in the permeate is neglected

$$J_i = \left(\frac{l}{P_i} + \frac{H_i}{k_L} \right)^{-1} \cdot p_i , \qquad (3)$$

where l is the membrane thickness, P is the permeability coefficient, H is Henry's law coefficient of the VOC in an aqueous solution in molar density and pressure dimension, k_L is the mass transfer coefficient in the boundary layer and subscript i refers to component i. In Chapter 3 it was explained how k_L can be calculated from pervaporation experiments with different membrane thicknesses.

In this paper, however, different membrane thicknesses can not be determined exactly, since composite membranes are used and one always should be aware of the unknown influence of the support layer. Another approach as used by a number of researchers is similar to the 'feed-velocity-variation' method [10,11]. The mass transfer coefficient k_L can be substituted by $a \cdot v^q$ and eqn (3) becomes after rearranging

$$\frac{H_i \cdot \rho_f \cdot x_{f,i}}{J_i} = \left(\frac{l}{P_i} + \frac{H_i}{a \cdot v^q} \right) , \qquad (4)$$

where v is the feed flow velocity and a and q are fitting constants. The reciprocal of the overall resistance ($1/k'_{ov}$), which is equal to the driving force over flux, can be plotted versus $1/v$ for a certain membrane module. Now, k_L can be calculated for each feed velocity by iteration of the following equation:

$$1/k'_{ov} = m + n*(1/v)^q \qquad (5)$$

[1] Commonly it is preferred to describe k in [m/s] and P is described in [Barrer]. Therefore, these units will be used. However, for calculations and in the equations the following units are used: P in [mol.m/(m^2.s.Pa)], p in [Pa], x in [mol/mol] and J in [mol/(m^2.s)].

with m and n as fitting parameters. Then m equals l/P and n equals H_i/a.

7.2.4 Composite membranes in pervaporation

Basically, transport of vapors in composite membranes is comparable to gas permeation and the solution-diffusion model is applicable. However, due to the effects of swelling phenomena and the possibility of capillary condensation in the support some additional aspects have to be discussed. The effect of capillary condensation is such that pores become 'blocked' due to condensation of the vapor molecules and the permeation rate will become much lower. The effect on the mass transfer equations has been described in several papers by Bode and Hoempler [12]. Upon increasing the permeate pressure capillary condensation will occur first in the smallest pores. This means that capillary condensation of toluene occurs in pores of poly(ether imide) with a pore radius of 2 nm if a toluene vapor pressure of 10 mbar or more is reached [13]. Water will condense in the same way as toluene but due to the high selective toplayer (EPDM) hardly any water vapor is present in the pores. Capillary condensation is of minor importance since the support membranes used in this research have pore sizes larger than 2 nm and during the pervaporation experiments a total permeate pressure of more than 1 mbar is never exceeded.

Another important effect may be the swelling of the toplayer material due to high sorption of the preferentially sorped component. As a result the flux of the slower component may be enhanced and selectivity decreases. However, in Chapters 3 and 4 of this thesis it was shown that for the removal of VOCs from water by pervaporation the selectivity is only a little affected by swelling.

7.3 MATERIALS AND METHODS

7.3.1 Materials

Ethylene-propylene-diene terpolymers were kindly supplied by *DSM-elastomers*. Toluene and ethanol have been purchased from *Merck* (for synthesis or analysis grade) and were used without further purification. Water was demineralized and ultrafiltrated.

7.3.2 Pervaporation

The experimental set-up for pervaporation has been described in Chapter 3. Instead of, the flat membrane cell, a transverse flow and a longitudinal outside flow module have been used.

7.3.3 Transverse flow module

A lab-scale transverse flow module (TFM) has been constructed (fig.4). In transverse flow the feed flows perpendicular along the membrane capillaries. The transverse flow module consists of 7 capillaries next to each other. The diameter of the module is 5 cm and the effective membrane area is 9-20 cm^2, which

depends on the capillary diameter. Defect-free composite membranes are potted into a TFM. A two component poly-urethane glue (purchased from *Morton Adhesives Europe*) is used as potting agent. A glueing procedure was developed to provide a very smooth surface at the side where the inside of the capillaries are connected to the vacuum. A Viton® O-ring which is softly pressed to the surface around the seven holes provides the sealing of the vacuum side. This TFM was tested both with dense silicon tubes and porous hydrophobic Accurel® membranes [14,15]. Reproducible results were obtained and the module remained leak-free. Various TFM's were prepared with different composite membranes with PEI or PES supports and EPDM as the selective toplayer.

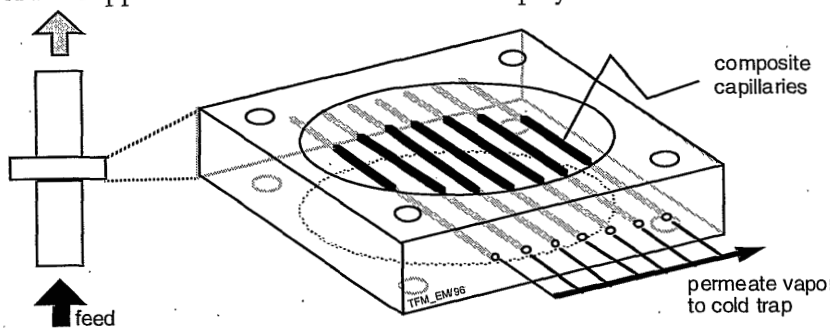

Figure 4 *Lab-scale transverse flow membrane module.*

7.3.4 Longitudinal outside flow module

A simple longitudinal outside flow module (LOM) has been developed with a tube diameter of 1 cm, which can be used both in gas permeation and pervaporation experiments. High Reynolds numbers of more than 11,000 can be achieved in this module. The membrane surface area ranges from 4 to 8 cm^2 depending on membrane diameter and lenght. One end of the module was connected to the vacuum. The other end was sealed with polyurethane. After the pervaporation experiment the membrane was dried overnight and a gas permeation experiment was performed to check whether the membrane was still defect-free[2].

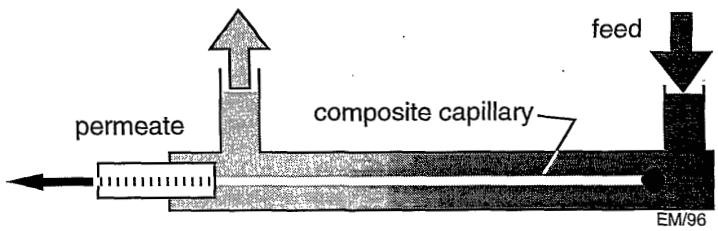

Figure 5 *Lab-scale longitudinal outside flow*

2 Due to the boundary layer resistance it is hard to conclude in pervaporation whether a membrane has defects or not. Yet, from gas permeation it is very easy to determine this.

7.4 RESULTS AND DISCUSSION

7.4.1 Determination of k_L and P/l

Flux measurements at different feed flow velocities in a transverse flow module (TFM) and a longitudinal outside flow module (LOM) were carried out to calculate both the membrane resistance and the mass transfer coefficient in the boundary layer. Capillaries were used with a diameter of 1.1 and 2 mm. Fig.6 shows typical results of a pervaporation experiment, where every point is the result of a 2 hour measurement.

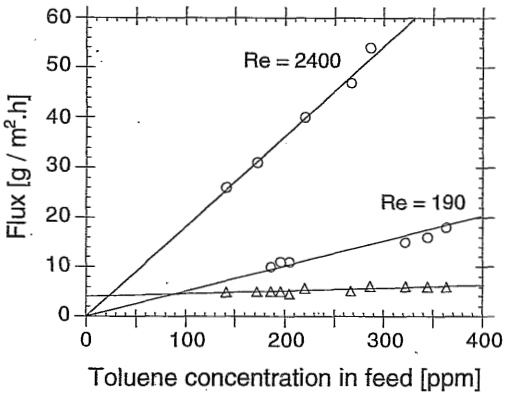

Figure 6 *Toluene (o) and water (Δ) fluxes versus the toluene concentration in the feed for two Reynolds numbers using CP2\D-composites in a TFM.*

It can be concluded that the toluene flux increases linearly with the toluene concentration in the feed. It is clear that both at high and low Reynolds this linear behaviour occurs. Consequently, the toluene flux can be normalized by a simple linear relation. Fig.6 also shows that the water flux increases marginally with increasing toluene concentration. This phenomenon has been predicted theoretically as described in Chapter 4 and has been shown for homogeneous EPDM-films (see Chapter 3).

Fig.7a shows the toluene and the water flux as a function of the Reynolds number (*Re*). It is clear that at low *Re* the toluene flux increases strongly with increasing *Re*, while at high *Re* this increase flattens off. The water flux is constant and is 5 g/(m^2.h). The effective toplayer thickness of EPDM for water is then 10 μm. (The intrinsic water flux is 0.5 g/(m^2.h) through a 100 μm thick homogeneous EPDM film at 26° C [16]. Fig.7b shows the same result plotted on different axes: the overall resistance to mass transfer versus the reciprocal feed flow velocity. From data-fitting values are obtained for the membrane resistance and the mass transfer coefficient in the liquid boundary layer. From this fit the membrane resistance can be obtained as well and a value of $3 \cdot 10^6$ m^2.s.Pa/mol is found. The effective toplayer thickness of EPDM for toluene is then 40 μm (with P_{tol} is 40 kBarrer which equals $1.36 \cdot 10^{-11}$ mol.m/ (m^2.s.Pa) [16]).

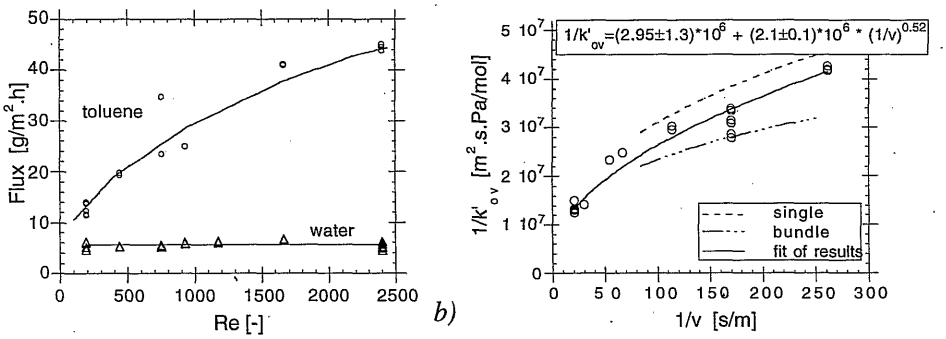

Figure 7 *a) Toluene (o) and water (Δ) fluxes versus Reynolds number with a TFM, b) overall resistance versus reciprocal feed flow velocity. (Two dashed lines have been added based on literature calculations with d_h = 2mm [6].)*

From eqn (5), k_L can be calculated at any feed flow velocity within the range of *Re* which have been covered. For a TFM with capillaries of 2 mm the $k_L = H/(2 \cdot 10^6)*(1/v)^{0.5}$, which is $6.7 \cdot 10^{-5}$ m/s for the maximum feed flow rate (*Re* is 2400 and v_{max} = 4.7 cm/s) and the feed temperature of 26° C (with: H = 648 Pa.m^3/mol). Similar k_L values for transverse flow were found in literature [3]. In fig.7b two additional curves have been drawn for a transverse flow of a single fiber and a bundle of fibers, respectively, as found in literature [6].

Fig.8 shows the results of the same composite membrane measured in an LOM. The *Re* are much higher compared to the TFM. High *Re* were applied to decrease the LBL-resistance.

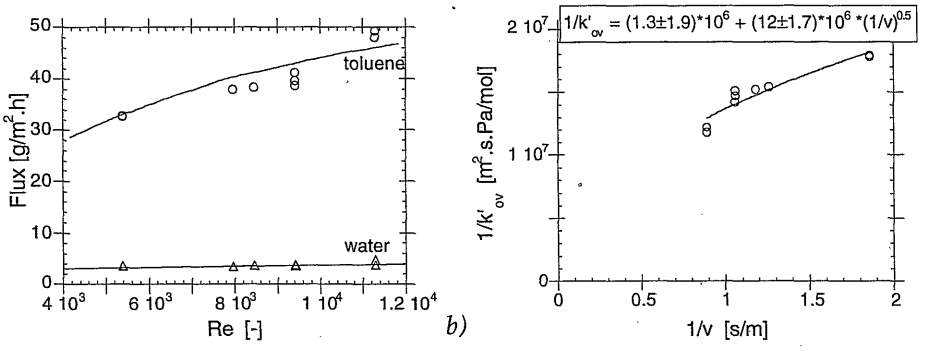

Figure 8 *a) Toluene (o) and water (Δ) fluxes versus Reynolds number using a LOM, b) overall resistance versus reciprocal feed flow velocity for CP2\D composites.*

Comparison of fig.7a and fig.8a clearly demonstrates the positive effect of TFM on the toluene flux. A toluene flux is found of about 45 g/m^2.h with a *Re* of 10,000 for the LOM and only 2,400 for the TFM. This flux decreases for the LOM to 30 g/m^2.h for a *Re* of 5,000. It must be concluded that the TFM, indeed, provides a much higher k_L value at a certain Reynolds number which effects the toluene flux in a positive way. For extreme high Reynolds numbers in the LOM the k_L

can be increased and becomes comparable to the TFM.

Fig.9a shows the results of a PEI-supported composite (JQ2). This composite has also a toplayer thickness as observed by SEM of 12 µm. A relatively high water flux of 12 g/(m^2.h) is combined with a maximum toluene flux of 23 g/(m^2.h), which is much lower than the CP2\D-composites. From the water flux a value for l_{eff} of 4 µm is obtained and from the toluene flux a value of 87 µm. In fig.9b the Sherwood-relation of Yang and Cussler has been depicted for 1.1 mm capillaries. However, the fitted data points of the JQ2-composite lie much higher, which indicates that the membrane resistance is higher for these membranes than the CP2\D membranes shown in fig.7b.

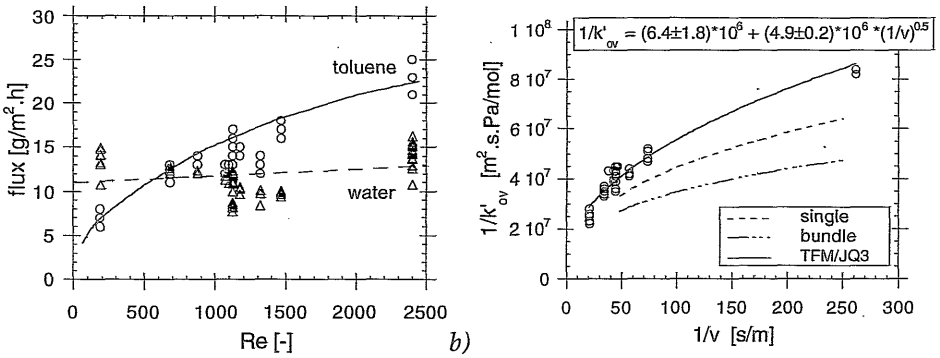

Figure 9 *a) Toluene (o) and water (Δ) fluxes versus Reynolds number for a TFM with composites with a PEI-support, b) overall mass transfer resistance versus reciprocal feed flow velocity. (Two dashed lines have been added based on literature calculations with d_h = 1.1mm [6],)*

The error in the estimate for the membrane resistance to toluene permeation is quite high since the error in the value for the abscissa is high. This is mainly due to a relative high resistance in the LBL. However, relative differences between various composites with the same diameter can be compared.

Table 2 summarizes the values found for the mass transfer coefficients in the liquid boundary layer for the two modules. It is clear that k_L for the LOM at extreme high *Re* is close to k_L for the TFM at much lower Reynolds number.

Table 2 *Mass transfer coefficients in the liquid boundary layer for TF and OF modules for different capillary diameters.*

Module type	Re [-]	Capillary diameter [mm]	k_L *10^5 [m/s]	Capillary diameter [mm]	k_L *10^5 [m/s]
Transverse flow	2400	2	6.7	1.1	2.9
Outside longitudinal flow	11,200	2	5.7	1.1	-

7.4.2 Separation factor

The separation factor decreases just a little with increasing toluene concentration in the feed (fig.10a), however, with increasing Reynolds number the separation factor increases strongly, due to an increased toluene flux at a constant toluene concentration and a constant water flux (fig.10b).

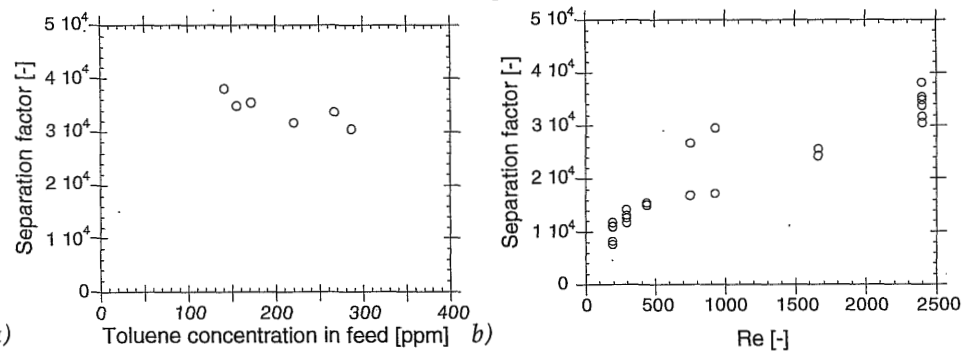

Figure 10 *a) Separation factor versus the toluene feed concentration at a fixed Re=2,400 and b) the Reynolds number in the feed at a fixed feed concentration of 250 ppm.*

Table 3 demonstrates clearly that the PES-supported composites show a high separation factor ranging from $35 \cdot 10^3$ to $90 \cdot 10^3$ and the PEI-supported membranes shows a separation factor of about $8 \cdot 10^3$. These lower separation factors for the latter membranes is mainly due to the low porosity of the porous support as will be explained more extensively in the next paragraph.

Table 3 *Separation factor of several composite membranes*

Support type	CP1*		CP2*				JQ2
Composite #	A	B	C	D	E	F	G
α (LOM) $*10^3$ [-]	70	30	48	52	80	82	-
α (TFM) $*10^3$ [-]	-	-	-	35	-	90	7.7

* CP1 and CP2 are PES-supported composite membranes and JQ2 is a PEI-supported composite membrane.

7.4.3 Toplayer thicknesses

The water flux is hardly affected by the support layer material since the permeability coefficient of water is higher for the support material than for the toplayer material [17]. The permeability of toluene and CO_2 is higher in EPDM than it is in PES (or PEI).

Table 4 *toplayer thickness from scanning electron microscopy (SEM) and effective thicknesses of composite membranes from CO_2, toluene and water permeation rates [μm].*

Composite type	$l_{eff}(CO_2)$	l_{SEM}	l_{eff}(tol/TFM)	l_{eff}(tol/LOM)	l_{eff}(water/TFM)	l_{eff}(water/LOM)
CP1\A	37	40	-	58	-	25
CP1\B	63	35	-	105	-	13
CP2\C	22	20	-	66	-	17
CP2\D	24	12	31	11	9	14
CP2\E	26	20	-	12	-	23
CP2\F	35	25	63	49	25	29
JQ2\G	33	12	39	-	4	-

Table 4 summarizes the various effective thicknesses as calculated via CO_2-permeation, toluene and water fluxes for several composites. For a certain composite A, C or F the various thicknesses are in rather good agreement, only the thickness from the toluene flux is somewhat higher. The other composites, on the other hand, show less comparable results. Composite G is very different and shows a low value for the thickness due to the high water flux, while the toplayer thickness as observed by SEM is somewhat higher. The effective thickness from CO_2 permeation is much higher which may be attributed to the influence of the support, which is different from the other results.

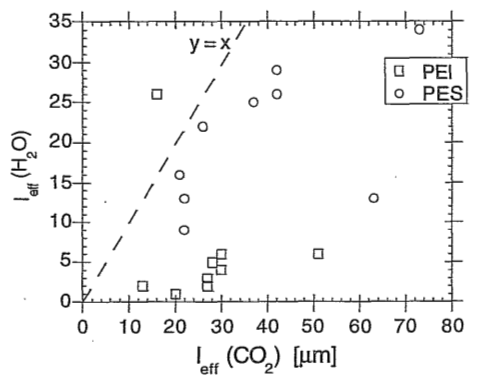

Figure 11 *The effective thickness of poly(ether imide) and poly(ether sulfone) supports calculated from CO_2 permeability measurements and water flux experiments.*

Comparison of the effective thicknesses of EPDM on PEI or PES supports calculated via CO_2-permeation and water flux experiments illustrates that the resistances are comparable for the PES-based composites, while for the PEI-based composites a relative smaller resistance to water transport is obtained (see fig.11). One can see from this figure that one PEI-composite lies much higher. This

membrane was coated 6 times with a 10 wt-% K578 solution, resulting in a thicker EPDM layer, and as a consequence the effect of the support layer is relatively smaller.

7.5 CONCLUSION

Composite membranes with poly(ether sulfone) (PES) or poly(ether imide) (PEI) as the porous support layer and with ethylene-propylene terpolymer (EPDM) as the toplayer material were characterized by pervaporation using a toluene/water solution. Toluene was selectively removed from an aqueous feed. A transverse flow (TFM) and a longitudinal outside flow module (LOM) were used to perform the pervaporation experiments. The mass transfer coefficient in the liquid boundary layer (k_L) was obtained as a function of the feed flow velocity. At a Reynolds number of 2400 the TFM shows a k_L of $6.7 \cdot 10^{-5}$ m/s. For the LOM a k_L value of $5.7 \cdot 10^{-5}$ m/s was found at extreme high Reynolds numbers of 11,000.

The toluene flux through the membrane was between 5 and 50 g/m^2.h for a toluene concentration in the feed of 250 ppm. The difference was mainly determined by the toplayer thickness and the feed flow velocity. Thinner toplayers and higher feed flow velocities result in higher toluene fluxes. The water flux decreased with increasing toplayer thickness and ranged from 1.5 to 12 g/m^2.h. The effective toplayer thicknesses as calculated via toluene and water fluxes were within the range of 4 to 100 μm. The separation factor ranges from 5,000 to 90,000 and this increases with increasing toplayer thickness and higher feed flow velocity.

The low porosity of the PEI supports (<1% [18]) resulted in a strong contribution on the pervaporation performance. The effective thickness as calculated from water fluxes for these membranes was much lower than for the composites which were supported with the PES capillaries (8% or 20% [18]), while the toluene fluxes were about the same.

ACKNOWLEDGEMENTS

Kees Plug and Krista Bouma are acknowledged for developing the pervaporation set-up. Also, they are acknowledged for the discussions concerning this topic. Lydia Versteeg is acknowledged for performing pervaporation experiments.

LIST OF SYMBOLS

Roman

a	activity	[-]
A	membrane area	[m^2]

b	semi-emperical parameter	[-]
c	concentration	[mol/m^3]
D	diffusion coefficient	[m^2/s]
H	Henry's law coefficient	[Pa. m^3/mol]
J	flux	[mol/(m^2.s)]
k	mass transfer coefficient	[m/s]
$m1$	fitting constant	[-]
$m2$	fitting constant	[-]
M	molecular weight	[g/mol]
p	(partial) pressure	[Pa]
p	fitting constant	[-]
P	permeability coefficient	[cm^3(STP).cm/(cm^2.s.cmHg] or [mol.m/(m^2.s.Pa)]
q	fitting constant	[-]
r	pore radius	[m]
r	fitting constant	[-]
R	universal gas constant	[J/(mol.K)]
Re	Reynolds number	[-]
s	fitting constant	[-]
Sc	Schmidt number	[-]
Sh	Sherwood number	[-]
STP	standard conditions: T=273.15 K and p=10^5 Pa	[-]
T	temperature	K
x	mole fraction in liquid	[mol/mol]
y	mole fraction in vapor	[mol/mol]

Greek symbols

α	separation factor for pervaporation	[-]
α_{id}	ideal selectivity for gas separation	[-]
γ	activity coefficient	[-]
ρ	density	[kg/m^3]
ρ_f	molar density	[mol/m^3]
σ	surface tension	[N/m]
τ	plasticizing coefficient	[-]

subscripts

f	feed
i	component i
L	stagnant liquid boundary layer
m	membrane
ov	overall
p	permeate side
tol	toluene
voc	volatile organic contaminant

w water

REFERENCES

[1] Strand, N.S., *Permeability separatory cell and apparatus and method of using the same*, USP 3,342,720 (1964).

[2] Futselaar, H., I.G.Rácz, Counter-current flow membrane module for liquid separations, EP 0,464,941 A1, 1990.

[3] Côté, P.L., R.P.Maurion, C.J.Lipski, *Frameless array of hollow fiber membranes and module containing a stack of arrays*, US 5104535, 1992.

[4] Bessarabov, D.G., A.V.Vorobiev, E.P.Jacobs, R.D.Sanderson, S.F.Timashev, *Separation of olefin/paraffin gaseous mixtures by means of facilitated-transport membranes based on metal-containing perfluorinated carbon-chain copolymers*, in: Bowen, W.R., R.W.Field, J.A.Howell (eds), Proceedings of Euromembrane '95, Bath, Anthony Rowe Ltd, Chippenham (UK), 1995, II-186.

[5] Meulen, ter, B.Ph., *Transfer device for the transfer of matter and/or heat from one medium flow to another medium flow*, WO 91/09668 (1991).

[6] Yang, M.-C., E.L.Cussler, *Designing hollow-fiber contactors*, AIChE Journal, 32 (1986) 1910-1916.

[7] Prasad, R., C.J.Runkle, *An improved hollow fiber module for mass transfer operations*, Proceedings of the NAMS, 6th, Breckenridge, Colorado (USA), 1994.

[8] Futselaar, H., *The transverse flow membrane module; construction, performance and applications*, PhD-thesis, University of Twente, Enschede (NL), 1993.

[9] Futselaar, H., *The transverse flow membrane module: application to pervaporation of volatile organic compounds*, in: Bowen, W.R., R.W.Field, J.A.Howell (eds), Proceedings of Euromembane '95, Bath (UK), Antony Rowe Ltd., Chippenham (UK), 1995, II-106.
Futselaar, H., C.P.Borges, A.C.Habert, R.Nobrega, *Removal of volatile organic contaminants from ground and waste waters by pervaporation*, Final report of COPPE/UFRJ, EEC/DG-XII CI1*-CT92-0081 Rio de Janeiro (BRA), 1996.

[10] Nijhuis, H.H., M.H.V.Mulder, C.A.Smolders, *Modeling pervaporation membrane performance in the removal of trace organics from water*, Proceedings of the 1990 Intern. Congress on Membrane and. Membrane processes, Chigago (USA), 1990, 319-321.

[11] Gooding, C., P.Hickey, P.Dettenberg, J.Cobb, *Mass transfer and permeate pressure effects in the pervaporation of VOCs from water*, in: R.Bakish (ed.), Proc.6th Int.Conf.Perv. Procs.Chem.Ind.; Ottawa (Canada), Bakish Materials Corp., Englewood (USA), 1992.
Hickey, P.J., C.H.Gooding, *Mass transfer in spiral wound pervaporation modules*, J.Membr.Sci, 92 (1994) 59-74.

[12] Bode, E., C.Hoempler, *Transport resistances during pervaporation through a composite membrane: experiments and model calculations*, J.Membr.Sci., 113 (1996) 43-56.

[13] Leemann, M., *Einsatz der Dampfpermeation zur Abtrennung und Rückgewinnung organischer Lösungsmittel aus Abluft - Verfahren und Verfahrenskombination*, Fortschrittberichte VDI Reihe 3 Nr.446, VDI Verlag GmbH, Düsseldorf (D), 1996.

[14] Borges, C.P., H.Futselaar, A.C.Habert, R.Nobrega, E.E.B.Meuleman, M.H.V.Mulder, *Removal of volatile organic contaminants from ground and waste waters by pervaporation*, Seminario internacional del agua, Mazatlan (MEX), 1994.

[15] Meuleman, E.E.B., M.H.V.Mulder, H.Strathmann, *Removal of volatile organic contaminants from ground and waste waters by pervaporation*, 2nd annual report, EEC/DG-XII CI1*-CT92-0081, 1995.

[16] Meuleman, E.E.B., Chapter 3 of this thesis, 1997.

[17] Borges, C.P., M.H.V.Mulder, C.A.Smolders, *Support effect of composite hollow fiber for removal of VOC's from water by pervaporation*, in: Habert, C., E.Drioli (eds), *Workshop CEE-Brazil on membrane separation processes*, Rio de Janeiro (BRA), 1992.

[18] Meuleman, E.E.B., Chapter 5 of this thesis, 1997.

LEVENSLOOP

Erik Meuleman werd op 20 oktober 1967 geboren in Goor. In 1986 behaalde hij zijn VWO-diploma aan het Twickel College in Hengelo (Ov.). Aansluitend begon hij de studie Chemische Technologie aan de Universiteit Twente. In 1988 werd de propaedeuse behaald. De stage werd bij AKZO in Obernburg (D) uitgevoerd en behelsde de bouw en automatisering van een opstelling waarmee het ontstaan van een vlak membraan kon worden gevolgd. De studie werd in 1992 onder leiding van dr. ir. Th. van den Boomgaard afgerond met een afstudeer-scriptie getiteld "Nabehandeling van hydrofiele ultrafiltratie-membranen" bij de vakgroep Membraantechnologie.

Op 1 november 1992 trad hij in dienst van dezelfde vakgroep, inmiddels geleid door Prof. dr. ing. H. Strathmann, als Assistent In Opleiding. Het aldaar uitgevoerde promotiewerk betrof de verwijdering van vluchtige organische stoffen uit water met behulp van pervaporatie en is beschreven in dit proefschrift. In het kader van de samenwerking binnen dit project met de groep van prof. dr. C. Habert en prof. dr. R. Nobrega van de Universiteit in Rio de Janeiro (UFRJ/COPPE) heeft hij twee maanden gewerkt in deze laboratoria om poreuze steunlagen te spinnen en composiet-membranen te produceren.

This thesis describes the improvement of the pervaporative removal of VOC's from water. High VOC-fluxes are obtained due to the use of a transverse flow membrane module, with which high mass transfer coefficients can be obtained. Furthermore, the water flux is strongly decreased because of the use of EPDM as the selective layer. In this study it was focused on the preparation of composite membranes. The top layer thickness has been varied between 2 and 100 µm onto a porous support.

ISBN 90 365 09 343